Management Strategy Evaluation for Sacramento River winter Chinook salmon

Arliss J. Winship[1,2] Michael R. O'Farrell[2]
Michael S. Mohr[2]

[1] Institute of Marine Sciences, University of California, Santa Cruz

Tel: +1-831-420-3963, E-mail: awinship@ucsc.edu

[2] Fisheries Ecology Division, Southwest Fisheries Science Center

National Marine Fisheries Service, 110 Shaffer Road, Santa Cruz, CA 95060, USA

February 28, 2012

Introduction

Sacramento River winter Chinook salmon (SRWC) is an endangered stock that is harvested incidentally in ocean fisheries. This stock was first listed as threatened under the Endangered Species Act (ESA) in 1989, and then downgraded to endangered in 1994. Most recently, in the 2010 Biological Opinion for ocean fisheries (NMFS (National Marine Fisheries Service), 2010), the National Marine Fisheries Service (NMFS) found that ocean fisheries are likely to jeopardize the continued existence of SRWC owing to a lack of measures and tools to constrain or reduce fishery impacts when this population's status is poor. NMFS offered a reasonable and prudent alternative (RPA) to comply with the ESA, which included (1) establishing thresholds related to the status of SRWC, (2) establishing fishery management objectives, and (3) development of analytical tools and assessment models that can implement the fishery objectives in the salmon fishery management process. This report documents a management strategy evaluation (MSE) used to develop a new management framework in the form of a harvest control rule. This work is relevant to component 2 of the RPA.

MSE is a computer simulation approach to evaluating the performance of alternative harvest management strategies with respect to management objectives (Hilborn, 1979; Butterworth & Punt, 1999; Cooke, 1999; Milner-Gulland *et al.*, 2001; Punt & Donovan, 2007). At the core of a MSE is an operating model. The operating model

has several components including the dynamics of the impacted population, measurement of that population, and the dynamics of harvest (Kell *et al.*, 1999; Rademeyer *et al.*, 2007). A set of candidate control rules are chosen that relate the target harvesting effort, impact rate, or harvest to the estimated status of the impacted population. Simulations are then conducted using the operating model to evaluate the performance of the different control rules in terms of conservation and fishery objectives. By modelling the entire system, including errors in the assessment of the impacted population and errors in the implementation of harvest control measures, MSE aims to replicate how a harvest strategy would perform in practice.

This report describes the development of an operating model and the evaluation of several different control rules for specifying annual ocean fishery impact rates. The performance of the different control rules were evaluated relative to previously defined conservation criteria for Central Valley salmonids (Lindley *et al.*, 2007) and the implications for ocean fisheries. The addendum to this report presents the performance results for an additional control rule proposed by the NMFS Southwest Region.

Methods

Operating model

An important feature of our operating model was stochasticity. Maturation and death are discrete events that occur with some expected probability within a given time frame for each individual. However, the occurrences of these events also involve an element of randomness whereby the actual maturation and survival rates in a finite population will vary from the expected probabilities. This randomness is referred to as demographic stochasticity and can be modelled using standard probability distributions for discrete events (e.g., binomial and multinomial). The variance in maturation and survival rates induced by demographic stochasticity is highest for small populations. It is also the case in nature that expected maturation and survival probabilities are rarely constant over time. For example, variation in environmental conditions results in variation in expected maturation and survival rates (environmental stochasticity). Variation in expected maturation and survival probabilities over time results in greater variation in the numbers of maturations and deaths than that specified by the binomial and multinomial distributions. Human processes are also subject to stochasticity. Measurements of natural systems are subject to random errors (e.g., estimated numbers of spawners from carcass surveys). The implementation of a management decision such as a fishery impact rate is a complex process involving the design of fishery control measures and subsequent fishing effort, which will never perfectly achieve the chosen rate in practice. It was vital that these sources of stochasticity were included in our operating model. Demographic and environmen-

tal stochasticity can affect the probability that a population will go extinct (Lande, 1993). Data that feed into a control rule will be uncertain so in order for the MSE to mimic reality the impact control rule can not have knowledge of the true state of the population. Deviations of realized impact rates from those specified by the control rule have obvious implications for the success of any management strategy.

At the core of our operating model was a model of the SRWC population. The population model was structured by origin (natural and hatchery), sex and age and had a time step of one year (Figs 1 and 2). The model tracked the number of fish on 1 March. We assumed that spawning adults, symbolized by S, entered the river on the last day of February. Their offspring (fry), J, along with hatchery-produced juveniles (pre-smolts), P, migrated back down the river during the following fall and winter and were assumed to enter the ocean on the last day of February one year later. Fish in the ocean were symbolized by O with fish being referred to as age-2 during their first year in the ocean and their age advancing 1 year every 1 March. Fish of age a that returned to the river to spawn were referred to as age-a even though spawning occurred during the summer following river entry. Aspects of our model and some of our notation follow several previous models for SRWC (Botsford & Brittnacher, 1998; Newman *et al.*, 2006; Newman & Lindley, 2006; O'Farrell *et al.*, 2011b).

For fish in the ocean on 1 March, the first modelled event each biological year was fishery impacts:

$$I_{osat} \sim \text{Binomial}\left(O_{osat}, i_{at}\right) \qquad \text{for} \quad 2 < a \leq A \tag{1}$$

where I_{osat} is the number of fish of origin o, sex s and age a that died during the fishing season following time t due to interactions with fisheries (harvest, release and drop-off mortality), O_{osat} is the number of fish of origin o, sex s and age a in the ocean at time t, i_{at} is the fishery impact rate on fish of age a during the fishing season following time t, and A is maximum age. The notation $x = \text{Binomial}\left(n, p\right)$ indicates that x is binomially distributed with sample size n and probability p. x represents the number of successes in n Bernoulli trials (two possible outcomes) with a probability of success of p. The number of successes will vary among sets of trials of size n by chance. The binomial distribution describes the distribution of the numbers of successes across sets of trials. In the case of Eq. 1, the number of fishery impacts I_{osat} represents the number of 'successes', the number of fish in the ocean O_{osat} represents the sample size, and the fishery impact rate i_{at} represents the probability of success.

Natural mortality was assumed to occur over winter after fishery impacts followed by sexual maturity completing the biological year:

$$\left[O_{os(a+1)(t+1)}, S_{osa(t+1)}\right] \sim \text{Multinomial}\left[O_{osat} - I_{osat}, n_a\left(1 - m_{sa}\right), n_a m_{sa}\right] \quad \text{for} \quad 2 < a < A \tag{2}$$

$$S_{osa(t+1)} \sim \text{Binomial}\left(O_{osat} - I_{osat}, n_a\right) \quad \text{for} \quad a = A \tag{3}$$

where S_{osat} is the number of fish of origin o, sex s and age a returning to the river at time t, n_a is the overwinter natural survival rate of fish of age a, and m_{sa} is the

probability that a fish of sex s and age a will mature into a spawner. The model assumed that the earliest age at which a fish could spawn was 2 years and that all fish matured by the maximum age. Fisheries were assumed to impact only fish of age 3 or older. We also assumed that fishery impact rates, natural survival rates and maturation rates were identical between natural-origin and hatchery-origin fish. This assumption is discussed further in the 'Parameterization' section. The notation $[x_1, x_2] = \text{Multinomial}\,(n, p_1, p_2)$ or $\mathbf{x} = \text{Multinomial}\,(n, \mathbf{p})$ indicates that the vector $\mathbf{x}$ is multinomially distributed with sample size n and probability vector $\mathbf{p}$. The multinomial distribution is analogous to the binomial distribution, but it is used for situations when there is more than two possible outcomes in each trial. p_1 represents the probability of the first outcome, p_2 represents the probability of the second outcome, etc. In the case of Eq. 2, there were three possible outcomes for a fish that survived fishery impacts: survived natural mortality and did not spawn, survived natural mortality and spawned, or succumbed to natural mortality. In our model we only kept track of the first two of these outcomes.

The numbers of natural-origin and hatchery-origin fish returning to spawn at age 2 and remaining in the ocean at age 3 were assumed to be functions of natural and hatchery production:

$$\begin{aligned}&\left[O_{(\text{natural})(\text{male})3(t+1)}, O_{(\text{natural})(\text{female})3(t+1)}, S_{(\text{natural})(\text{male})2(t+1)}, S_{(\text{natural})(\text{female})2(t+1)}\right] \sim \\ &\quad \text{Multinomial}\left[J_t, 0.5n_{2t}\left(1-m_{(\text{male})2}\right), 0.5n_{2t}\left(1-m_{(\text{female})2}\right), 0.5n_{2t}m_{(\text{male})2}, 0.5n_{2t}m_{(\text{female})2}\right]\end{aligned} \tag{4}$$

$$\begin{aligned}&\left[O_{(\text{hatchery})(\text{male})3(t+1)}, O_{(\text{hatchery})(\text{female})3(t+1)}, S_{(\text{hatchery})(\text{male})2(t+1)}, S_{(\text{hatchery})(\text{female})2(t+1)}\right] \sim \\ &\quad \text{Multinomial}\left[P_t, 0.5hn_{2t}\left(1-m_{(\text{male})2}\right), 0.5hn_{2t}\left(1-m_{(\text{female})2}\right), 0.5hn_{2t}m_{(\text{male})2}, 0.5hn_{2t}m_{(\text{female})2}\right]\end{aligned} \tag{5}$$

where J_t is the number of fry produced in natural spawning areas by spawners who entered the river at time $t-1$, n_{2t} is the juvenile survival rate of natural-origin fry from time t to time $t+1$ (freshwater outmigration and their first year in the ocean), P_t is the number of pre-smolts released into the river by the hatchery, and h is the juvenile survival rate of hatchery-origin pre-smolts as a multiple of the survival rate of natural-origin fry. We assumed a juvenile sex ratio of 1:1. Eqs 4-5 incorporated demographic stochasticity in the sex ratio, maturation rate and survival rate of juveniles.

Freshwater rearing, outmigration and the first year in the ocean are critical life stages for young salmon, and it has been hypothesized that variation in the environmental conditions experienced during these stages may cause substantial variation in natural juvenile growth and survival rates and ultimately the number of fish that return to the river to spawn (Friedland, 1998; Beamish & Mahnken, 2001; Wells *et al.*, 2007; Lindley *et al.*, 2009). We modelled the effect of variation in environmental conditions on juvenile survival by allowing the juvenile survival rate to vary over time according to a first-order autoregressive process whose marginal distribution

was a beta distribution (McKenzie, 1985):

$$n_{2t} = 1 - U_t \left[1 - W_t n_{2(t-1)}\right] \tag{6}$$

where

$$U_t \sim \text{Beta}\left(\beta_{n_2}, \alpha_{n_2} - p_{n_2}\right) \tag{7}$$

$$W_t \sim \text{Beta}\left(p_{n_2}, \alpha_{n_2} - p_{n_2}\right) \tag{8}$$

for $0 < p_{n_2} < \alpha_{n_2}$. Note that U_t and W_t were independent of each other and $n_{2(t-1)}$. Eqs 6-8 allow for positive autocorrelation in n_{2t} over time. The parameters of these beta distributions (α_{n_2}, β_{n_2}, p_{n_2}) were determined by specifying the mean, CV and autocorrelation of n_{2t} (μ_{n_2}, CV_{n_2}, ρ_{n_2}) and using the following relationships:

$$\alpha_{n_2} = \frac{1 - \mu_{n_2}\left(1 + CV_{n_2}^2\right)}{CV_{n_2}^2} \tag{9}$$

$$\beta_{n_2} = \frac{\frac{1}{\mu_{n_2}} - 2 + \mu_{n_2} + \left(\mu_{n_2} - 1\right) CV_{n_2}^2}{CV_{n_2}^2} \tag{10}$$

$$p = \frac{\alpha_{n_2} + \beta_{n_2}}{1 + \frac{\beta_{n_2}}{\rho_{n_2}\alpha_{n_2}}} \tag{11}$$

where $0 < \rho_{n_2} < 1$. Eq. 11 was derived based on McKenzie (1985). The sequence of juvenile survival rates was initialized by setting $n_{21} = \mu_{n_2}$. Autocorrelation in juvenile survival rates over time was intended to reflect autocorrelation in environmental conditions over time (e.g., sequences of consecutive good or bad years). Demographic stochasticity in juvenile survival rates was modelled (Eqs 4-5) in addition to the stochasticity described here (Eqs 6-8). The value used for CV_{n_2} was estimated from data at escapement levels of hundreds or thousands of spawners so we allowed for additional variance in realized juvenile survival rates at very small population sizes.

Livingston Stone National Fish Hatchery obtains new broodstock each year by capturing returning natural-origin spawners (in very few cases, hatchery-origin SRWC have been used for broodstock) in the Keswick Dam fish trap. Thus, not all natural-origin fish returning to the river contribute to natural production. The numbers of fish that spawned in the river were calculated as follows:

$$R_{osat} = \begin{cases} S_{osat} & \text{for} \quad o = \text{hatchery} \\ S_{osat} - B_{sat} & \text{for} \quad o = \text{natural} \end{cases} \tag{12}$$

where R_{osat} is the number of fish of origin o, sex s and age a that returned to the river at time t and subsequently spawned in the river and B_{sat} is the number of natural-origin fish of sex s and age a that returned to the river at time t and were subsequently removed from the river for broodstock.

We assumed that there was a targeted total broodstock for each sex, B^{target}, but that the total broodstock for each sex actually taken in a given year, B_t^{sex}, was constrained by the number of returning natural-origin spawners. We assumed that at most 20% of returning natural-origin spawners were taken as broodstock:

$$B_t^{\text{sex}} = \min\left\{B^{\text{target}}, \text{round}\left[0.2\sum_{a=2}^{A} S_{(\text{natural})(\text{female})at}\right], \text{round}\left[0.2\sum_{a=2}^{A} S_{(\text{natural})(\text{male})at}\right]\right\} \tag{13}$$

Eq. 13 assumed that the numbers of broodstock taken were determined by the sex with the fewest returning spawners. It is possible that the hatchery would be unable to obtain 20% of returning natural-origin spawners if abundance was low and $< 20\%$ of spawners entered the trap. If this was the case, the number of broodstock taken (and subsequent hatchery production) would be lower than specified by Eq 13.

The total male broodstock was assumed to be equal to the female broodstock, and broodstock was partitioned stochastically among ages according the age composition of returning fish:

$$[B_{s2t}, \ldots, B_{sAt}] \sim \text{Multinomial}\left[B_t^{\text{sex}}, \frac{S_{(\text{natural})s2t}}{\sum_{a=2}^{A} S_{(\text{natural})sat}}, \ldots, \frac{S_{(\text{natural})sAt}}{\sum_{a=2}^{A} S_{(\text{natural})sat}}\right] \tag{14}$$

Between 2003 and 2010 the annual numbers of male and female spawners taken as broodstock were usually similar, although 9% more females were taken overall (D. Killam, pers. comm.).

The expected number of fry produced in the wild was assumed to be a density-dependent function of the number of eggs produced following the Beverton-Holt stock-recruitment relationship (Beverton & Holt, 1957). Furthermore, it was assumed that the number of fry produced per female spawner would vary over time due to variation in fecundity and the rate of survival of eggs to the fry stage driven by variation in environmental conditions. This stochasticity in production was assumed to be greater than that dicatated by demographic stochasticity alone. We modelled stochasticity in the number of fry produced in the wild using a bias-corrected lognormal distribution. The following equations described the production of natural-origin fry in our model:

$$J_{t+1} \sim \text{round}\left\{\text{Lognormal}\left[\log\left(r_t F_t\right) - 0.5\sigma^2_{\log J}, \sigma^2_{\log J}\right]\right\} \tag{15}$$

$$r_t = \frac{\theta_1 g}{1 + \theta_2 g F_t} \tag{16}$$

$$F_t = \sum_{o}\sum_{a=2}^{A} R_{o(\text{female})at} \tag{17}$$

where $\text{Lognormal}\left(\mu, \sigma^2\right)$ is a lognormal distribution with mean μ and variance σ^2 on the log-scale, F_t is the total number of natural-origin and hatchery-origin females who entered the river at time t and subsequently spawned in the river, r_t is the

number of fry produced per female spawner, g is the number of eggs produced per female spawner, θ_1 is the maximum rate of successful egg deposition, incubation, hatching and survival to the fry stage, and θ_2 is a parameter specifying the strength of density dependence. Eq. 16 follows the parameterization of Newman & Lindley (2006) where θ_1 is equal to $\frac{1}{\beta}$ in the original parameterization presented by Beverton & Holt (1957) and θ_2 is equal to $\frac{\alpha}{\beta}$ in the original parameterization. We assumed that the number of male spawners did not limit the number of fry produced. We specified the CV of natural production (CV_J) and then calculated the variance on the log scale as:

$$\sigma^2_{\log J} = \log\left(1 + CV_J^2\right) \tag{18}$$

Hatchery production was modelled by assuming that all females taken for broodstock were spawned and that each of these females ultimately produced 3000 hatchery-origin pre-smolts for release into the river:

$$P_{t+1} = \text{round}\left[3000 B_t^{\text{sex}}\right] \tag{19}$$

We estimated the number of pre-smolts released per broodstock female from the numbers of female spawners taken as broodstock between 2006-2009 and the corresponding numbers of hatchery-origin pre-smolts released from those brood years (K. Niemela, pers. comm.).

Fishery impact rates were modelled as follows:

$$i_{at} = 1 - e^{\log\left[1-(c_t+\delta)\right]v_a} \tag{20}$$

where c_t is the realized impact rate south of Point Arena following time t, δ is the additional fishery impact rate north of Point Arena, and v_a is the relative instantaneous impact rate on age a. The realized impact rate was assumed to be distributed according to a beta distribution whose mean was the impact rate specified by the impact control rule (the maximum allowable impact rate):

$$c_t \sim \text{Beta}\left(\alpha_{c_t}, \beta_{c_t}\right) \tag{21}$$

where

$$\alpha_{c_t} = \frac{1 - \mu_{c_t}\left(1 + CV_c^2\right)}{CV_c^2} \tag{22}$$

$$\beta_{c_t} = \frac{\frac{1}{\mu_{c_t}} - 2 + \mu_{c_t} + \left(\mu_{c_t} - 1\right) CV_c^2}{CV_c^2}, \tag{23}$$

μ_{c_t} was the impact rate specified by the control rule at time t and CV_c was the coefficient of variation of the realized impact rate relative to the maximum allowable impact rate. The deviations of the realized impact rate from that specified by the control rule were intended to capture the unpredictable complexities of the real process of trying to design fishery controls to achieve a specific maximum allowable impact rate. For some simulation scenarios (see below), c_t was restricted to be

≤ 0.35 to prevent unrealistic realized impact rates. This constraint was implemented by truncating the beta distribution in Eq. 21 (i.e., discarding values higher than 0.35 and resampling until a permissible value was obtained). Demographic stochasticity in the realized impact rate was modelled (Eq. 1) in addition to the stochasticity described here (Eq. 21). As with CV_{n_2}, the value used for CV_c was estimated from data at escapement levels of hundreds or thousands of fish so we allowed for additional variance in realized impact rates at very small population sizes.

Six different impact control rules were considered (Fig. 3). The first three of these had a constant maximum allowable impact rate (i.e., μ_{c_t} did not change over time). The other three control rules specified the maximum allowable impact rate as a function of the mean estimated number of spawners over the past T years:

$$\mu_{c_t} = \min\left\{\phi_1 + \frac{\phi_2 - \phi_1}{\phi_4 - \phi_3}\max\left[\bar{N}_{tT}^{\text{spawn}} - \phi_3, 0\right], \phi_2\right\} \tag{24}$$

where $\bar{N}_{tT}^{\text{spawn}}$ is the mean estimated number of spawners per year during the T years preceding t, ϕ_1 was the minimum value that the maximum allowable impact rate could be, ϕ_2 was the maximum value that the maximum allowable impact rate could be, ϕ_3 was the threshold mean estimated number of spawners below which the maximum allowable impact rate was set to its minimum value, and ϕ_4 was the mean estimated number of spawners above which the maximum allowable impact rate was set to its maximum value. We used the geometric mean estimated number of spawners:

$$\bar{N}_{tT}^{\text{spawn}} = \left(\prod_{u=t-T}^{t-1}\hat{N}_u^{\text{spawn}}\right)^{\frac{1}{T}} \tag{25}$$

where $\hat{N}_t^{\text{spawn}}$ were simulated estimates of the numbers of spawners over time. These simulated estimates had two components: 1) the total numbers of spawners that were removed as broodstock ($2B_t^{\text{sex}}$), which were assumed to be known, and 2) estimates of the number of fish spawning in the river as though actual carcass surveys were being conducted. Errors in the estimates of the number of fish spawning in the river were assumed to conform to a bias-corrected lognormal distribution so that:

$$\hat{N}_t^{\text{spawn}} \sim \text{round}\left\{\text{Lognormal}\left[\log\left(\sum_o\sum_s\sum_{a=2}^{A}R_{osat}\right) - 0.5\sigma^2_{\log\hat{N}^{\text{spawn}}}, \sigma^2_{\log\hat{N}^{\text{spawn}}}\right]\right\} + 2B_t^{\text{sex}} \tag{26}$$

We specified the CV of these spawner estimates ($CV_{\hat{N}^{\text{spawn}}}$) and then calculated the variance on the log scale as in Eq. 18. Eq. 26 assumed that the true number of fish spawning in the river was the mean of the lognormal distribution. It is important to note that the impact rate specified by the control rule was a function of the simulated data not the true number of spawners.

Initialization

The natural population was initialized at the beginning of the simulation by specifying the initial number of females spawning in the river, $F_{(\text{natural})1}$. The vector of initial numbers of natural-origin fish of each sex, age and maturity status, $\mathbf{N}_1$, was then calculated from $F_{(\text{natural})1}$ and the stable age distribution specified by a pre-simulation deterministic transition matrix, $\left(\mathbf{X}_{\text{natural}} + \mathbf{Z}_{(\text{natural})0}\right)\mathbf{Y}_0$ (Appendix A). The stable age distribution was proportional to the eigenvector corresponding to the dominant eigenvalue of this matrix. The pre-simulation matrix was intended to approximate the dynamics of the population just prior to the start of the simulation. For consistency we assumed that these dynamics conformed to the assumed density-dependent dynamics in the simulation. Thus, the number of juveniles produced per female spawner just prior to the simulation, r_0, was set equal to r_1, which was calculated from $F_{(\text{natural})1}$ and Eq. 16. We also allowed for pre-simulation fishery impacts specified by the impact rates i_{a0}. It is important to note that if the initial population was below the equilibrium population size, the stable age distribution defined by the pre-simulation matrix would never be realized even theoretically because r_t would change over time according to its assumed density dependence. Furthermore, the removal of natural-origin spawners for broodstock and the contribution of hatchery-origin spawners to natural production were not represented in the natural stable age distribution. Despite these inconsistencies, we felt that this stable age distribution provided a reasonably realistic approximate natural age distribution with which to start the simulations with.

The hatchery-origin population was initialized at the beginning of the simulation in the same way as the natural population but using the initial number of hatchery-origin pre-smolts, P_1, and the pre-simulation deterministic transition matrix, $\left(\mathbf{X}_{\text{hatchery}} + \mathbf{Z}_{(\text{hatchery})0}\right)\mathbf{Y}_0$.

Parameterization

Model parameter values are presented in Table 1. We assumed a maximum age of 4 years. The initial number of natural-origin females spawning in the river was set to 1475, the average estimated number of natural-origin females spawning in the river from 2008-2010. The initial and future target broodstock (B_0^{sex} and B^{target}, respectively) were set to 50 females and 50 males. This broodstock was assumed to produce 150000 pre-smolts following our assumption of 3000 pre-smolts per female. This assumed hatchery production reflected the average hatchery production in recent years (2006-2009).

We obtained several of the parameter values that we used in the simulations from a statistical model that we developed for SRWC (Winship *et al.*, 2011). The structure of the population model in that analysis was similar to the population

component of our operating model, thus, the parameters were transferable between models. The parameter values that we took from the statistical analysis included the stock-recruitment parameters (g, θ_1, θ_2, CV_J), sexual maturation probabilities (m_{sa}), juvenile survival probabilities (μ_{n_2}, CV_{n_2}, h) and the CV of estimates of the number of fish spawning in the river ($CV_{\hat{N}^{\text{spawn}}}$). We used median posterior estimates from the statistical model because the posterior probability distributions were sometimes heavily skewed and medians are less affected by parameter transformations. The value of $CV_{\hat{N}^{\text{spawn}}}$ was set to the mean of our annual estimates from the statistical model (total number of fish spawning in the river). There were no available estimates of the autocorrelation in juvenile survival probabilities over time. Furthermore, we did not feel that the lengths of the data time-series (Winship *et al.*, 2011) were sufficient to reliably estimate this parameter. Instead, we explored two different scenarios with respect to temporal autocorrelation in juvenile survival rates. In the first of these scenarios we assumed no autocorrelation, and in the second we assumed an autocorrelation of 0.5. The values that we chose for ρ_{n_2} were somewhat arbitrary because of the lack of information about what a realistic level of autocorrelation might be. Nevertheless, we felt that the values 0 and 0.5 bracketed a range that likely contained a realistic value. We explored two other preliminary autocorrelation scenarios ($\rho_{n_2} = 0.3$ and 0.6) and found that increasing or decreasing ρ_{n_2} generally increased or decreased the autocorrelation effects described in the 'Results' section.

We assumed a constant natural annual survival probability of 80% for ages $\geq$ 3 following assumptions in models by CDFG (California Department of Fish and Game) (1989) and O'Farrell *et al.* (2011b). Our model assumed that the survival rates of hatchery-origin and natural-origin fish older than age 2 were identical. The average age distributions of hatchery-origin and natural-origin spawners were similar between 2001-2009 (USFWS (United States Fish and Wildlife Service), 2010), which is consistent with similar survival rates conditional on similar maturation rates.

The impact rate specified by the control rule was assumed to be the age-3 impact rate ($v_3 = 1$). Fish were assumed to be invulnerable to fishery-related mortality during their first year in the ocean (i.e., $v_2 = 0$). Estimated age-4 impact rates were variable between 2001-2007 and based on small sample sizes (O'Farrell *et al.*, 2011b) so we made the simplifying assumption that the instantaneous age-4 impact rate was twice that of the age-3 impact rate ($v_4 = 2$). The contributions of fishery impacts north of Point Arena to the overall impact rate were also variable between 2000-2007, but we assumed that $\delta = 0.006$, the average value. The pre-simulation age-3 impact rate, $i_{3\,0}$, was assumed to be 0.2 (O'Farrell *et al.*, 2011b). The CV of the realized impact rate relative to that specified by the control rule, CV_c, was calculated from an analysis of estimated impact rates for SRWC (O'Farrell *et al.*, 2011b) and hindcast impact rates from a preliminary version of the SRWC harvest model (O'Farrell *et al.*, 2011a).

Performance-testing simulations

To illustrate our MSE framework we conducted a series of preliminary performance-testing simulations.

We evaluated the performance of six different control rules that specified a wide range of maximum allowable fishery impact rates. The set of control rules represented no fishing, historical fishing levels, current fishing levels and three control rules where the maximum allowable impact rate was reduced as stock status declined. The control rule parameter values used for these performance-testing simulations were: rule 0 – $c_t = 0$; rule 1 – $c_t = 0.25$; rule 2 – $c_t = 0.2$; rule 3 – $\phi_1 = 0.1$, $\phi_2 = 0.2$, $\phi_3 = 833\frac{1}{3}$ and $\phi_4 = 1041\frac{2}{3}$; rule 4 – $\phi_1 = 0$, $\phi_2 = 0.2$, $\phi_3 = 0$ and $\phi_4 = 1041\frac{2}{3}$; rule 5 – $\phi_1 = 0$, $\phi_2 = 0.2$, $\phi_3 = 833\frac{1}{3}$ and $\phi_4 = 1041\frac{2}{3}$ (Fig. 3).

Control rule 1 was intended to represent a situation where fishing opportunity and effort were similar to historical levels. It is not possible to directly estimate fishery impact rates prior to the implementation of SRWC-focused protective measures, first instituted in 1994, because of data limitations. The largest difference in ocean fisheries between the pre-1994 "baseline" period and current fisheries was the presence of February and March recreational fisheries in areas south of Point Arena. Available data from the late 1960s suggest that recreational fisheries in these months likely harvested substantial numbers of SRWC (O'Farrell *et al.*, 2011b). Using historical fishing effort estimates and estimates of the impact rate per unit effort, we inferred the age-3 impact rate south of Point Arena for the baseline era prior to the protective measures. A general description of the method follows.

For the south of Point Arena area, the monthly (March–November), recreational age-3 impact rate per unit effort was estimated from cohort reconstructions for the current era, defined as 2000-2009 (O'Farrell *et al.*, 2011b). The recreational age-3 impact rate in the baseline era was then inferred by (1) assuming that the February impact rate per unit effort was equivalent to the March impact rate per unit effort, (2) multiplying the month-specific, recreational impact rate per unit effort by the month-specific average recreational effort for years 1976–1993, (3) summing the resulting impact rates over months February–November, and (4) multiplying the baseline age-3 recreational fishery impact rate by a factor of 1/0.69. The denominator of the fraction in (4) represents the proportion of the age-3 impact rate attributed to the recreational fishery, estimated for the current era. This procedure results in a mean age-3 impact rate for the baseline period of 0.25.

Control rule 2, a constant age-3 impact rate, was intended to represent current era ocean fisheries, which have been reduced relative to the historic level owing to the SRWC consultation standard. Control rule 2 is therefore defined as a constant age-3 impact rate of 0.20, which was the mean age-3 impact rate estimated from cohort reconstructions for years 2000-2007 (O'Farrell *et al.*, 2011b).

Control rules 3-5 incorporated increasingly conservative features to control rule 2, in the form of lower age-3 impact rates at reduced levels of stock status (Fig. 3). The mean spawner levels at which reductions in impact rate occurred were chosen based on thresholds of the population size risk criterion defined by Lindley *et al.* (2007).

Control rule 3 specifies an age-3 impact rate of 0.20 (ϕ_2) at mean spawner levels greater than $1041\frac{2}{3}$ (ϕ_4). Between mean spawner levels of $1041\frac{2}{3}$ and $833\frac{1}{3}$ (ϕ_3), the impact rate declines linearly from 0.20 to 0.10 (ϕ_1). At mean spawner levels less than or equal to $833\frac{1}{3}$, the impact rate is 0.10. The threshold value of $833\frac{1}{3}$ was chosen to represent the situation where the total population size was 2500 spawners, the threshold for a low risk of extinction for the population size criterion defined by Lindley *et al.* (2007). The threshold value of $1041\frac{2}{3}$ was chosen to represent the situation where the number of spawners in a given year would be reduced to $833\frac{1}{3}$ by an impact rate of 0.20. Control rule 3 therefore allows the mean impact rate experienced in recent years under the current SRWC consultation standard, unless the mean number of spawners reaches a defined threshold, at which time the impact rate is reduced to a *de minimis* level. The *de minimis* impact rate of 0.10 is representative of other *de minimis* exploitation rates for ESA listed salmon stocks.

Control rule 5 specifies an age-3 impact rate of 0.20 (ϕ_2) at mean spawner levels greater than $1041\frac{2}{3}$ (ϕ_4). Between mean spawner levels of $1041\frac{2}{3}$ and $833\frac{1}{3}$ (ϕ_3), the impact rate declines linearly from 0.20 to zero (ϕ_1). Justification for threshold values of mean spawner levels is the same as described for control rule 3. Control rule 5 contains the most conservative features of all control rules considered (with exception to the no fishing control rule), as it results in the closure of all fisheries when the average spawner level is less than or equal to the low risk threshold for the population size risk criterion (Lindley *et al.*, 2007).

Control rule 4 was designed to represent an intermediate level of conservatism between control rules 3 and 5. This control rule specifies an age-3 impact rate of 0.20 (ϕ_2) at mean spawner levels greater than $1041\frac{2}{3}$ (ϕ_4). Between mean spawner levels of $1041\frac{2}{3}$ and zero (ϕ_3), the impact rate declines linearly from 0.20 to zero (ϕ_1).

For control rules 2-5 we assumed that the maximum realized impact rate was 0.35 (the realized impact rate was a stochastic realization of the impact rate specified by the control rule; Eq. 21).

For comparison we also present the results of simulations with no fishery impacts south of Point Arena (i.e., $c_t = 0$), referred to as control rule 0.

The six control rules were tested under all combinations of two sets of scenarios. The first set of three simulation scenarios explored different values of T, the number of years of data input to the control rule (Eqs 24-25). In Scenario 'a' only the most recent escapement was input to the control rule ($T = 1$). In Scenario 'b' the geometric mean of the previous three escapements was input ($T = 3$). In Scenario

'c' $T = 5$.

The second set of two simulation scenarios considered different levels of autocorrelation in juvenile survival rates over time, ρ_{n_2} (Eq. 11). In the first of these scenarios we assumed no autocorrelation in juvenile survival rate, and in the second we assumed an autocorrelation of 0.5. All other parameters were set at the values presented in Table 1.

For each combination of control rule and scenario 20000 stochastic simulations were conducted for a time period of 100 years. We evaluated five performance metrics primarily related to the extinction risk criteria presented by Lindley *et al.* (2007) for Sacramento River Chinook salmon. The first performance metric was annual escapement, which equalled the total number of male and female natural- and hatchery-origin spawners each year ($\sum_o \sum_s \sum_{a=2}^{A} S_{osat}$). The second performance metric was 'population size' as defined by Lindley *et al.* (2007): the sum of three years (one generation) of escapement ($\sum_o \sum_s \sum_{a=2}^{A} \sum_{u=t}^{t-2} S_{osau}$). The distinction between escapement and population size is important with respect to performance criteria. For example, Lindley *et al.* (2007) present criteria for assessing extinction risk based on population size, but there may also be interest in escapement criteria. The third performance metric was the 10-year log trend in escapements, which is related to the extinction risk criteria based on 'population decline' presented by Lindley *et al.* (2007). The fourth performance metric was generational changes in population size, which was related to the extinction risk criteria based on 'catastrophe' presented by Lindley *et al.* (2007). While our model did not incorporate catastrophic events as defined by Lindley *et al.* (2007), we were interested in how the environmental variability that was incorporated in our model would affect the classification of population changes in terms of the catastrophe criteria. The catastrophe performance metric was calculated over 12 years of escapement, which equalled 10 years of population sizes. Note that these population sizes were not independent as there was temporal overlap in the escapements used to calculate sequential population sizes. Each generational change was calculated from the ratio of each pair of these 10 population sizes that were 3 years apart. Thus, the catastrophe performance metric was based on 7 generational changes in population size. The fifth performance metric was the proportion of years in which hatchery-origin fish composed 10% or more of the escapement. This last metric is relevant to the 'hatchery influence' extinction risk criteria presented by (Lindley *et al.*, 2007).

In addition to the extinction risk criteria, we evaluated several performance metrics relevant to the fishery. First we examined the proportion of time that the conservative features of control rules 3-5 were activated. We also examined how frequently the maximum allowable impact rate changed under these control rules, and the durations of continuous periods of time when the maximum allowable impact rate was less than its maximum value. Finally, we examined the realized impact rates under all of the control rules.

Results

Performance-testing simulations

Time-series of escapements simulated by the model seemed plausible in the context of the observed dynamics of SRWC during the past 40 years (Figs 4-5). The majority of simulated escapements were within the range of estimated historical escapements, although much higher escapements occurred in the simulations (> 50000 spawners). Large declines were observed in some of the simulations as were extended periods of low escapement. It is important to keep in mind that the historical time series of escapement data represents only one replicate of 40 years while the simulation results represent what might have happened in 20000 different realizations of a 100-year time series. As expected, allowing for autocorrelation in juvenile survival rates resulted in relatively smoother changes in escapement over time and more frequent protracted periods of low or high escapement (Fig. 5). The long-term mean annual escapement in simulations without fishery impacts south of Point Arena was about 23000-24000 spawners, but when fishery impacts were allowed under control rule 1 the mean escapement dropped to about 10000 spawners. Mean escapement was a bit higher under the more conservative control rules 2-5, about 13000 spawners. Differences among the long-term mean escapements under control rules 2-5 were small (< 1000 spawners).

The distributions of final population sizes in the simulations reflected similar patterns as those observed in annual escapements (Figs 6-7). The mean final population sizes were about three times the long-term mean annual escapements for corresponding control rules and scenarios. This result was expected because population size was calculated as the sum of three years of escapement. The distributions of population sizes were highly positively skewed with modes and medians less than the means. Thus, $> 50\%$ of final population sizes were less than the mean final population size. Allowing for fishery impacts under control rule 1 resulted in a $> 50\%$ reduction in final population size. This reduction was less under control rules 2-5, and differences in final population size among control rules 2-5 were relatively small. Differences in final population size among the three T scenarios (a, b and c) were also small. Allowing for autocorrelation in juvenile survival rates increased the variance in final population size (Fig. 7).

With respect to the 'population size' extinction risk criteria of Lindley *et al.* (2007), the vast majority of simulations resulted in low extinction risk (Figs 8-9). Fishery impacts under control rules 1-5 resulted in higher probabilities of moderate and high risk (Figs 8-11). The risk was highest when juvenile survival rates were autocorrelated over time, although the proportions of runs with high risk were small (1%) and only 9% of these simulations resulted in moderate risk (Figs 9, 11). It is also worth noting that there were small probabilities of moderate and high risk even in the absence of fishery impacts south of Point Arena, when juvenile survival

rates were autocorrelated over time (Fig. 9). Performance with respect to these extinction risk criteria tended to improve from control rule 1 through control rule 5 especially in the presence of autocorrelated juvenile survival rates (Figs 9, 11). However, differences in performance among control rules 3-5 were small ($\leq 1\%$).

With respect to the 'population decline' extinction risk criteria of Lindley *et al.* (2007), there was substantial probability of moderate and high risk even in the absence of fishery impacts south of Point Arena (Figs 12-13). The dynamics of our operating model were such that the population fluctuated around an equilibrium size, sometimes increasing and sometimes decreasing. Thus, about 50% of the time the population was expected to be declining, sometimes at a rate greater than 10% per year. As a result, the population often met the decline-based criteria for moderate or high extinction risk. Fishery impacts under control rules 2-5 increased the probability of moderate and high extinction risk by decreasing the equilibrium mean escapement and increasing the probability that escapement was ≤ 500 spawners at least once in the last 6 years. Autocorrelation in juvenile survival rates also increased the probability of escapements ≤ 500 resulting in higher risk attributable to this metric.

With respect to the 'catastrophe' extinction risk criteria of Lindley *et al.* (2007), the environmental variability inherent to our model resulted in small probabilities of a catastrophic decline in population size during the last 10 years of the simulations (Figs 14-15). The probability of high risk ($\geq 90\%$) was at most 2% (scenario with autocorrelation in juvenile survival rates; Fig. 15). The probabilities of at least one lesser but substantial decline ($\geq 50\%$; our definition of moderate risk) were much higher (up to 50%). Performance with respect to these criteria varied little among control rules. It is important to note that our model did not incorporate catastrophic events, however, the environmental variability that was incorporated resulted in generational changes in population size that could have been classified as moderate or high risk according to the 'catastrophe' criteria of Lindley *et al.* (2007).

The mean frequency of years when $> 10\%$ of spawners were of hatchery origin was about 1 in 10 in the absence of fishery impacts south of Point Arena and autocorrelation in juvenile survival rates (Fig. 16). This mean frequency increased to about 4 in 10 with fishery impacts under control rule 1 and about 3 in 10 under control rules 2-5. The frequency increased with increasing fishery impacts because the impacts reduced the size of the natural-origin population and thus natural production while hatchery production remained constant. Autocorrelation in juvenile survival rates increased the mean frequency of years with $> 10\%$ of spawners of hatchery-origin to as much as 1 in 2 under control rule 1 (Fig. 17). Differences in this performance metric were small among T scenarios and among control rules 2-5, although there was some indication that the frequency decreased from rule 2 through rule 5 when juvenile survival rates were autocorrelated (Fig. 17).

The probability of escapement being > 20000 spawners was 38-42% in the absence of fishery impacts south of Point Arena across all simulation scenarios (Figs

18-21). This probability dropped to 13-15% when there were fishery impacts south of Point Arena under control rule 1, and was between 18-21% under control rules 2-5. Differences in this probability among control rules 2-5 were small. Allowing for autocorrelation in juvenile survival rates tended to result in slightly higher probabilities of escapement > 20000 under control rules 1-5 (Figs 19, 21). Differences in T did not have large effects on the probability of escapement > 20000. For historical context, estimates of SRWC escapement from counts at Red Bluff Diversion Dam on the Sacramento River exceeded 20000 in 9 of 39 years between 1970-2008. However, the years with escapement > 20000 occurred at the beginning of the time series, and the dynamics during that time period might have been different from the more recent dynamics that we estimated using our statistical model and applied to our forward projections.

For the majority of years in the simulations the maximum allowable impact rate specified by control rules 3-5 was equal to its maximum value, 0.2 (Figs 22-23). Population size was usually greater than the thresholds inherent to these control rules at which a lower impact rate would have been specified. Nevertheless, there were substantial proportions of time during which control rules 3-5 dictated a scaling back of the impact rate and thus fishing opportunity. Maximum allowable impact rates < 0.1 occurred under control rules 4 and 5, and maximum allowable impact rates of 0 (i.e., no fishing effort) occurred under control rule 5. The proportion of years with a maximum allowable impact rate less than its maximum value was greatest under Scenario a where only the most recent estimate of escapement was input to the control rule (Fig. 22). The 3-year and 5-year means that were input to the control rules under Scenarios b and c fluctuated less than the most recent escapement value so there were fewer years when the input to the control rule was low enough to trigger a lower impact rate. As discussed above, autocorrelation in juvenile survival rates resulted in a higher probability of lower population sizes, thus autocorrelation resulted in control rules 3-5 more frequently specifying an impact rate less than the maximum (Fig. 23).

Because the impact rate specified by control rules 3-5 was usually its maximum value, the maximum allowable impact rate was mostly stable over time (Fig. 24). The proportions of years when the maximum allowable impact rate decreased or increased were approximately equal. The impact rate changed more frequently when only the most recent estimate of escapement was input to the control rule than when 3-year or 5-year means were input. Autocorrelation in juvenile survival rates resulted in higher proportions of years when the impact rate changed because of the higher frequency of escapements below the control rules' upper escapement thresholds (Fig. 25). The specified impact rate changed most frequently under control rule 4, which had the largest range of escapements over which the impact rate was specified to change (Fig. 3).

The periods of time for which control rules 3-5 specified a scaling back of the maximum allowable impact rate varied depending on the number of years of escapement

data input to the control rule and the level of autocorrelation in juvenile survival rates (Figs 26 and 27). When we assumed no autocorrelation in juvenile survival rates and the specified impact rate was a function of only the most recent estimate of escapement (Scenario a) the impact rate was usually scaled back for only a single year at a time ($> 80\%$ of occurrences of scaling back; Fig. 26). Over 99% of occurrences of the impact rate being scaled back lasted for 5 years or less. When 3-year or 5-year means were input to the control rule scaling back of the specified impact rate lasted for ≥ 2 years more than half of the time and lasted longer than 5 years 9-17% of the time. When we assumed that there was autocorrelation in juvenile survival rates, the average time that the specified impact rate was scaled back lengthened (Fig. 27). When the control rule operated on the most recent estimate of escapement the impact rate was scaled back for longer than a year 38-39% of time. When 3-year or 5-year means were input to the control rule scaling back of the specified impact rate lasted for ≥ 2 years 75-82% of the time and lasted longer than 5 years 30-38% of the time.

Although the maximum allowable impact rate was usually 0.25 (control rule 1) or 0.2 (control rules 2-5), the assumed stochastic errors in achieving the maximum allowable impact rate resulted in a wide range of realized age-3 impact rates south of Point Arena. The bulk of the distributions were between 0.1-0.4 under control rule 1, but we assumed a maximum realized impact rate of 0.35 under control rules 2-5 (Figs 28-29). Within T scenarios, the lower tails of these distributions tended to be longer as the control rule became more conservative and specified an increasing frequency of impact rates < 0.2. In the case of control rule 5, realized impact rates were as low as zero. The lower tails of the distributions of realized impact rates were also longer and heavier when the juvenile survival rate was assumed to be autocorrelated over time.

Discussion

We constructed a MSE to inform the choice of a new management framework for SRWC in the form of a fishery impact rate control rule. The operating model used in the MSE was parameterized based on a statistical model, a cohort reconstruction, and auxiliary analyses. We examined several simulation scenarios including a scenario with reduced precision of spawner abundance estimates and two scenarios with respect to autocorrelation in juvenile survival rates over time. We feel that the two autocorrelation scenarios bracketed the range of realistic levels of autocorrelation. The simulation scenario with an autocorrelation of 0.5 represented the worst case scenario, in terms of conservation risk, among the scenarios that we examined.

The MSE was used to evaluate the performance, in terms of conservation benefit and fishery cost, of several control rules with a wide range of conservative features. The set of control rules represented no fishing, historical fishing levels, current fishing

levels and three control rules where the impact rate was reduced as stock status declined.

While we evaluated the performance of these control rules with respect to a variety of criteria, the most pertinent criterion with regard to developing a management framework was the population size risk criterion. Other performance metrics were much less informative for a variety of reasons. With respect to the population decline risk criterion, our model structure (density dependence) resulted in the population fluctuating around an equilibrium level with relatively equal frequencies of increase and decrease. In addition, the population decline risk criterion is of most relevance at low population size, which is represented more directly by the population size risk criterion. With respect to the hatchery risk criterion, Livingston Stone National Fish Hatchery is a best-practices fish hatchery and there is little basis for quantitative guidelines regarding hatchery straying from best-practices hatcheries (Lindley *et al.*, 2007). With respect to a recovery criterion, we examined the probability of annual escapement exceeding 20000 (NMFS, 1997; Botsford & Brittnacher, 1998). However, 20000 spawners is not a well-established recovery target and the ocean fishery is not solely responsible for recovery. Finally, with respect to the catastrophe risk criterion, Lindley *et al.* (2007) developed this criterion to capture large, rapid declines in population size that were not a result of "normal environmental variation". It is difficult to predict the probability of occurrence and magnitude of catastrophes that might befall SRWC so we did not incorporate catastrophes in our model. Nevertheless, the environmental variability that was incorporated sometimes resulted in very large, rapid declines in population size. Presumably the catastrophe risk criterion would be considered in the event of an identifiable catastrophe. We therefore focus here on results pertaining to the population size risk criterion for making inference about conservation benefits provided by alternative control rules.

The three-year geometric mean number of spawners is an appropriate metric for use in determining the maximum allowable age-3 impact rate through a control rule. Escapement in salmon populations can be highly variable, and single years of low or high escapement may not accurately reflect stock status. On the other hand, use of the five-year geometric mean could result in a control rule that is too slow to respond to changes in stock status, with relatively distant escapement values affecting current management. We focus here on results when the three-year geometric mean number of spawners was input to the control rules.

Control rules 3-5 reduce the maximum allowable age-3 impact rate as stock status declines, and the breakpoints in these control rules correspond to published thresholds for the population size risk criterion (Lindley *et al.*, 2007). There was little to no difference in risk among control rules 3-5 in terms of the population size risk criterion. Under our worst-case scenario (autocorrelation in juvenile survival rate = 0.5), there was moderate risk 4-5% of the time and high risk $< 1\%$ of the time. When we assumed no autocorrelation in juvenile survival rate, there was moderate or high risk $< 1\%$ of the time. Control rules 3-5 reduced the probability of moderate

or high risk by $> 50\%$ relative to historical levels of fishing (control rule 1), and resulted in noticeable risk reduction relative to current levels of fishing (control rule 2). Furthermore, there is relatively little to be gained in terms of risk reduction by more conservative control rules than those developed here, as the elimination of all fisheries still resulted in moderate or high risk in 1% of the simulations for the worst-case scenario.

While there was little difference in terms of the conservation benefits resulting from control rules 3-5, there would have been large differences in the costs to the fishery. The conservative features of these control rules (i.e., reductions in the maximum allowable impact rate below its maximum value) were invoked 7-9% of the time under our worst-case scenario. Control rule 3 allows for a *de minimis* age-3 impact rate of 0.1 when stock status is poor, and the specified impact rate was equal to this value 1% of the time when there was no autocorrelation in juvenile survival rate and 9% of the time when there was autocorrelation in juvenile survival rate. Control rules 4-5 allowed for impact rates < 0.1 and complete closure of the recreational and commercial fisheries. Control rule 5 specified a zero impact rate $< 1\%$ of the time and 5% of the time without and with autocorrelation, respectively. An impact rate of 0.1 would require heavy reductions in both commercial and recreational fishing opportunity south of Point Arena, but would permit some *de minimis* fishery impacts, allowing some access to abundant target stocks. Impact rates below 0.1 would dramatically reduce fishing opportunity relative to what has been typical levels under the current consultation standard.

In conclusion, among the range of control rules considered, control rule 3 provided conservation benefits relative to the control rules that approximated historical and current rates of fishery impacts and resulted in similar levels of conservation benefits as control rules 4-5. However, control rule 3 would have resulted in the lowest fishery cost among the set of control rules 3-5, primarily because it allowed for some *de minimis* fishery impacts to occur. Our results suggested that the population size risk incurred by the *de minimis* fishery impact rate under control rule 3 was negligible, but the reduction in fishery cost relative to control rules 4-5 was substantial.

Table 1. Model parameters and values.

Parameter	Description	Dimensions	Value
A	max. age		4
$F_{(\text{natural})1}$	initial number of natural-origin females spawning in the river		1475
g	number of eggs per female spawner		4900
θ_1	max. egg-to-fry survival rate		0.301
θ_2	strength of density dependence		1.38e-08
CV_J	CV of recruitment stochasticity		0.105
n_a, μ_{n2}	natural survival rate	$a \in \{2, \ldots, A\}$	$n_2 = \mu_{n_2} = 0.00370$ $n_{3+} = 0.8$
CV_{n_2}	CV of juvenile survival rate		0.836
ρ_{n_2}	autocorrelation in juvenile survival rate		0, 0.5
h	hatchery-origin juvenile survival rate		2.06
m_{sa}	maturation rate	$s \in \{\text{male}, \text{female}\}$ $a \in \{2, \ldots, A-1\}$	$m_{(\text{male})2} = 0.139$ $m_{(\text{male})3} = 0.903$ $m_{(\text{female})2} = 0.000628$ $m_{(\text{female})3} = 0.960$
B_0^{sex}, B^{target}	broodstock	$t \in \{1, 2, \ldots, T-1\}$	50
λ^{P}	pre-simulation rate of change in hatchery production		1
v_a	relative impact rate	$a \in \{3, \ldots, A\}$	$v_3 = 1$ $v_4 = 2$
CV_c	CV of realized impact rate		0.315
$i_{3\,0}$	pre-simulation age-3 impact rate		0.2
$CV_{\hat{N}^{\text{spawn}}}$	CV of observation error		0.08

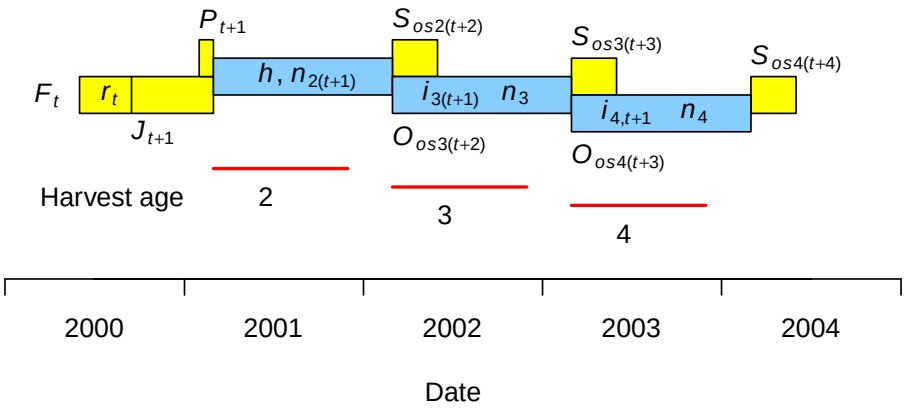

Figure 1. Model life history of Sacramento River winter Chinook salmon. This example timeline is for fish whose brood year is 2000 (offspring of female spawners in 2000, F_t). Yellow represents freshwater phases and blue represents marine phases. Model ages correspond to 1 March. Spawners are assumed to enter the river on the last day of February and to spawn on 1 June. Numbers of fish are symbolized with capital letters (J_t = natural-origin fry, P_t = hatchery-origin pre-smolts, O_{osat} = fish in the ocean, and S_{osat} = spawners). Natural survival rates (r_t = egg to fry, h = hatchery-origin pre-smolt outmigration and first year in ocean, n_{2t} = natural-origin fry outmigration and first year in ocean, n_a = ages 3 and older) and fishery impact rates (i_{at}) are symbolized with lower case letters. Red lines indicate the time period of the marine fisheries (1 March - 30 November). Note that harvest age is equivalent to the age at which the fish could spawn next. The removal of natural-origin spawners for hatchery broodstock is not represented in this figure.

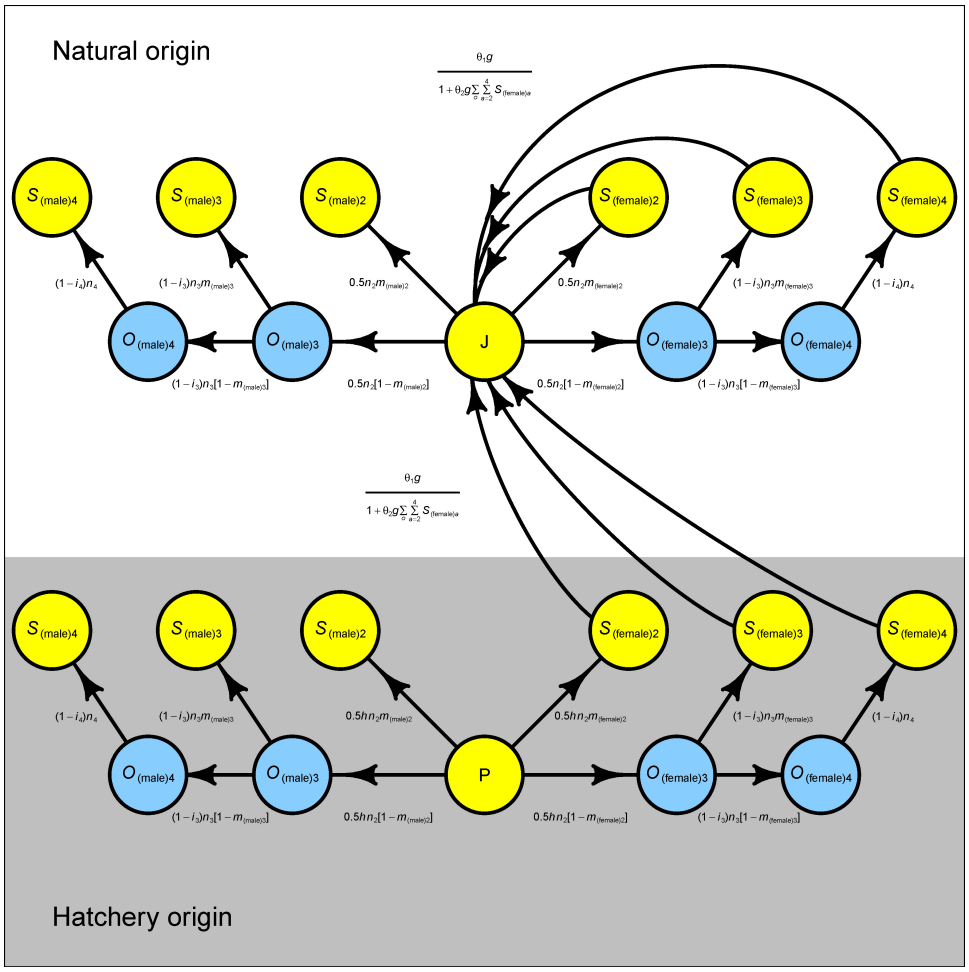

Figure 2. Model life cycle of Sacramento River winter Chinook salmon. Yellow represents freshwater phases and blue represents marine phases. The grey shaded box indicates hatchery-origin fish as distinct from natural-origin fish. Circles represent the numbers of fish in each state (J = natural-origin fry, P = hatchery-origin pre-smolts, O_{sa} = fish in the ocean, and S_{sa} = spawners). The indexing of states by origin, o, has been suppressed in this figure. Transitions between states include fishery impact rates (i_a) and natural survival (n_a, h), maturation (m_{sa}) and reproductive rates. The removal of natural-origin spawners for hatchery broodstock and subsequent hatchery production is not represented in this figure.

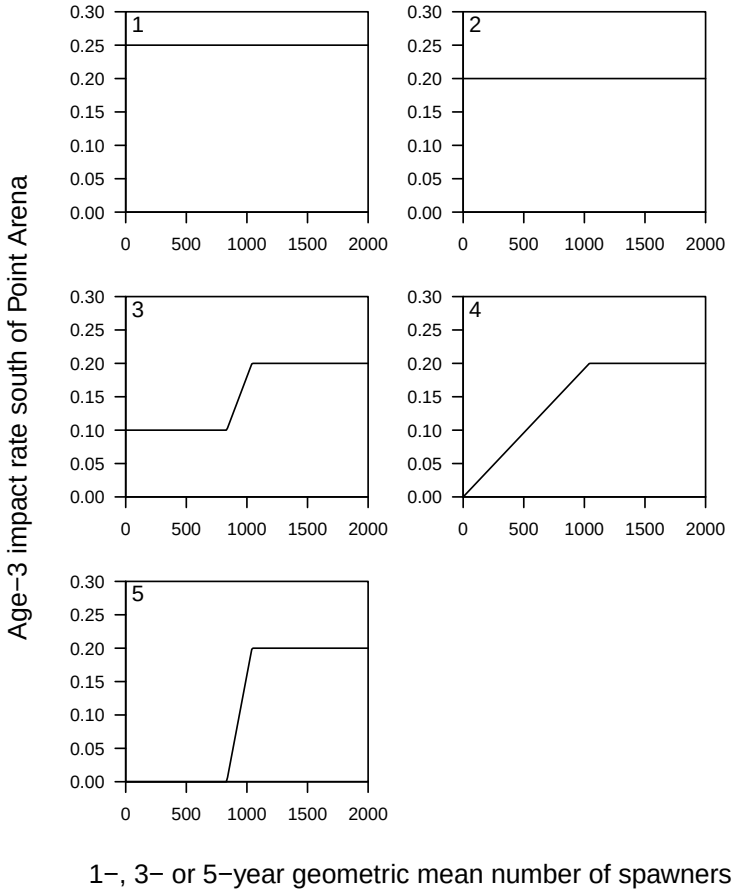

Figure 3. Impact control rules 1-5. The x-axis is the mean estimated total male and female natural- and hatchery-origin spawner escapement ($\bar{N}_{tT}^{\text{spawn}}$).

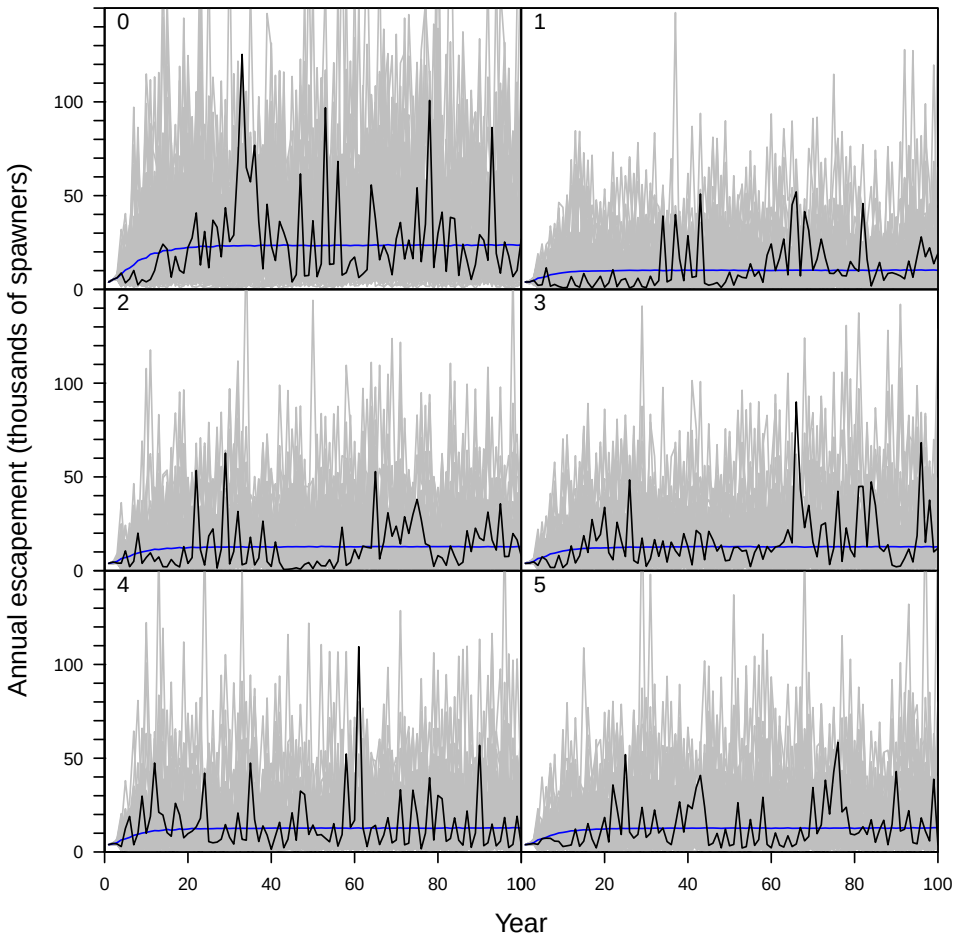

Figure 4. Simulated time-series of escapement over a 100-year period. The 3-year geometric mean estimated escapement was input to the control rule in any given year (Scenario b) and there was no temporal autocorrelation in juvenile survival rates. Panels 0-5 represent control rules 0-5 as described in the text. The grey lines represent 100 simulations for each control rule. The blue lines represent the mean escapement in each year across 20000 simulations. The black lines represent a single, randomly chosen simulation.

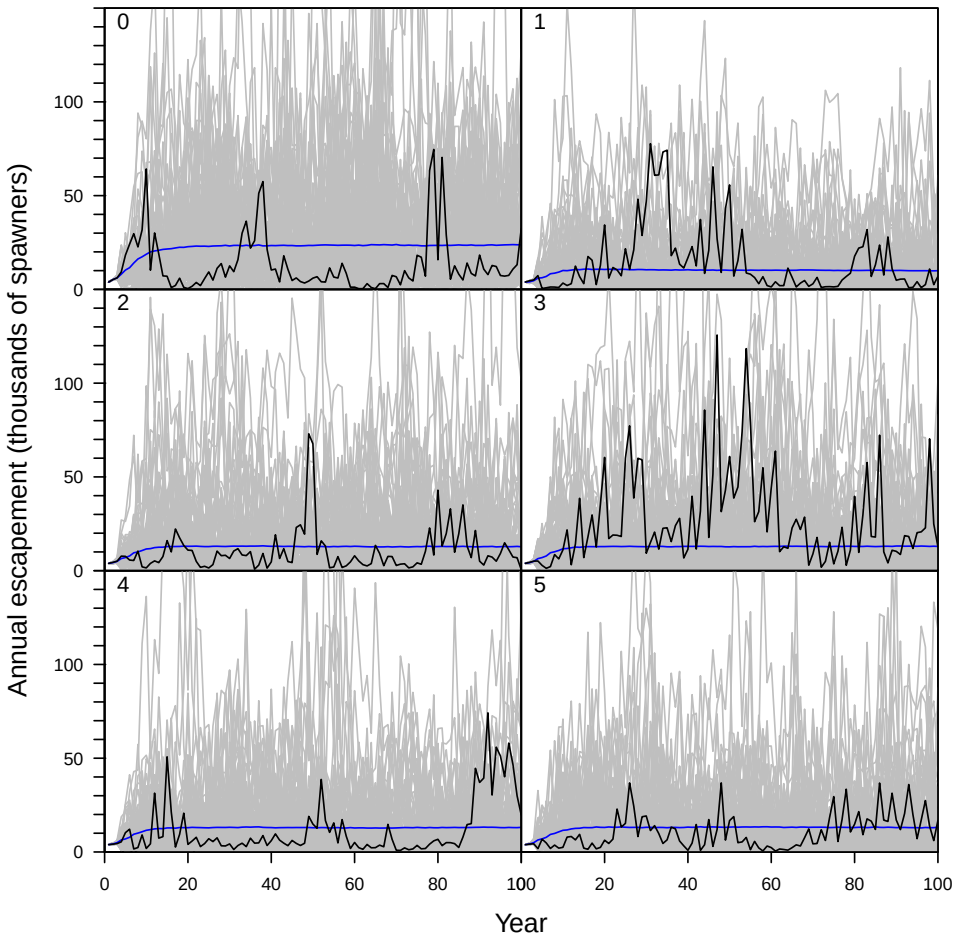

Figure 5. Simulated time-series of escapement over a 100-year period. The 3-year geometric mean estimated escapement was input to the control rule in any given year (Scenario b) and we assumed a temporal autocorrelation of 0.5 in juvenile survival rates. Panels 0-5 represent control rules 0-5 as described in the text. The grey lines represent 100 simulations for each control rule. The blue lines represent the mean escapement in each year across 20000 simulations. The black lines represent a single, randomly chosen simulation.

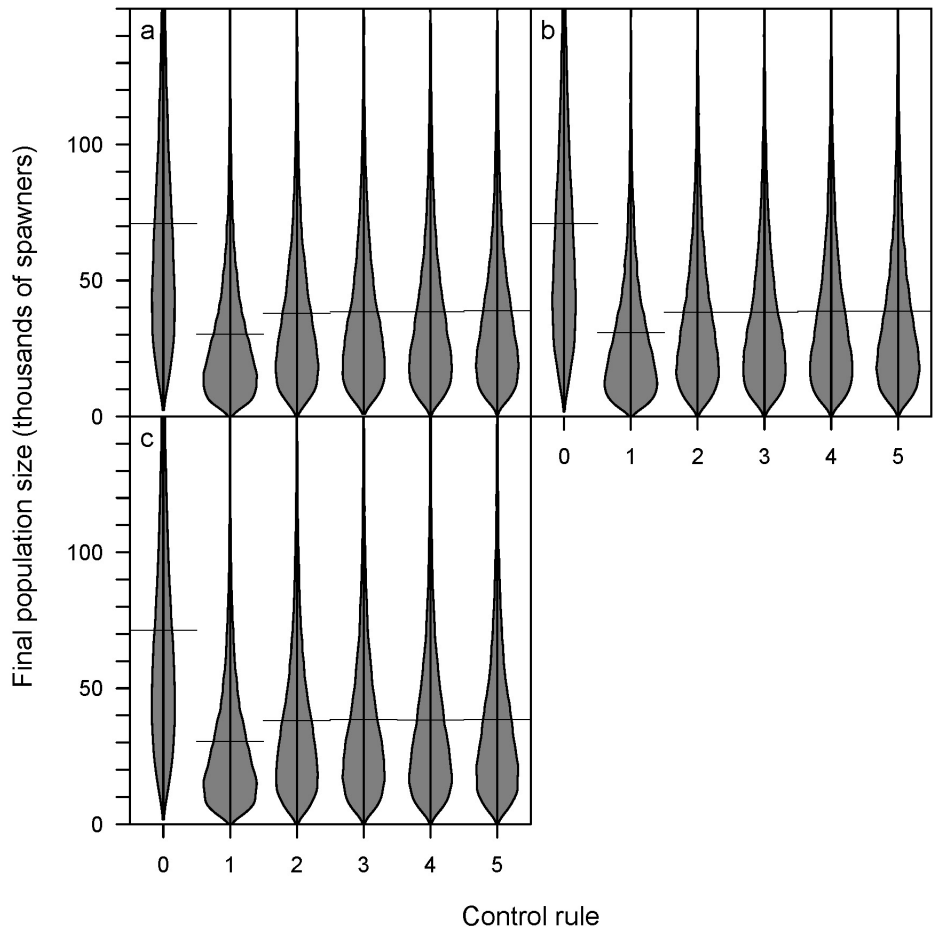

Figure 6. Distribution of final population size in 20000 100-year simulations for each of three T scenarios (a-c) and 6 control rules (0-5) assuming no temporal autocorrelation in juvenile survival rates. Final population size was calculated as the sum of escapements during the last three years of a simulation. Scenarios and control rules are described in the text. The horizontal lines represent the means of the distributions.

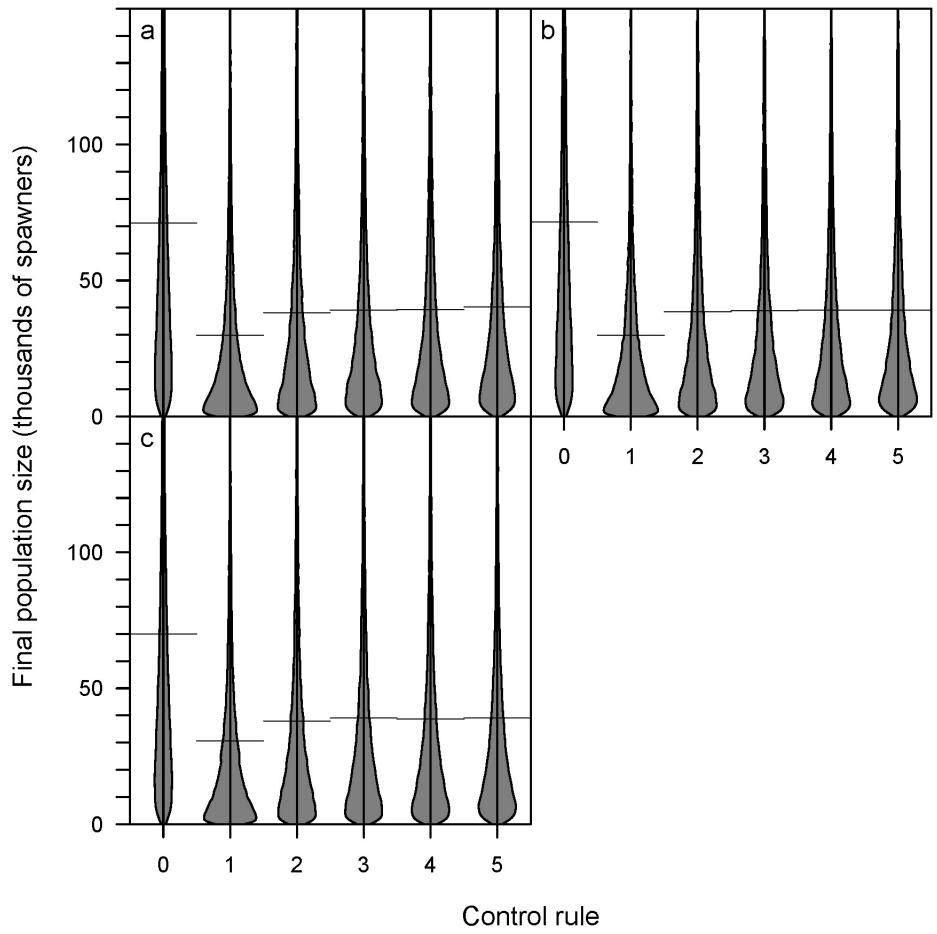

Figure 7. Distribution of final population size in 20000 100-year simulations for each of three T scenarios (a-c) and 6 control rules (0-5) assuming a temporal autocorrelation of 0.5 in juvenile survival rates. Final population size was calculated as the sum of escapements during the last three years of a simulation. Scenarios and control rules are described in the text. The horizontal lines represent the means of the distributions.

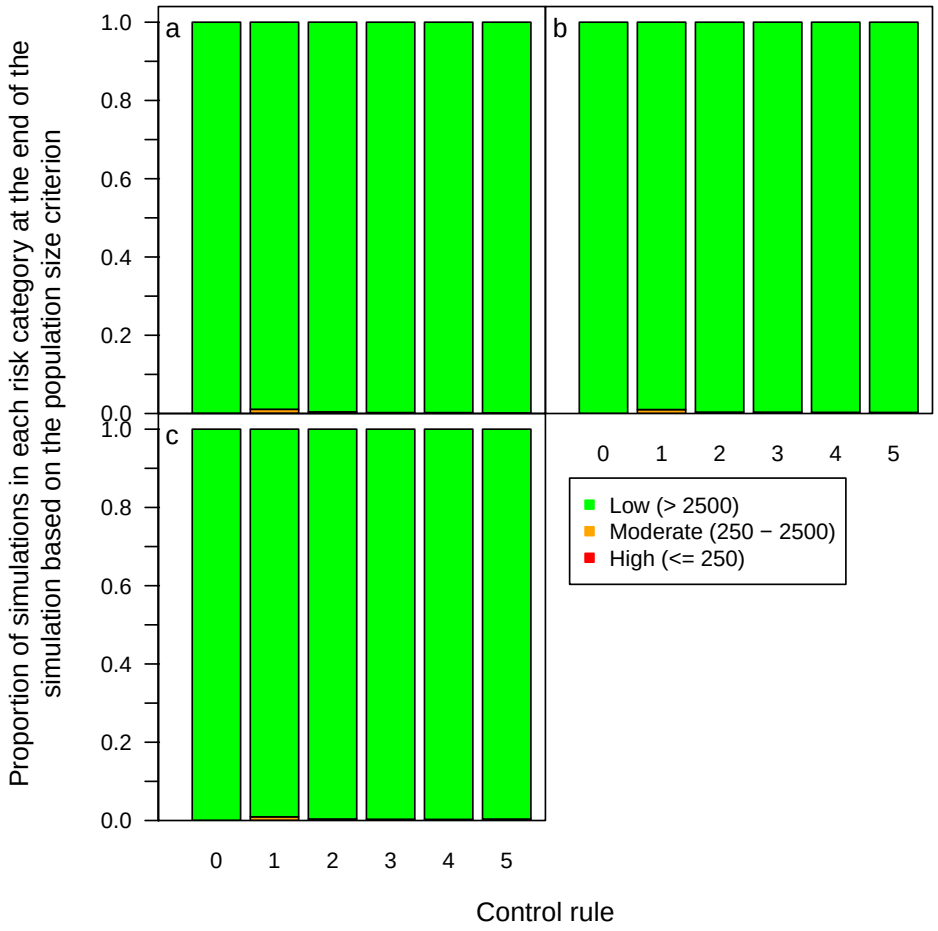

Figure 8. Proportions of 20000 100-year simulations whose final population sizes met each of three extinction risk categories based on 'population size' defined by Lindley *et al.* (2007). We assumed no temporal autocorrelation in juvenile survival rates. Final population size was calculated as the sum of escapements during the last three years of a simulation. Results are shown for each of three T scenarios (a-c) and 6 control rules (0-5), which are described in the text.

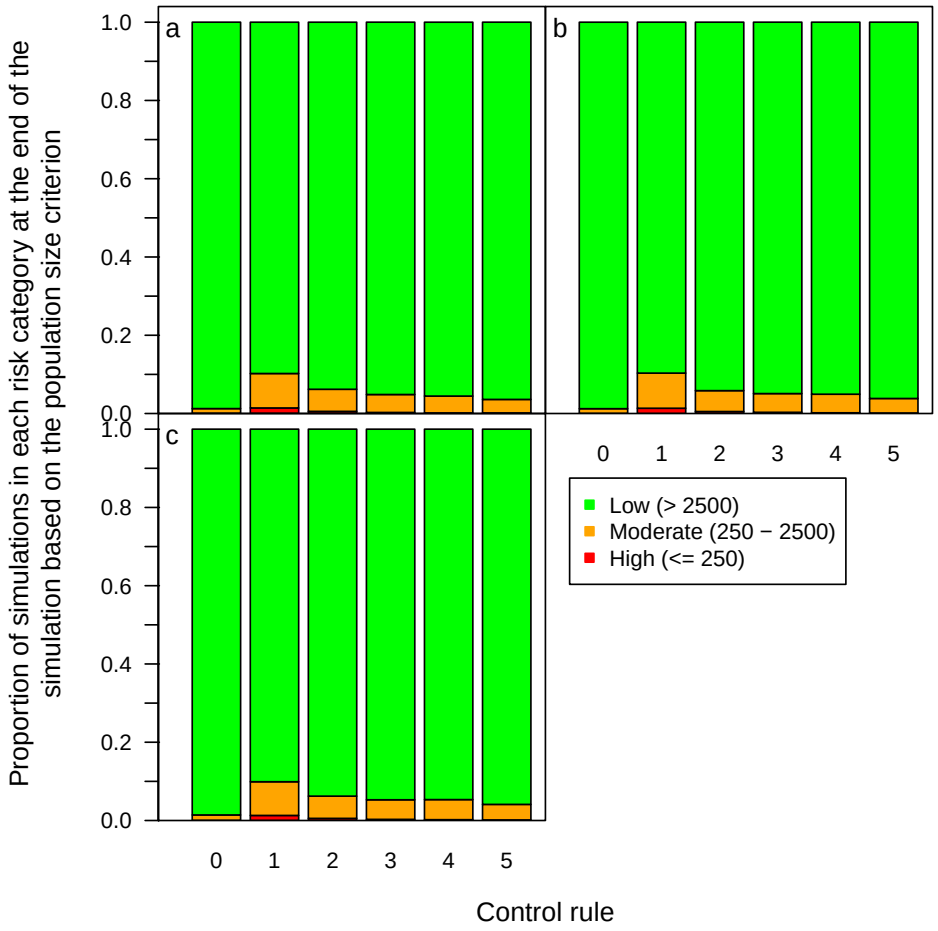

Figure 9. Proportions of 20000 100-year simulations whose final population sizes met each of three extinction risk categories based on 'population size' defined by Lindley *et al.* (2007). We assumed a temporal autocorrelation of 0.5 in juvenile survival rates. Final population size was calculated as the sum of escapements during the last three years of a simulation. Results are shown for each of three T scenarios (a-c) and 6 control rules (0-5), which are described in the text.

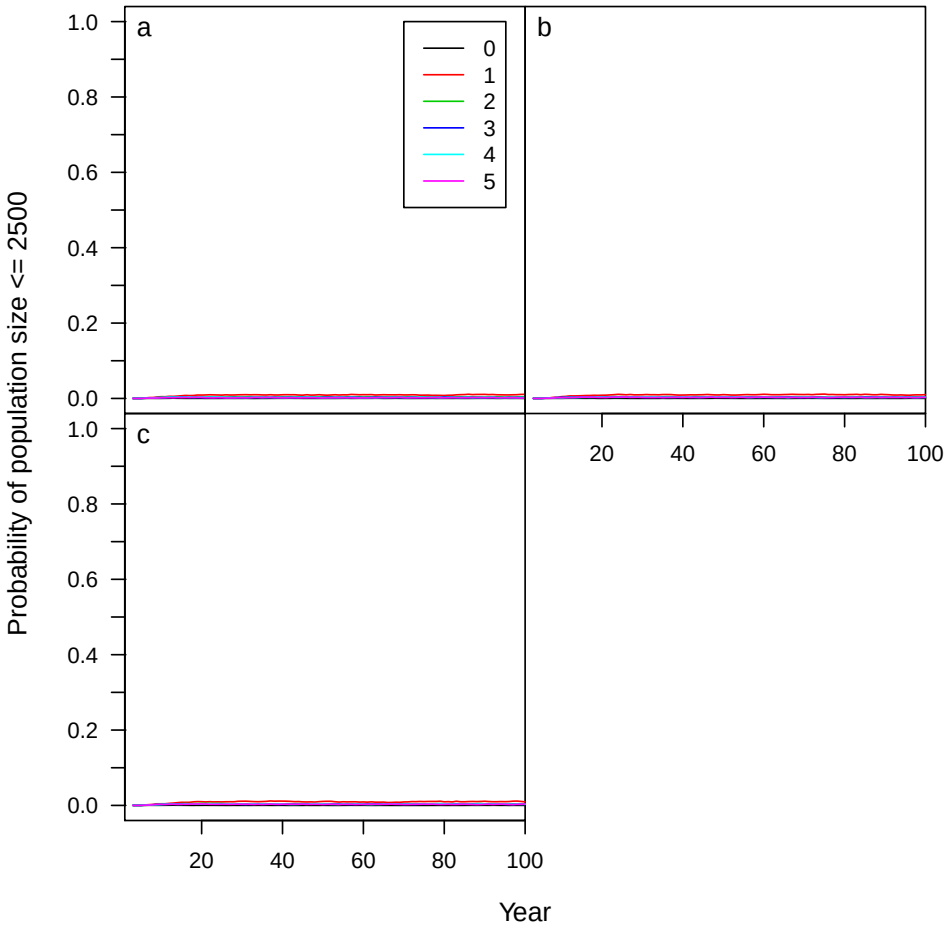

Figure 10. Proportion of 20000 simulations in which population size was $\leq$ 2500 spawners over the course of a 100-year simulation period. We assumed no temporal autocorrelation in juvenile survival rates. Population size was calculated as the sum of the escapements in the previous 3 years. Results are shown for each of three T scenarios (a-c) and 6 control rules (0-5), which are described in the text.

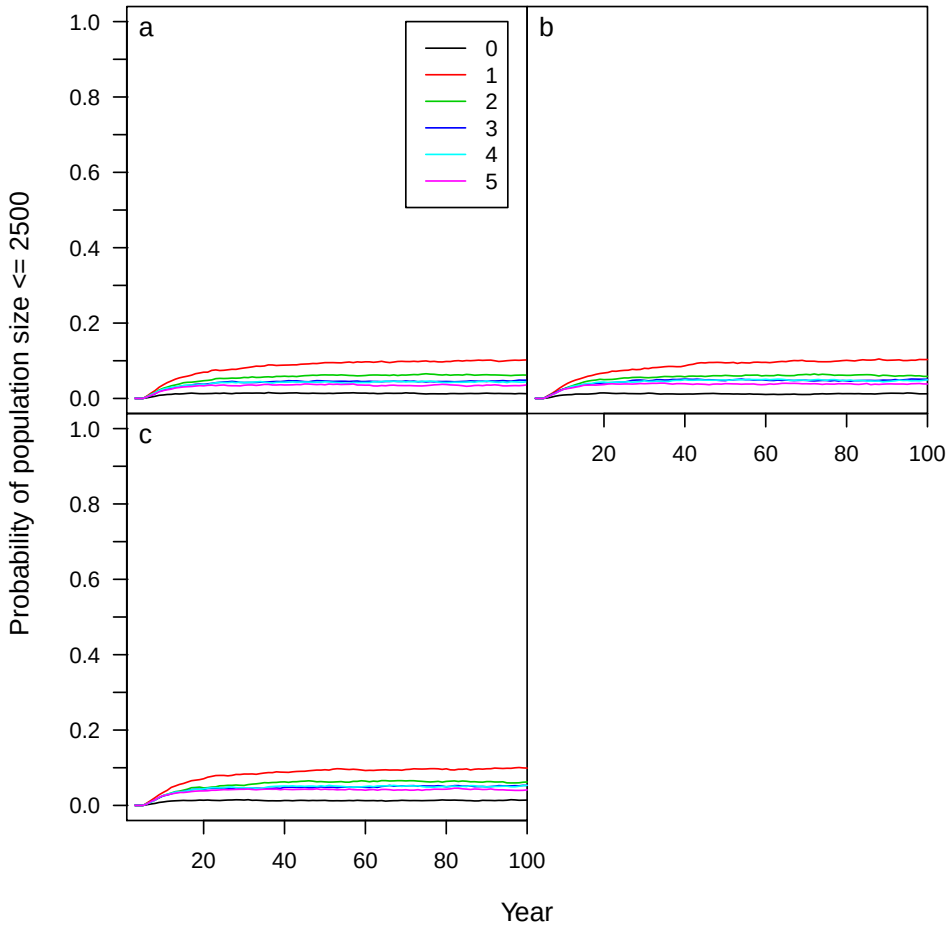

Figure 11. Proportion of 20000 simulations in which population size was $\leq$ 2500 spawners over the course of a 100-year simulation period. We assumed a temporal autocorrelation of 0.5 in juvenile survival rates. Population size was calculated as the sum of the escapements in the previous 3 years. Results are shown for each of three T scenarios (a-c) and 6 control rules (0-5), which are described in the text.

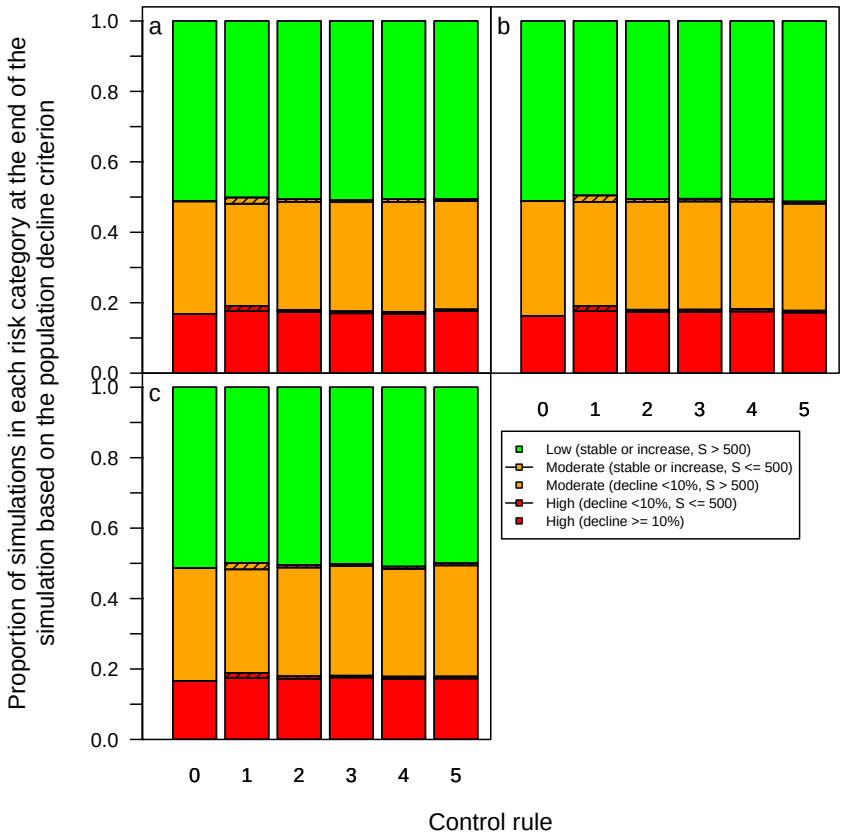

Figure 12. Proportions of 20000 100-year simulations whose final six escapements (S) and population trends met each of three extinction risk categories based on 'population decline' defined by Lindley *et al.* (2007). We assumed no temporal autocorrelation in juvenile survival rates. S$\leq$ 500 indicates that there was at least one escapement during the final six years (two generations) of the simulation that was $\leq$ 500 spawners, while S$>$ 500 indicates that all of the last six escapements were more than 500 spawners. Population trend was calculated as the slope of the linear regression of the log of the final 10 escapements on year (Lindley *et al.*, 2007). We assumed that a slope $<= \log(0.9)$ indicated a decline $\geq$ 10% and that a slope $> \log(0.999)$ indicated a stable or increasing trend. Trend was not calculated if there was one or more zero escapements during the final 10 years so in some cases the total proportions do not sum to 1. However, zero escapements were rare in the simulations shown here so the sum of the proportions was always very close to one. Results are shown for each of three T scenarios (a-c) and 6 control rules (0-5), which are described in the text.

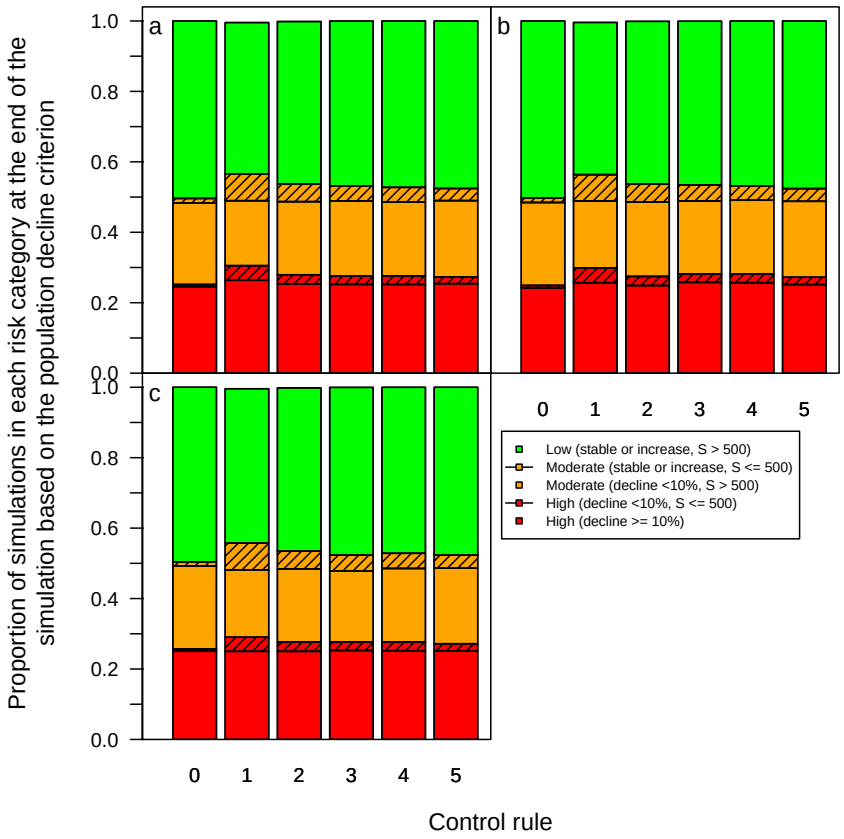

Figure 13. Proportions of 20000 100-year simulations whose final six escapements (S) and population trends met each of three extinction risk categories based on 'population decline' defined by Lindley *et al.* (2007). We assumed a temporal autocorrelation of 0.5 in juvenile survival rates. S$\leq$ 500 indicates that there was at least one escapement during the final six years (two generations) of the simulation that was $\leq$ 500 spawners, while S$>$ 500 indicates that all of the last six escapements were more than 500 spawners. Population trend was calculated as the slope of the linear regression of the log of the final 10 escapements on year (Lindley *et al.*, 2007). We assumed that a slope $<= \log(0.9)$ indicated a decline $\geq$ 10% and that a slope $> \log(0.999)$ indicated a stable or increasing trend. Trend was not calculated if there was one or more zero escapements during the final 10 years so in some cases the total proportions do not sum to 1. However, zero escapements were rare in the simulations shown here so the sum of the proportions was always very close to one. Results are shown for each of three T scenarios (a-c) and 6 control rules (0-5), which are described in the text.

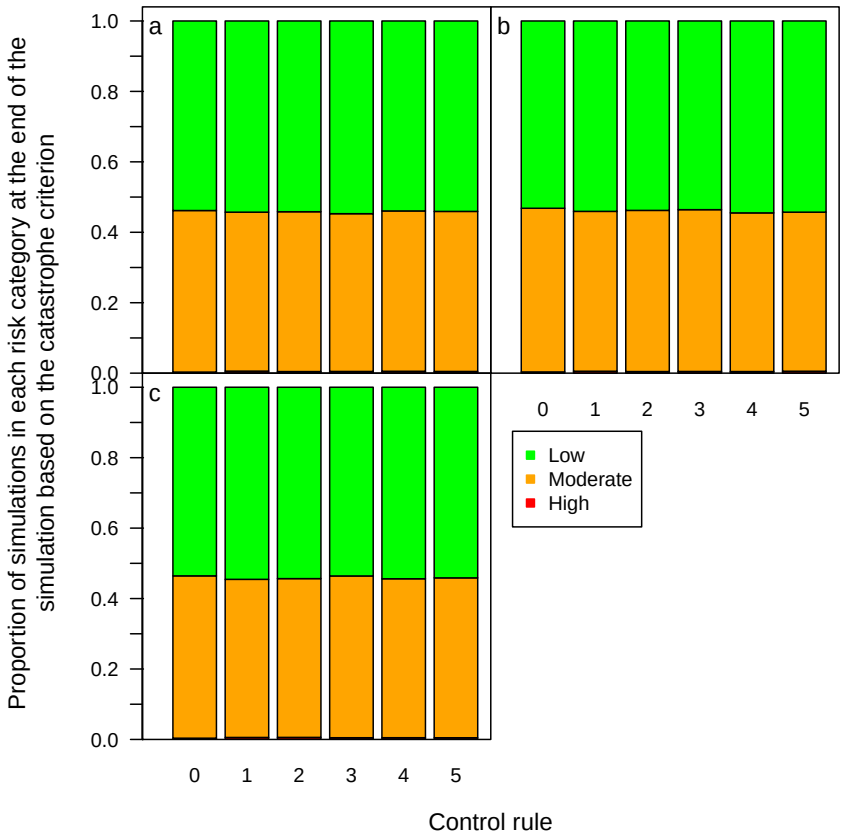

Figure 14. Proportions of 20000 100-year simulations whose population changes during the last 10 years met each of three extinction risk categories based on 'catastrophe' defined by Lindley *et al.* (2007). We assumed no temporal autocorrelation in juvenile survival rates. Population changes were calculated as proportional differences between pairs of population sizes three years (one generation) apart (Lindley *et al.*, 2007). Thus, during the last 10 years of each simulation there were 7 population changes. High risk was assigned to simulations in which there was at least one population decline $\geq 90\%$. Moderate risk was assigned to simulations in which there was at least one population decline $\geq 50\%$, but none $\geq 90\%$. Simulations that did not meet the conditions for high or moderate risk were assigned low risk. Population changes were ignored if the population went extinct. Results are shown for each of three T scenarios (a-c) and 6 control rules (0-5), which are described in the text.

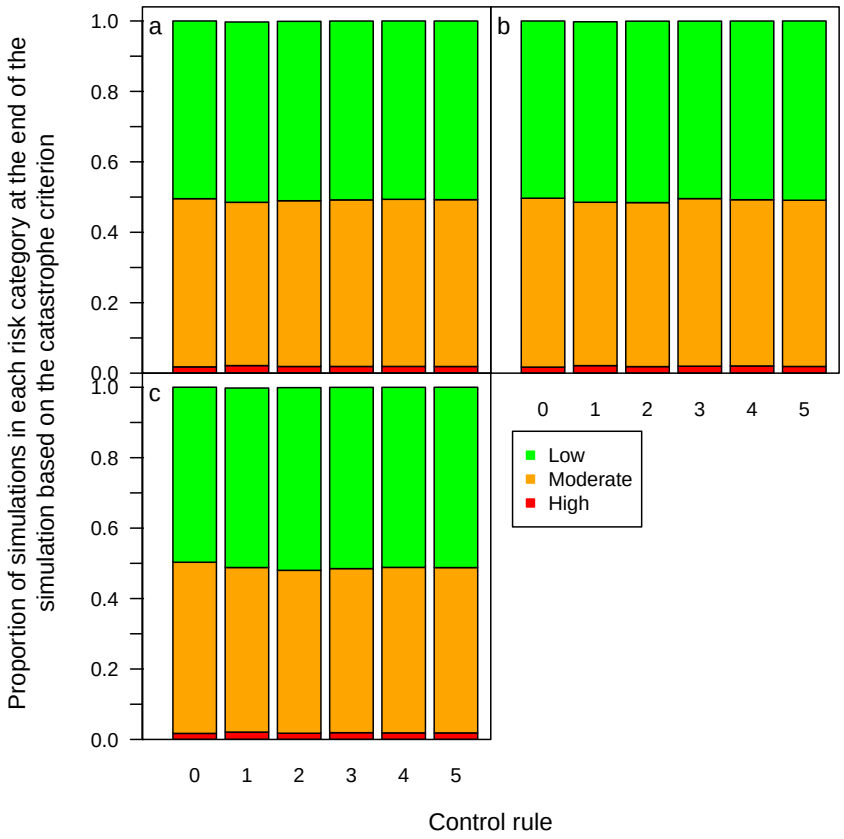

Figure 15. Proportions of 20000 100-year simulations whose population changes during the last 10 years met each of three extinction risk categories based on 'catastrophe' defined by Lindley *et al.* (2007). We assumed a temporal autocorrelation of 0.5 in juvenile survival rates. Population changes were calculated as proportional differences between pairs of population sizes three years (one generation) apart (Lindley *et al.*, 2007). Thus, during the last 10 years of each simulation there were 7 population changes. High risk was assigned to simulations in which there was at least one population decline $\geq 90\%$. Moderate risk was assigned to simulations in which there was at least one population decline $\geq 50\%$, but none $\geq 90\%$. Simulations that did not meet the conditions for high or moderate risk were assigned low risk. Population changes were ignored if the population went extinct. Results are shown for each of three T scenarios (a-c) and 6 control rules (0-5), which are described in the text.

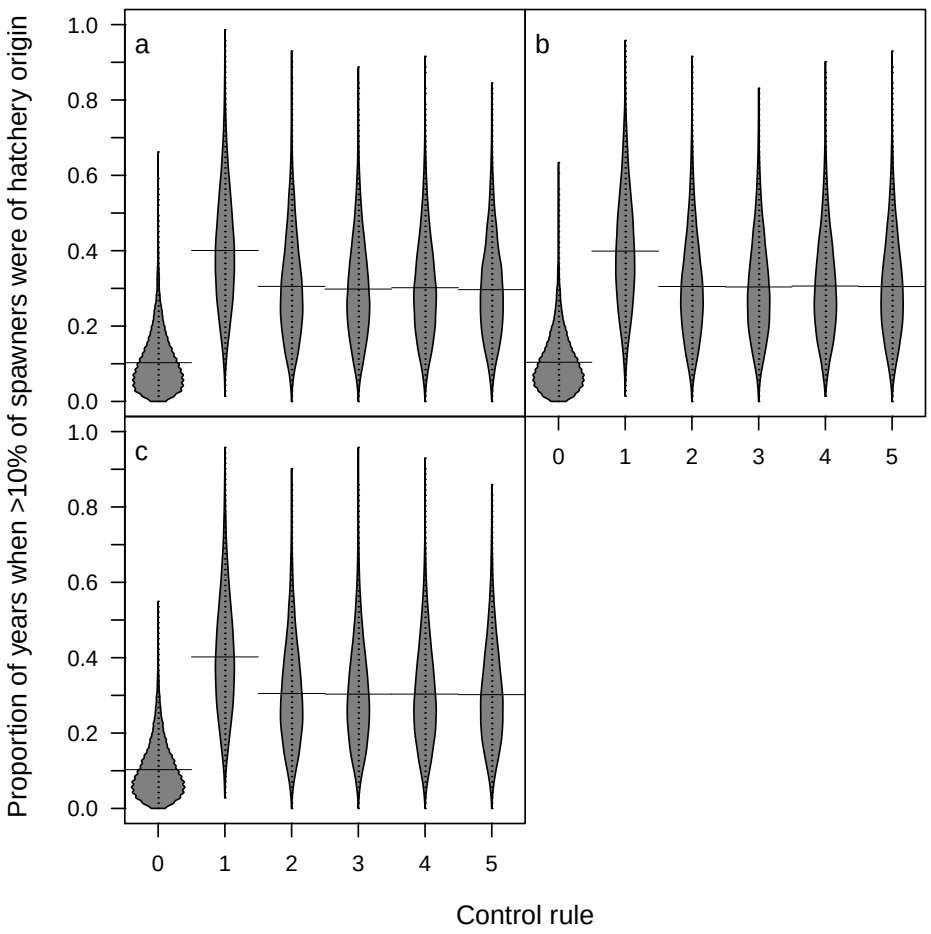

Figure 16. Distribution of the proportion of years during which $> 10\%$ of spawners were of hatchery origin across 20000 simulations. Proportions were calculated based on years 30-100 of 100-year simulations; the first 29 years were not included to ignore transient changes in spawner composition early in the simulation as a result of initial conditions. We assumed no temporal autocorrelation in juvenile survival rates. Results are shown for each of three T scenarios (a-c) and 6 control rules (0-5), which are described in the text. The horizontal lines represent the means of the distributions.

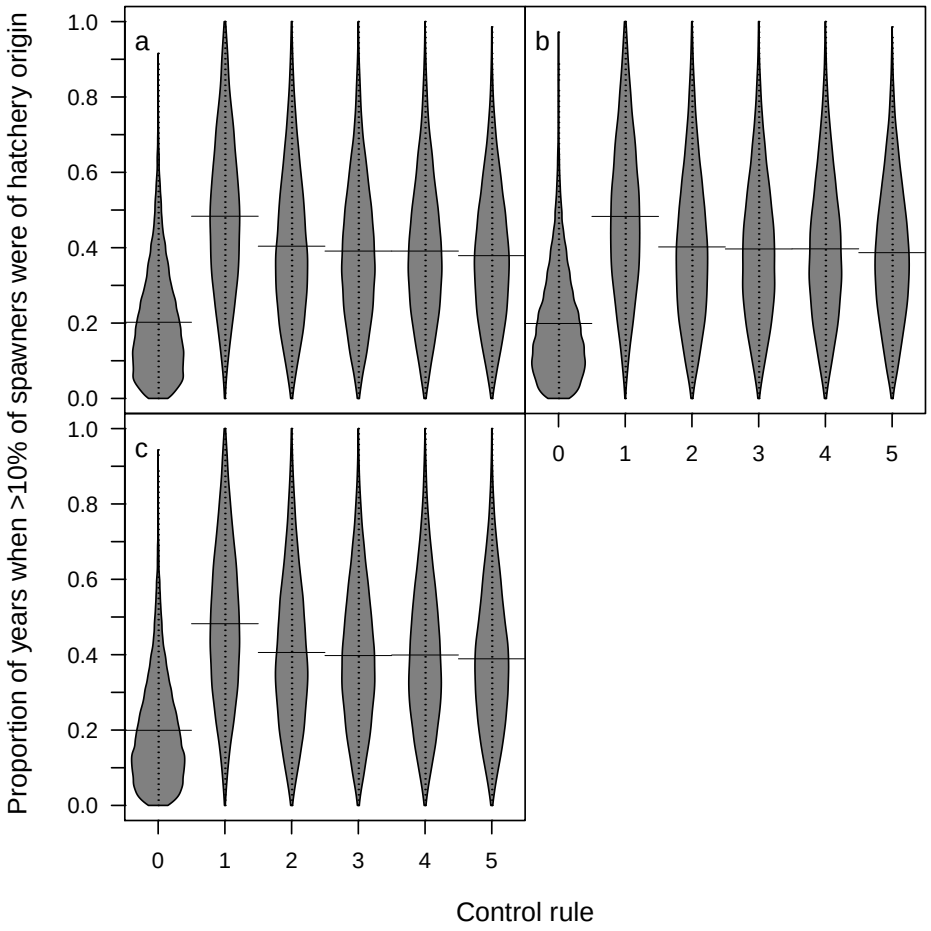

Figure 17. Distribution of the proportion of years during which $> 10\%$ of spawners were of hatchery origin across 20000 simulations. Proportions were calculated based on years 30-100 of 100-year simulations; the first 29 years were not included to ignore transient changes in spawner composition early in the simulation as a result of initial conditions. We assumed a temporal autocorrelation of 0.5 in juvenile survival rates. Results are shown for each of three T scenarios (a-c) and 6 control rules (0-5), which are described in the text. The horizontal lines represent the means of the distributions.

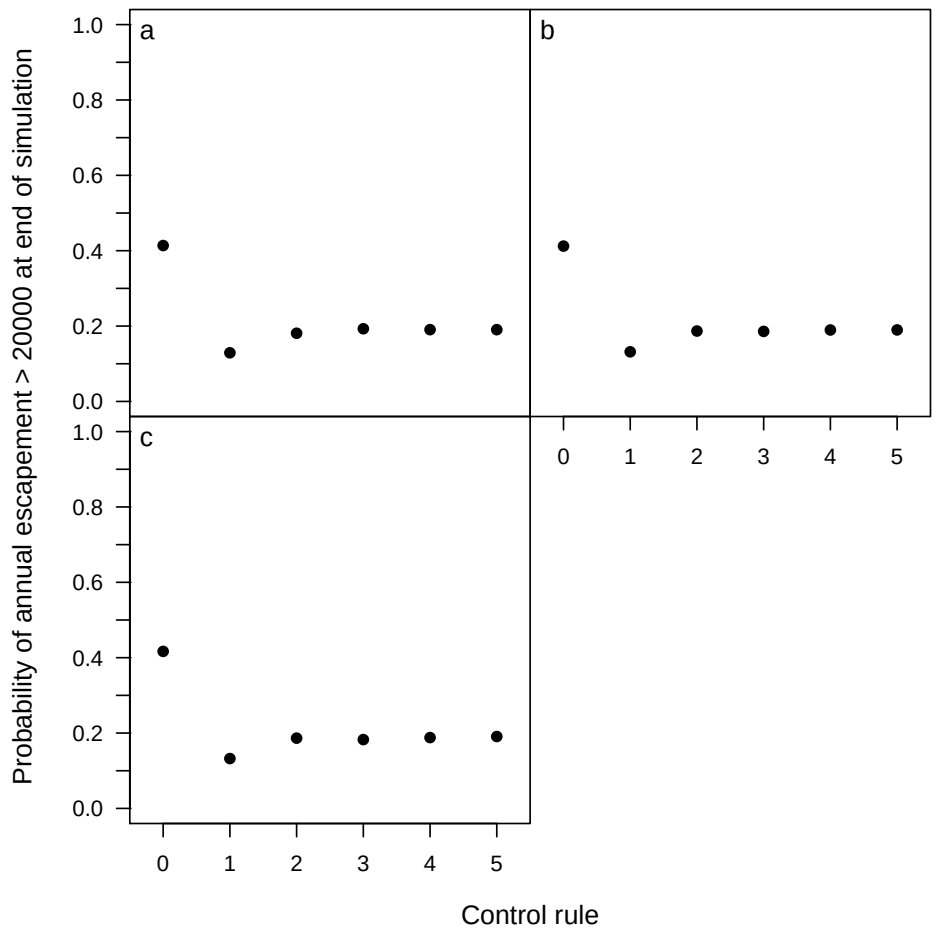

Figure 18. Proportion of 20000 100-year simulations whose final annual escapement was > 20000 spawners. We assumed no temporal autocorrelation in juvenile survival rates. Results are shown for each of three T scenarios (a-c) and 6 control rules (0-5), which are described in the text.

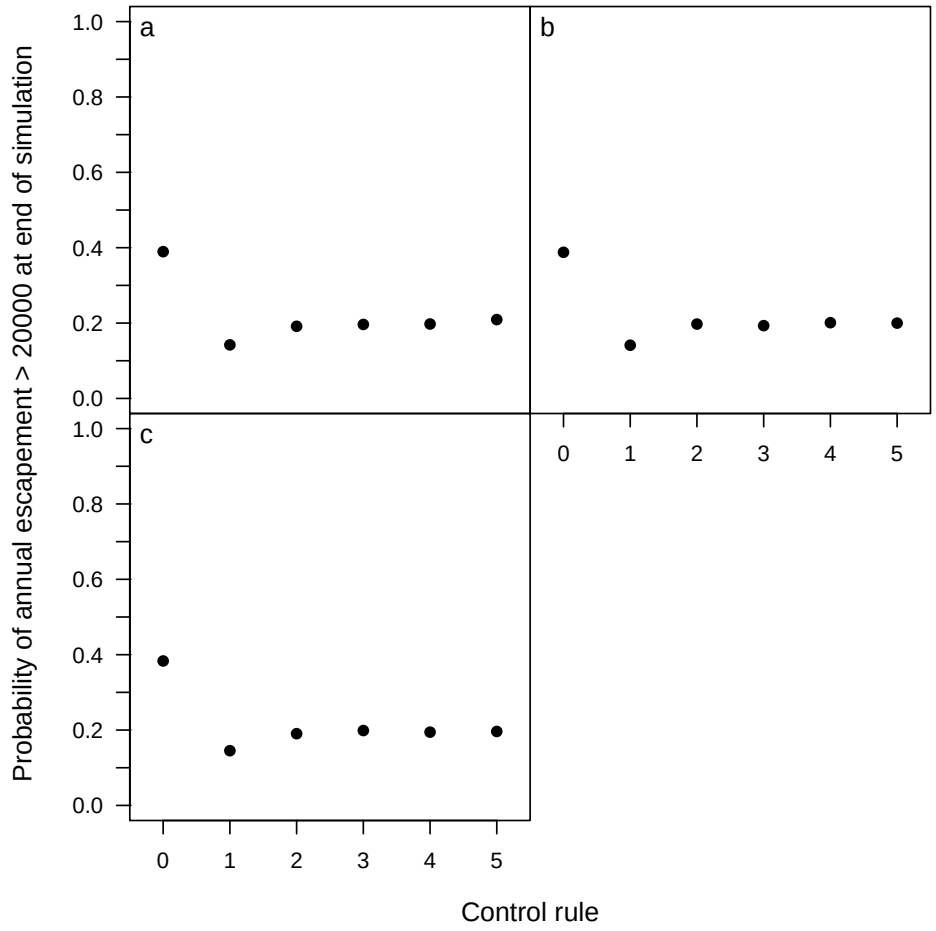

Figure 19. Proportion of 20000 100-year simulations whose final annual escapement was > 20000 spawners. We assumed a temporal autocorrelation of 0.5 in juvenile survival rates. Results are shown for each of three T scenarios (a-c) and 6 control rules (0-5), which are described in the text.

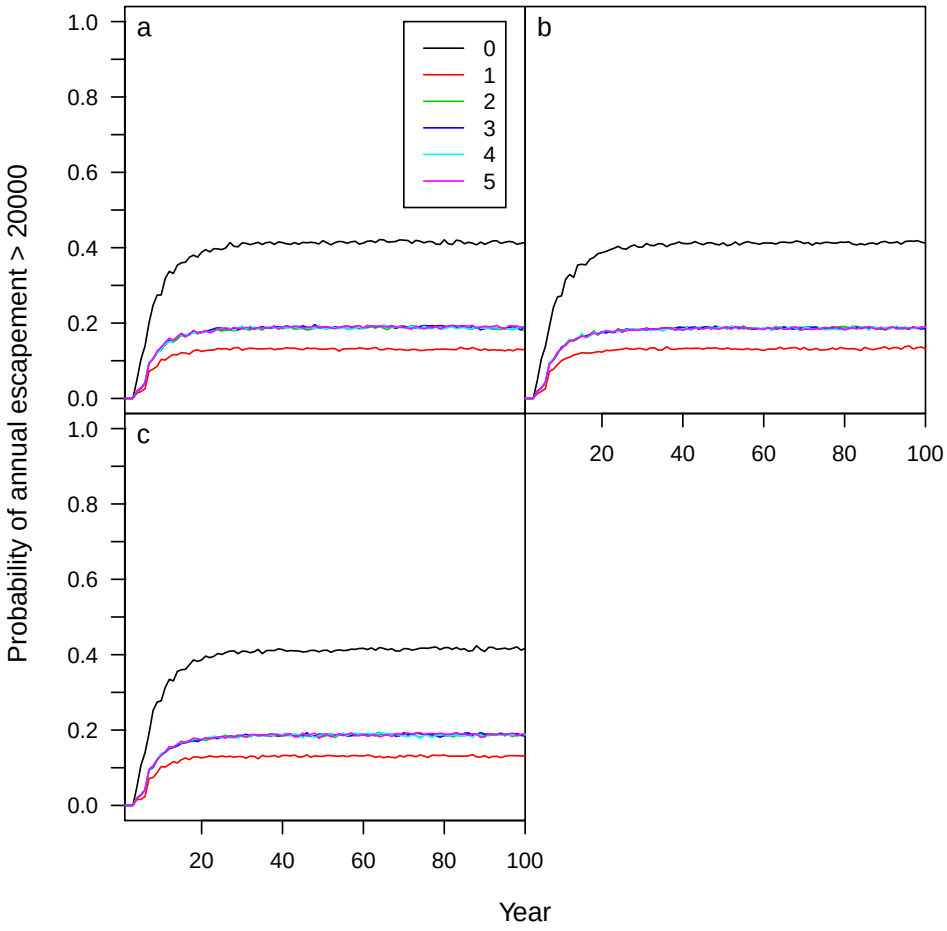

Figure 20. Proportion of 20000 simulations in which annual escapement was $>$ 20000 spawners over the course of a 100-year simulation period. We assumed no temporal autocorrelation in juvenile survival rates. Results are shown for each of three T scenarios (a-c) and 6 control rules (0-5), which are described in the text.

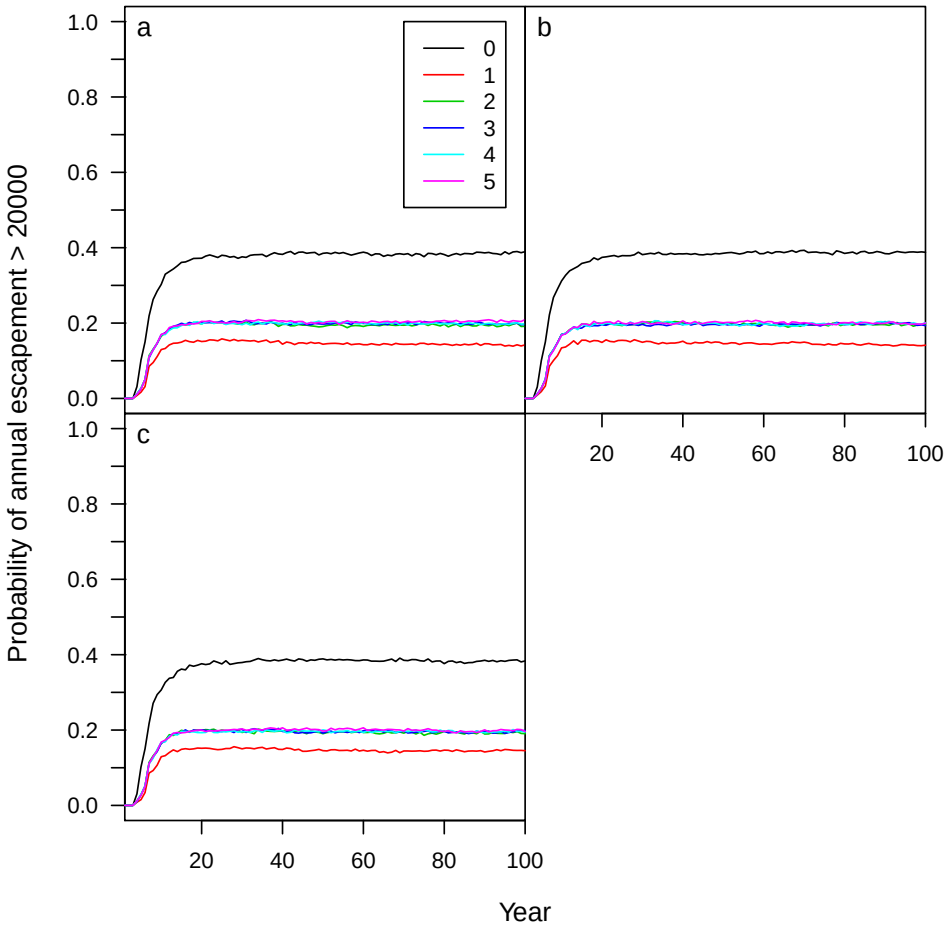

Figure 21. Proportion of 20000 simulations in which annual escapement was $>$ 20000 spawners over the course of a 100-year simulation period. We assumed a temporal autocorrelation of 0.5 in juvenile survival rates. Results are shown for each of three T scenarios (a-c) and 6 control rules (0-5), which are described in the text.

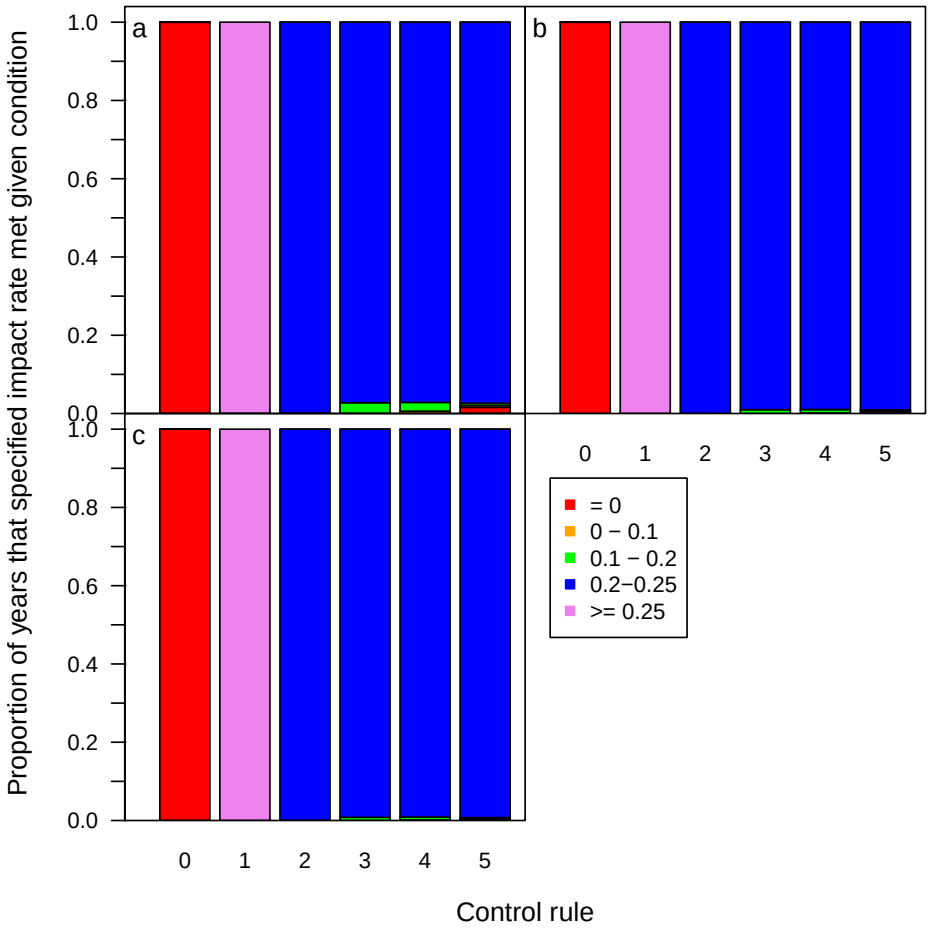

Figure 22. Proportions of annual impact rates specified by the control rule that met each of four categories across 20000 100-year simulations. Impact rates were only calculated for years 30-99 (i.e., 1400000 impact rates are represented by each vertical bar). The first 29 years were not included to ignore transient changes in population size early in the simulation as a result of initial conditions. We assumed no temporal autocorrelation in juvenile survival rates. Results are shown for each of three T scenarios (a-c) and 6 control rules (0-5), which are described in the text.

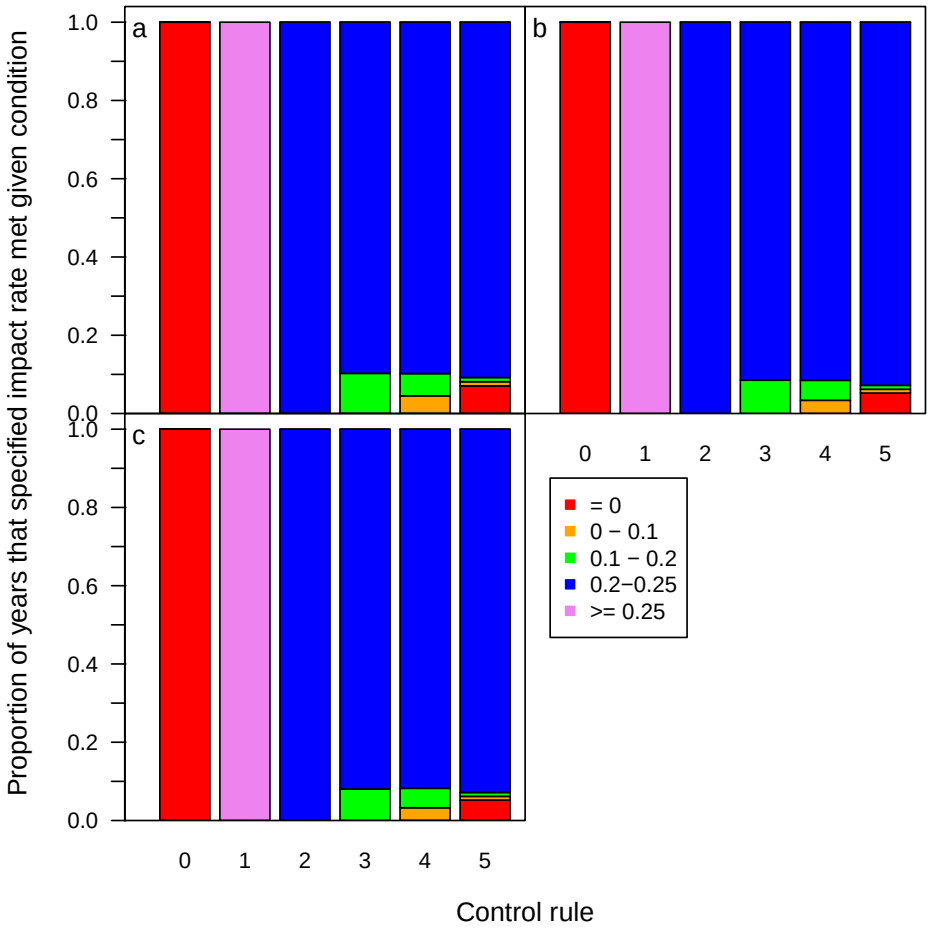

Figure 23. Proportions of annual impact rates specified by the control rule that met each of four categories across 20000 100-year simulations. Impact rates were only calculated for years 30-99 (i.e., 1400000 impact rates are represented by each vertical bar). The first 29 years were not included to ignore transient changes in population size early in the simulation as a result of initial conditions. We assumed a temporal autocorrelation of 0.5 in juvenile survival rates. Results are shown for each of three T scenarios (a-c) and 6 control rules (0-5), which are described in the text.

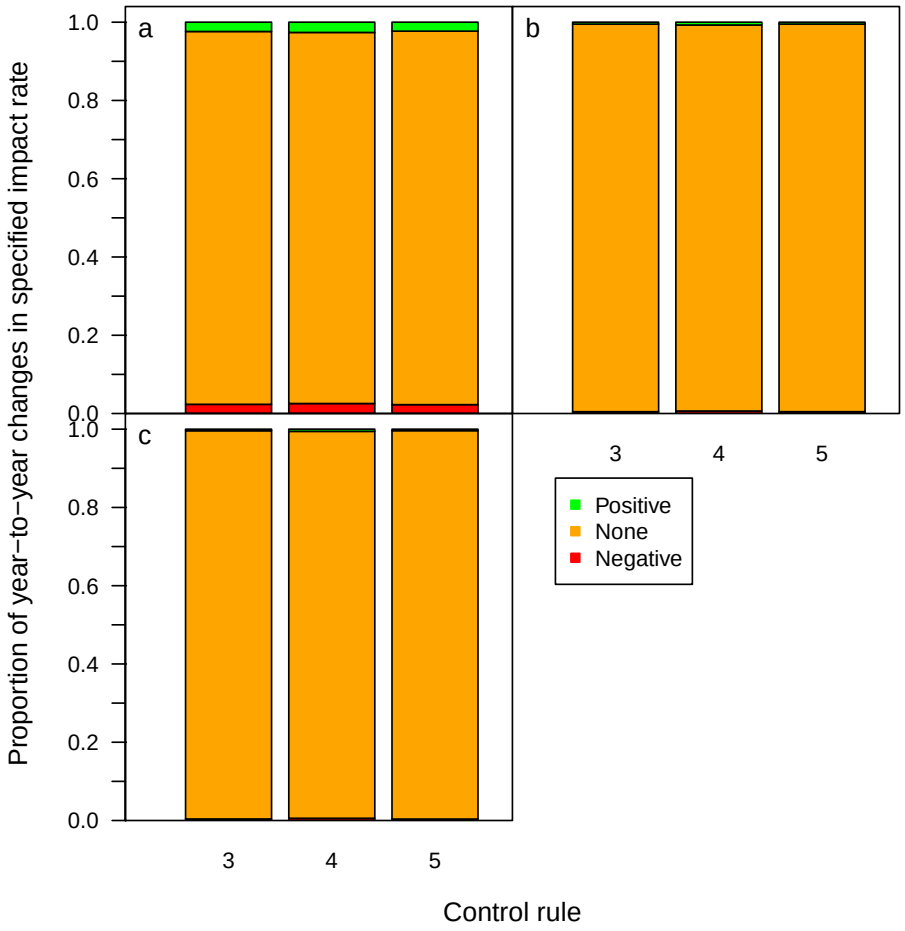

Figure 24. Proportions of year-to-year changes in the impact rate specified by the control rule that fell into each of three categories: negative, no change, and positive. Results are shown for years 30-99 of 20000 100-year simulations. The first 29 years of each simulation were not included to ignore transient changes in dynamics early in the simulation as a result of initial conditions. We assumed no temporal autocorrelation in juvenile survival rates. Results are shown for each of three T scenarios (a-c) and 3 control rules (3-5), which are described in the text.

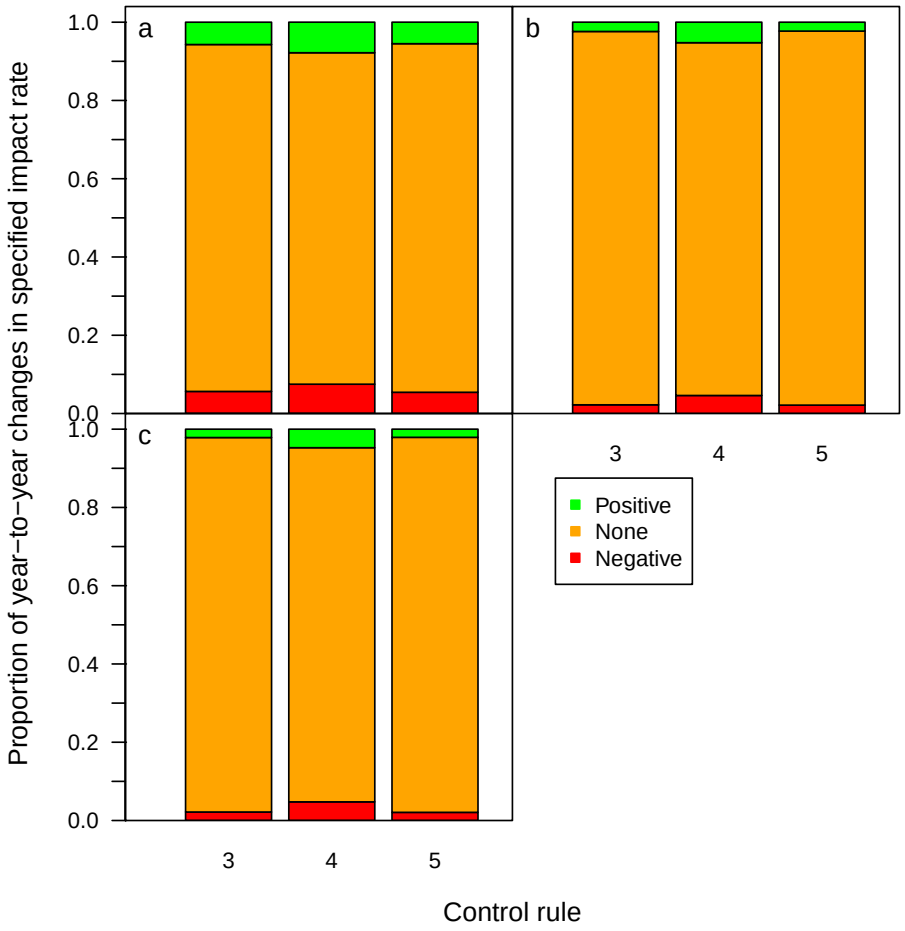

Figure 25. Proportions of year-to-year changes in the impact rate specified by the control rule that fell into each of three categories: negative, no change, and positive. Results are shown for years 30-99 of 20000 100-year simulations. The first 29 years of each simulation were not included to ignore transient changes in dynamics early in the simulation as a result of initial conditions. We assumed a temporal autocorrelation of 0.5 in juvenile survival rates. Results are shown for each of three T scenarios (a-c) and 3 control rules (3-5), which are described in the text.

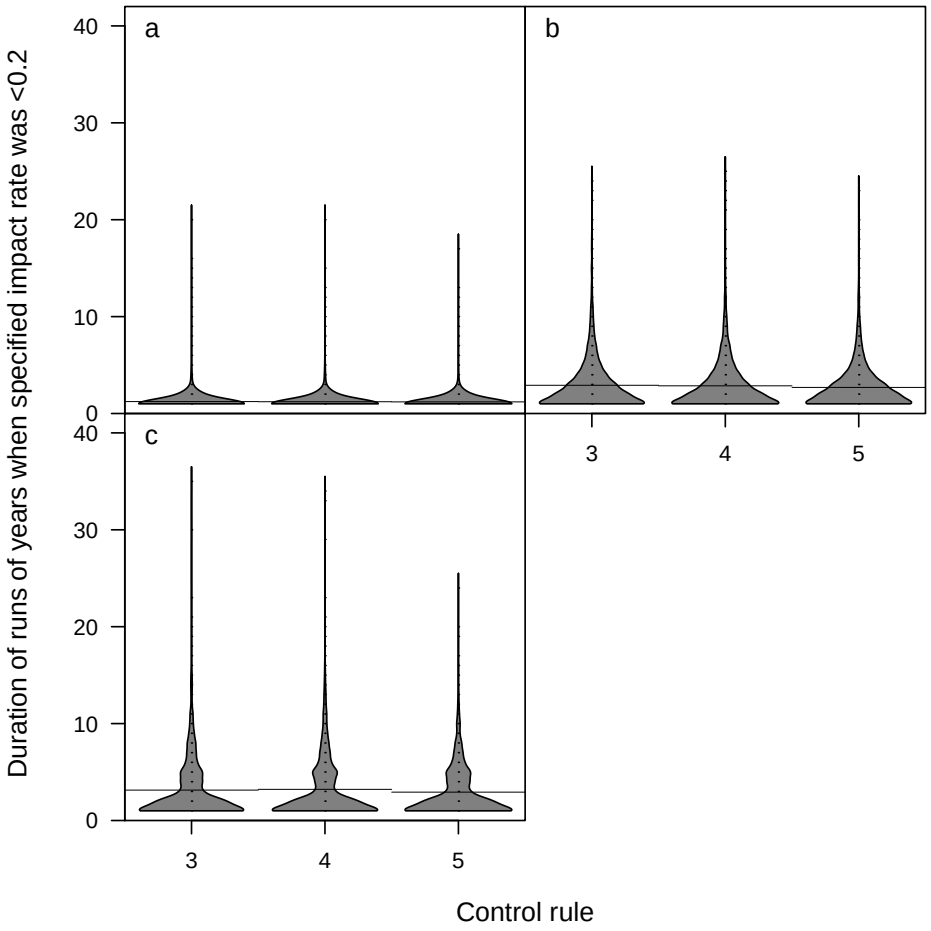

Figure 26. Distribution of lengths of runs of years when the impact rate specified by the control rule was < 0.2. Results are shown for years 30-99 of 20000 100-year simulations. The first 29 years of each simulation were not included to ignore transient changes in dynamics early in the simulation as a result of initial conditions. We assumed no temporal autocorrelation in juvenile survival rates. Results are shown for each of three T scenarios (a-c) and 3 control rules (3-5), which are described in the text. The horizontal lines represent the means of the distributions.

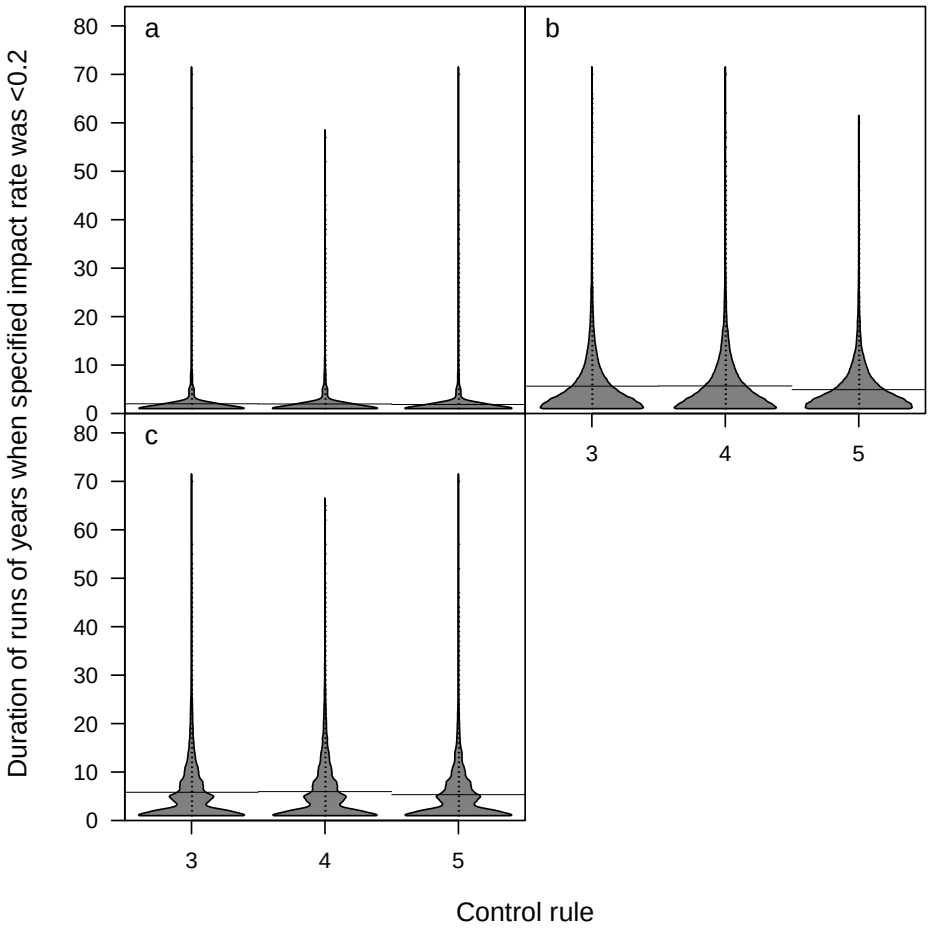

Figure 27. Distribution of lengths of runs of years when the impact rate specified by the control rule was < 0.2. Results are shown for years 30-99 of 20000 100-year simulations. The first 29 years of each simulation were not included to ignore transient changes in dynamics early in the simulation as a result of initial conditions. We assumed a temporal autocorrelation of 0.5 in juvenile survival rates. Results are shown for each of three T scenarios (a-c) and 3 control rules (3-5), which are described in the text. The horizontal lines represent the means of the distributions.

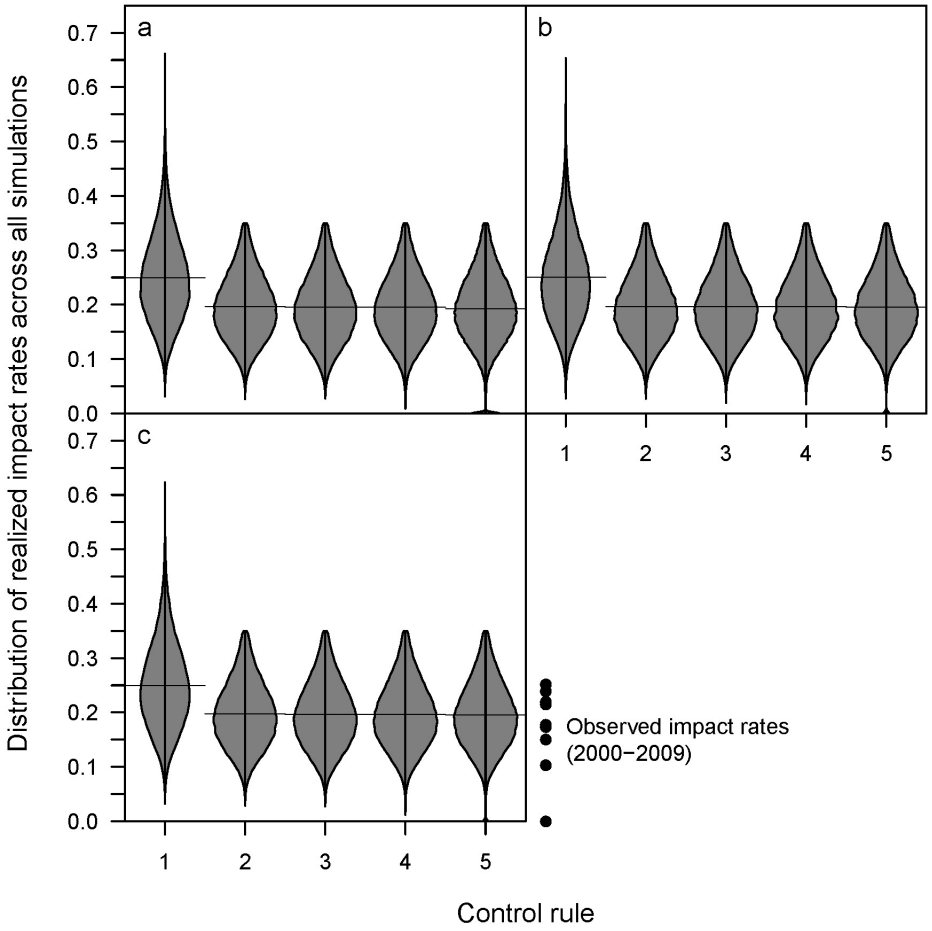

Figure 28. Distribution of realized annual age-3 impact rates south of Point Arena. Each distribution represents 100000 annual realized impact rates sampled from 20000 100-year simulations. The assumed impact rate north of point Arena ($\delta = 0.006$) was a constant addition to the realized impact rates shown here. Only impact rates from years 30-99 were plotted to exclude transient changes early in the simulation as a result of initial conditions. We assumed no temporal autocorrelation in juvenile survival rates. Results are shown for each of three T scenarios (a-c) and 5 control rules (1-5), which are described in the text. The horizontal lines represent the means of the distributions. Actual estimated impact rates for years 2000-2009 are shown as points to the right of the lower panel.

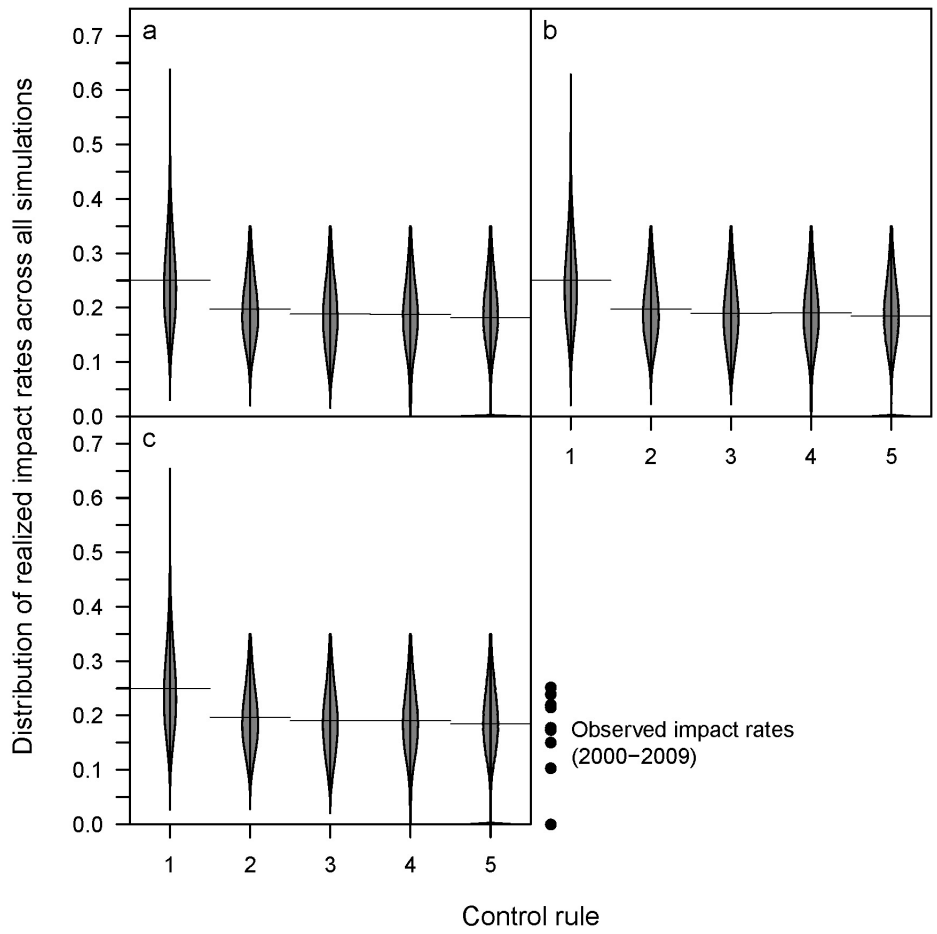

Figure 29. Distribution of realized annual age-3 impact rates south of Point Arena. Each distribution represents 100000 annual realized impact rates sampled from 20000 100-year simulations. The assumed impact rate north of point Arena ($\delta = 0.006$) was a constant addition to the realized impact rates shown here. Only impact rates from years 30-99 were plotted to exclude transient changes early in the simulation as a result of initial conditions. We assumed a temporal autocorrelation of 0.5 in juvenile survival rates. Results are shown for each of three T scenarios (a-c) and 5 control rules (1-5), which are described in the text. The horizontal lines represent the means of the distributions. Actual estimated impact rates for years 2000-2009 are shown as points to the right of the lower panel.

Appendix A Matrix equations

For the purpose of initializing our full stochastic population model we used a simplified deterministic population model represented by the following matrix equations (Leslie, 1945; Caswell, 2000). This simplified model ignored the removal of natural-origin spawners for broodstock and the contribution of hatchery-origin spawners to natural production.

$$\mathbf{N}_{t+1} = \left(\mathbf{X}_{\text{natural}} + \mathbf{Z}_{(\text{natural})t}\right) \mathbf{Y}_t \mathbf{N}_t \tag{A.1}$$

$$\mathbf{H}_{t+1} = \left(\mathbf{X}_{\text{hatchery}} + \mathbf{Z}_{(\text{hatchery})t}\right) \mathbf{Y}_t \mathbf{H}_t \tag{A.2}$$

$\mathbf{X}_{\text{natural}} =$

$$\begin{Bmatrix}
0 & 0 & 0 & 0 & 0 & 0 & 0 & 0 & 0 & 0 & 0 \\
0.5n_2\left[1-m_{(\text{male})2}\right] & 0 & 0 & 0 & 0 & 0 & 0 & 0 & 0 & 0 & 0 \\
0 & n_3\left[1-m_{(\text{male})3}\right] & 0 & 0 & 0 & 0 & 0 & 0 & 0 & 0 & 0 \\
0.5n_2m_{(\text{male})2} & 0 & 0 & 0 & 0 & 0 & 0 & 0 & 0 & 0 & 0 \\
0 & n_3m_{(\text{male})3} & 0 & 0 & 0 & 0 & 0 & 0 & 0 & 0 & 0 \\
0 & 0 & n_4 & 0 & 0 & 0 & 0 & 0 & 0 & 0 & 0 \\
0.5n_2\left[1-m_{(\text{female})2}\right] & 0 & 0 & 0 & 0 & 0 & 0 & 0 & 0 & 0 & 0 \\
0 & 0 & 0 & 0 & 0 & 0 & n_3\left[1-m_{(\text{female})3}\right] & 0 & 0 & 0 & 0 \\
0.5n_2m_{(\text{female})2} & 0 & 0 & 0 & 0 & 0 & 0 & 0 & 0 & 0 & 0 \\
0 & 0 & 0 & 0 & 0 & 0 & n_3m_{(\text{female})3} & 0 & 0 & 0 & 0 \\
0 & 0 & 0 & 0 & 0 & 0 & 0 & n_4 & 0 & 0 & 0
\end{Bmatrix} \tag{A.3}$$

$\mathbf{X}_{\text{hatchery}} =$

$$\begin{Bmatrix}
0 & 0 & 0 & 0 & 0 & 0 & 0 & 0 & 0 & 0 & 0 \\
0.5hn_2\left[1-m_{(\text{male})2}\right] & 0 & 0 & 0 & 0 & 0 & 0 & 0 & 0 & 0 & 0 \\
0 & n_3\left[1-m_{(\text{male})3}\right] & 0 & 0 & 0 & 0 & 0 & 0 & 0 & 0 & 0 \\
0.5hn_2m_{(\text{male})2} & 0 & 0 & 0 & 0 & 0 & 0 & 0 & 0 & 0 & 0 \\
0 & n_3m_{(\text{male})3} & 0 & 0 & 0 & 0 & 0 & 0 & 0 & 0 & 0 \\
0 & 0 & n_4 & 0 & 0 & 0 & 0 & 0 & 0 & 0 & 0 \\
0.5hn_2\left[1-m_{(\text{female})2}\right] & 0 & 0 & 0 & 0 & 0 & 0 & 0 & 0 & 0 & 0 \\
0 & 0 & 0 & 0 & 0 & 0 & n_3\left[1-m_{(\text{female})3}\right] & 0 & 0 & 0 & 0 \\
0.5hn_2m_{(\text{female})2} & 0 & 0 & 0 & 0 & 0 & 0 & 0 & 0 & 0 & 0 \\
0 & 0 & 0 & 0 & 0 & 0 & n_3m_{(\text{female})3} & 0 & 0 & 0 & 0 \\
0 & 0 & 0 & 0 & 0 & 0 & 0 & n_4 & 0 & 0 & 0
\end{Bmatrix} \tag{A.4}$$

$$\mathbf{Y}_t = \begin{Bmatrix} 1 & 0 & 0 & 0 & 0 & 0 & 0 & 0 & 0 & 0 & 0 \\ 0 & 1-i_{3t} & 0 & 0 & 0 & 0 & 0 & 0 & 0 & 0 & 0 \\ 0 & 0 & 1-i_{4t} & 0 & 0 & 0 & 0 & 0 & 0 & 0 & 0 \\ 0 & 0 & 0 & 1 & 0 & 0 & 0 & 0 & 0 & 0 & 0 \\ 0 & 0 & 0 & 0 & 1 & 0 & 0 & 0 & 0 & 0 & 0 \\ 0 & 0 & 0 & 0 & 0 & 1 & 0 & 0 & 0 & 0 & 0 \\ 0 & 0 & 0 & 0 & 0 & 0 & 1-i_{3t} & 0 & 0 & 0 & 0 \\ 0 & 0 & 0 & 0 & 0 & 0 & 0 & 1-i_{4t} & 0 & 0 & 0 \\ 0 & 0 & 0 & 0 & 0 & 0 & 0 & 0 & 1 & 0 & 0 \\ 0 & 0 & 0 & 0 & 0 & 0 & 0 & 0 & 0 & 1 & 0 \\ 0 & 0 & 0 & 0 & 0 & 0 & 0 & 0 & 0 & 0 & 1 \end{Bmatrix} \tag{A.5}$$

$$\mathbf{Z}_{(\text{natural})t} = \begin{Bmatrix} 0 & 0 & 0 & 0 & 0 & 0 & 0 & 0 & r_t & r_t & r_t \\ 0 & 0 & 0 & 0 & 0 & 0 & 0 & 0 & 0 & 0 & 0 \\ 0 & 0 & 0 & 0 & 0 & 0 & 0 & 0 & 0 & 0 & 0 \\ 0 & 0 & 0 & 0 & 0 & 0 & 0 & 0 & 0 & 0 & 0 \\ 0 & 0 & 0 & 0 & 0 & 0 & 0 & 0 & 0 & 0 & 0 \\ 0 & 0 & 0 & 0 & 0 & 0 & 0 & 0 & 0 & 0 & 0 \\ 0 & 0 & 0 & 0 & 0 & 0 & 0 & 0 & 0 & 0 & 0 \\ 0 & 0 & 0 & 0 & 0 & 0 & 0 & 0 & 0 & 0 & 0 \\ 0 & 0 & 0 & 0 & 0 & 0 & 0 & 0 & 0 & 0 & 0 \\ 0 & 0 & 0 & 0 & 0 & 0 & 0 & 0 & 0 & 0 & 0 \\ 0 & 0 & 0 & 0 & 0 & 0 & 0 & 0 & 0 & 0 & 0 \end{Bmatrix} \tag{A.6}$$

$$\mathbf{Z}_{(\text{hatchery})t} = \begin{Bmatrix} \lambda_t^{\text{P}} & 0 & 0 & 0 & 0 & 0 & 0 & 0 & 0 & 0 & 0 \\ 0 & 0 & 0 & 0 & 0 & 0 & 0 & 0 & 0 & 0 & 0 \\ 0 & 0 & 0 & 0 & 0 & 0 & 0 & 0 & 0 & 0 & 0 \\ 0 & 0 & 0 & 0 & 0 & 0 & 0 & 0 & 0 & 0 & 0 \\ 0 & 0 & 0 & 0 & 0 & 0 & 0 & 0 & 0 & 0 & 0 \\ 0 & 0 & 0 & 0 & 0 & 0 & 0 & 0 & 0 & 0 & 0 \\ 0 & 0 & 0 & 0 & 0 & 0 & 0 & 0 & 0 & 0 & 0 \\ 0 & 0 & 0 & 0 & 0 & 0 & 0 & 0 & 0 & 0 & 0 \\ 0 & 0 & 0 & 0 & 0 & 0 & 0 & 0 & 0 & 0 & 0 \\ 0 & 0 & 0 & 0 & 0 & 0 & 0 & 0 & 0 & 0 & 0 \\ 0 & 0 & 0 & 0 & 0 & 0 & 0 & 0 & 0 & 0 & 0 \end{Bmatrix} \tag{A.7}$$

$$\mathbf{N}_t = \begin{bmatrix} J_t \\ O_{(\text{natural})(\text{male})3t} \\ O_{(\text{natural})(\text{male})4t} \\ S_{(\text{natural})(\text{male})2t} \\ S_{(\text{natural})(\text{male})3t} \\ S_{(\text{natural})(\text{male})4t} \\ O_{(\text{natural})(\text{female})3t} \\ O_{(\text{natural})(\text{female})4t} \\ S_{(\text{natural})(\text{female})2t} \\ S_{(\text{natural})(\text{female})3t} \\ S_{(\text{natural})(\text{female})4t} \end{bmatrix} \tag{A.8}$$

$$\mathbf{H}_t = \begin{bmatrix} P_t \\ O_{(\text{hatchery})(\text{male})3t} \\ O_{(\text{hatchery})(\text{male})4t} \\ S_{(\text{hatchery})(\text{male})2t} \\ S_{(\text{hatchery})(\text{male})3t} \\ S_{(\text{hatchery})(\text{male})4t} \\ O_{(\text{hatchery})(\text{female})3t} \\ O_{(\text{hatchery})(\text{female})4t} \\ S_{(\text{hatchery})(\text{female})2t} \\ S_{(\text{hatchery})(\text{female})3t} \\ S_{(\text{hatchery})(\text{female})4t} \end{bmatrix} \tag{A.9}$$

where λ_t^{P} is the rate of change in the number of hatchery-origin pre-smolts released into the river from time t to time $t+1$.

Acknowledgements

We thank D. Lawson, S. Lindley and W. Satterthwaite for insightful comments and discussion. We would like to thank Livingston Stone National Fish Hatchery for collecting the hatchery data used in our study and K. Niemela (U.S. Fish and Wildlife Service) for making these data available to us. We would like to thank A. Grover and D. Killam for providing carcass survey data that included the numbers of fish taken by the hatchery as broodstock. A remark by A. M. Starfield helped crystallize the idea that the historical time series of escapement can be thought of as one realization of a stochastic process.

References

Beamish, R. J. & Mahnken, C. (2001). A critical size and period hypothesis to explain natural regulation of salmon abundance and the linkage to climate and climate change. *Prog. Oceanogr.*, **49**, 423–437.

Beverton, R. J. H. & Holt, S. J. (1957). *On the dynamics of exploited fish populations*, *Volume 11*. *Fish and Fisheries*. Chapman and Hall, London.

Botsford, L. W. & Brittnacher, J. G. (1998). Viability of Sacramento River winter-run chinook salmon. *Conserv. Biol.*, **12**, 65–79.

Butterworth, D. S. & Punt, A. E. (1999). Experiences in the evaluation and implementation of management procedures. *ICES J. Mar. Sci.*, **56**, 985–998.

Caswell, H. (2000). *Matrix population models: construction, analysis, and interpretation*. Sinauer Associates, Sunderland, Massachusetts.

CDFG (California Department of Fish and Game) (1989). Description of winter Chinook ocean harvest model 1. Ocean Salmon Project Report, CDFG, Sacramento, California.

Cooke, J. G. (1999). Improvement of fishery-management advice through simulation testing of harvest algorithms. *ICES J. Mar. Sci.*, **56**, 797–810.

Friedland, K. D. (1998). Ocean climate influences on critical Atlantic salmon (*Salmo salar*) life history events. *Can. J. Fish. Aquat. Sci.*, **55(Suppl. 1)**, 119–130.

Hilborn, R. (1979). Comparison of fisheries control systems that utilize catch and effort data. *J. Fish. Res. Board Can.*, **36**, 1477–1489.

Kell, L. T., O'Brien, C. M., Smith, M. T., Stokes, T. K. & Rackham, B. D. (1999). An evaluation of management procedures for implementing a precautionary approach in the ICES context for North Sea plaice (*Pleuronectes platessa* L.). *ICES J. Mar. Sci.*, **56**, 834–845.

Lande, R. (1993). Risks of population extinction from demographic and environmental stochasticity and random catastrophes. *Am. Nat.*, **142**, 911–927.

Leslie, P. H. (1945). On the use of matrices in certain population mathematics. *Biometrika*, **33**, 183–212.

Lindley, S. T., Grimes, C. B., Mohr, M. S., Peterson, W., Stein, J., Anderson, J. T., Botsford, L. W., Bottom, D. L., Busack, C. A., Collier, T. K., Ferguson, J., Garza, J. C., Grover, A. M., Hankin, D. G., Kope, R. G., Lawson, P. W., Low, A., MacFarlane, R. B., Moore, K., Palmer-Zwahlen, M., Schwing, F. B., Smith, J., Tracy, C., Webb, R., Wells, B. K. & Williams, T. H. (2009). What caused the Sacramento River fall Chinook stock collapse? NOAA Technical Memorandum NOAA-TM-NMFS-SWFSC-447, National Marine Fisheries Service, Santa Cruz, CA, USA.

Lindley, S. T., Schick, R. S., Mora, E., Adams, P. B., Anderson, J. J., Greene, S., Hanson, C., May, B. P., McEwan, D. R., MacFarlane, R. B., Swanson, C. & Williams, J. G. (2007). Framework for assessing viability of threatened and endangered Chinook salmon and steelhead in the Sacramento-San Joaquin Basin. *San F. Estuar. Wat. Sci.*, **5**, http://repositories.cdlib.org/jmie/sfews/vol5/iss1/art4.

McKenzie, E. (1985). An autoregressive process for beta random variables. *Manage. Sci.*, **31**, 988–997.

Milner-Gulland, E. J., Shea, K., Possingham, H., Coulson, T. & Wilcox, C. (2001). Competing harvesting strategies in a simulated population under uncertainty. *Anim. Conserv.*, **4**, 157–167.

Newman, K. B., Buckland, S. T., Lindley, S. T., Thomas, L. & Fernández, C. (2006). Hidden process models for animal population dynamics. *Ecol. Appl.*, **16**, 74–86.

Newman, K. B. & Lindley, S. T. (2006). Accounting for demographic and environmental stochasticity, observation error, and parameter uncertainty in fish population dynamics models. *N. Am. J. Fish. Manage.*, **26**, 685–701.

NMFS (1997). NMFS proposed recovery plan for the Sacramento River winter-run chinook salmon. Technical report, National Marine Fisheries Service, Southwest Region, Long Beach, California.

NMFS (National Marine Fisheries Service) (2004). Authorization of ocean salmon fisheries developed in accordance with the Pacific Coast Salmon Plan and proposed protective measures during the 2004 through 2009 fishing seasons as it affects Sacramento River winter Chinook salmon. Endangered Species Act Section 7 Consultation Supplemental Biological Opinion, NMFS, Long Beach, California.

NMFS (National Marine Fisheries Service) (2010). Authorization of ocean salmon fisheries pursuant to the Pacific Coast Salmon Fishery Management Plan and additional protective measures as it affects Sacramento River winter Chinook salmon. Endangered Species Act Section 7 Consultation Biological Opinion, NMFS, Long Beach, California. Available from http://swr.nmfs.noaa.gov/pdf/Final_Harvest_BiOp_043010.pdf (accessed February 2012).

O'Farrell, M. R., Allen, S. & Mohr, M. S. (2011a). The winter-run harvest model (WRHM). Draft report, NMFS, Santa Cruz, California. Available from http://www.pcouncil.org/wp-content/uploads/C1a_ATT3_WRHM_NOV2011BB.pdf (accessed February 2012).

O'Farrell, M. R., Mohr, M. S. & Grover, A. M. (2011b). Sacramento River winter Chinook cohort reconstruction: analysis of ocean fishery impacts. Draft report, NMFS, Santa Cruz, California. Available from http://www.pcouncil.org/wp-content/uploads/C1a_ATT2_SACTO_COHORT_NOV2011BB.pdf (accessed February 2012).

Punt, A. E. & Donovan, G. P. (2007). Developing management procedures that are robust to uncertainty: lessons from the International Whaling Commission. *ICES J. Mar. Sci.*, **64**, 603–612.

Rademeyer, R. A., Plagányi, É. E. & Butterworth, D. S. (2007). Tips and tricks in designing management procedures. *ICES J. Mar. Sci.*, **64**, 618–625.

USFWS (United States Fish and Wildlife Service) (2010). *Upper Sacramento River winter Chinook salmon carcass survey 2009 annual report*. USFWS, Red Bluff, California. Available from http://www.fws.gov/redbluff/getReport.aspx?id=89 (accessed February 2012).

Wells, B. K., Grimes, C. B. & Waldvogel, J. B. (2007). Quantifying the effects of wind, upwelling, curl, sea surface temperature and sea level height on growth and maturation of a California Chinook salmon (*Oncorhynchus tshawytscha*) population. *Fish. Oceanogr.*, **16**, 363–382.

Winship, A. J., O'Farrell, M. R. & Mohr, M. S. (2011). Estimation of parameters for management strategy evaluation for Sacramento River winter-run Chinook salmon. Draft report, NMFS, NOAA, Santa Cruz, CA.

Addendum

Following completion of this report, the NMFS Southwest Region requested that the Southwest Fisheries Science Center (SWFSC) evaluate a new SRWC management framework for ocean salmon fisheries. Upon receiving this request, the SWFSC performed a MSE on this framework and the other management frameworks evaluated in the original report. This addendum reports the results from this new MSE.

The new Southwest Region management framework consists of two components. The first component specifies that the yearly season and size-limit minimum restrictions first specified in the NMFS 2004 Biological Opinion (NMFS, 2004) remain in place, regardless of population status:

> *The recreational season between Point Arena and Pigeon Point shall open no earlier than the first Saturday in April and close no later than the second Sunday in November; the recreational season between Pigeon Point and the U.S./Mexico Border shall open no earlier than the first Saturday in April and close no later than the first Sunday in October. The minimum size limit shall be at least 20 inches total length.*
>
> *The commercial season between Point Arena and the U.S./Mexico border shall open no earlier than May 1 and close no later than September 30, with the exception of an October season conducted Monday through Friday between Point Reyes and Point San Pedro, which shall end no later than October 15. The minimum size limit shall be at least 26 inches total length.*

The second component of the framework specifies that in addition, during periods of low abundance, the allowable age-3 impact rate on SRWC south of Point Arena is limited according to a control rule (Fig. A.3a) that is a function of the most recent 3-year geometric mean number of spawners ($T = 3$ scenario). If the 3-year geometric mean number of spawners is less than 500, the maximum allowable age-3 impact rate is zero. For a geometric mean number of spawners between 500 and 4000, the maximum allowable age-3 impact rate is a linearly increasing function from 0.10 to 0.20. For a geometric mean number of spawners between 4000 and 5000, the maximum allowable age-3 impact rate is 0.20. At mean spawner levels greater than 5000, the age-3 impact rate is not specifically limited.

For purposes of performing a MSE on the Southwest Region management framework, we combined the two framework components into a single control rule "SWR" as shown in Fig. A.3b by setting the maximum allowable age-3 impact rate to 0.20 for mean spawner levels greater than 5000. The control rule SWR is a reasonable approximation of this management framework given that estimates of the age-3 impact rate derived from SRWC cohort reconstructions (O'Farrell *et al.*, 2011b) under the season and size-limit restrictions of the first component have averaged 0.20. As

with all other simulations in this report, the realized impact rate (which would be estimated postseason) was not necessarily equal to the maximum allowable impact rate, but was specified by a distribution informed by expected deviations between the maximum allowable and realized impact rates.

The results of the MSE are presented in Figs A.4-A.29. The numbering sequence used for these figures is the same as that used in the main report; e.g., Fig. 5 in the main report corresponds with Fig. A.5 in this addendum. While the SWR framework results are only presented for the $T = 3$ scenario, the results from all other management frameworks and T scenarios are presented in these figures for comparison.

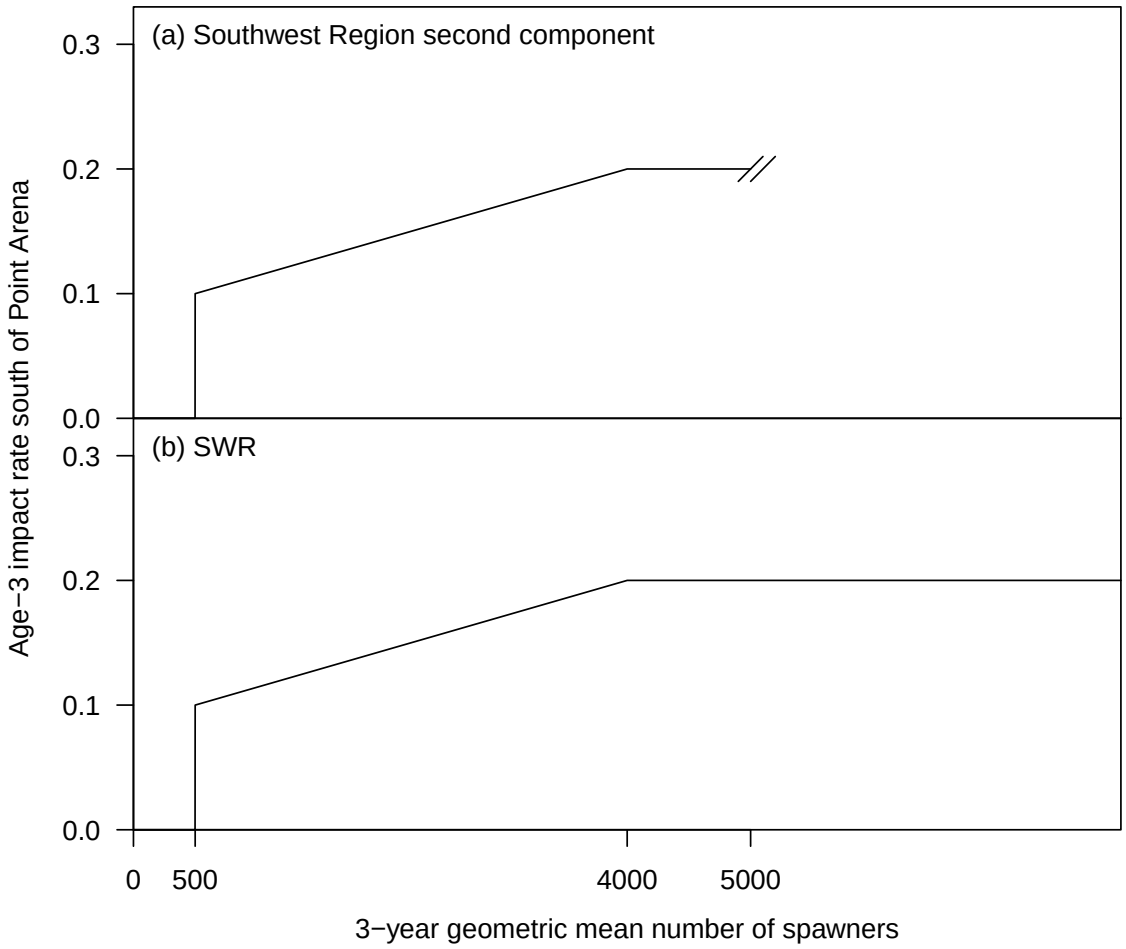

Figure A.3. Age-3 impact rate control rules. The number of spawners refers to the total male and female, natural- and hatchery-origin, spawner escapement as estimated through the carcass survey ($\bar{N}_{tT}^{\text{spawn}}$). Southwest Region management framework second component (a): above 5,000 spawners the impact rate is not specifically limited. The MSE was performed using the "SWR" control rule shown in panel (b), in which the maximum allowable impact rate above 5,000 spawners was 0.2 (see text).

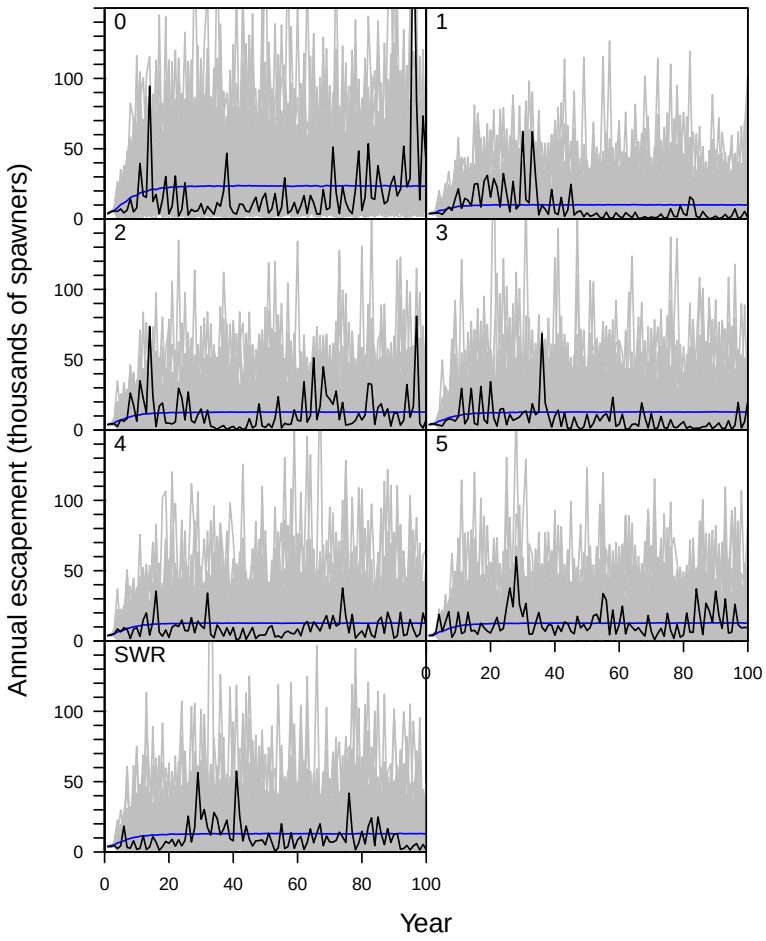

Figure A.4. Simulated time-series of escapement over a 100-year period. The 3-year geometric mean estimated escapement was input to the control rule in any given year (Scenario b) and there was no temporal autocorrelation in juvenile survival rates. Panels 0-5 and 'SWR' represent control rules 0-5 and 'SWR' as described in the text. The grey lines represent 100 simulations for each control rule. The blue lines represent the mean escapement in each year across 20000 simulations. The black lines represent a single, randomly chosen simulation.

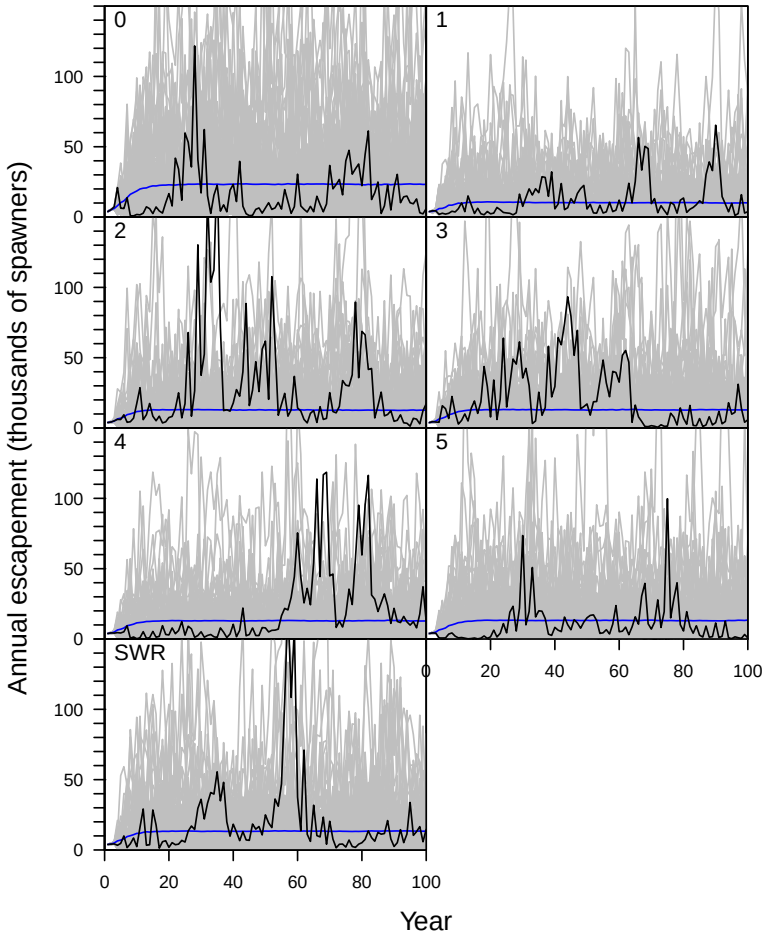

Figure A.5. Simulated time-series of escapement over a 100-year period. The 3-year geometric mean estimated escapement was input to the control rule in any given year (Scenario b) and we assumed a temporal autocorrelation of 0.5 in juvenile survival rates. Panels 0-5 and 'SWR' represent control rules 0-5 and 'SWR' as described in the text. The grey lines represent 100 simulations for each control rule. The blue lines represent the mean escapement in each year across 20000 simulations. The black lines represent a single, randomly chosen simulation.

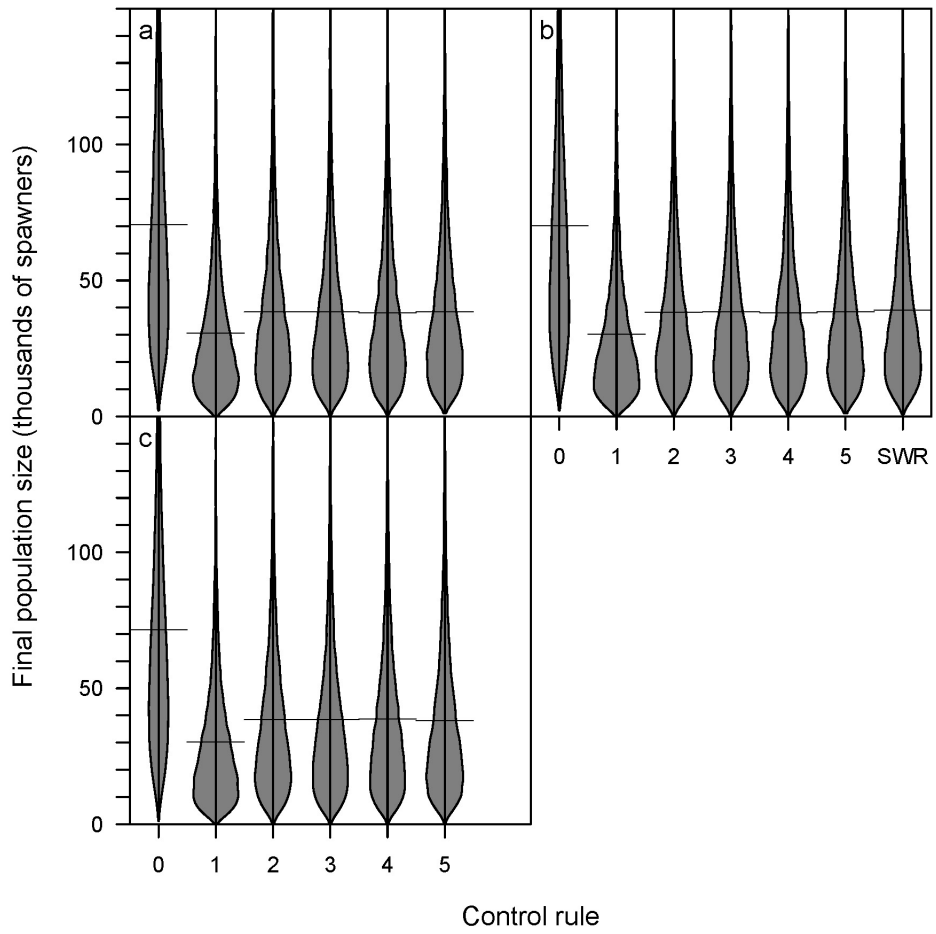

Figure A.6. Distribution of final population size in 20000 100-year simulations for each of three T scenarios (a-c) and 7 control rules (0-5 and 'SWR') assuming no temporal autocorrelation in juvenile survival rates. Final population size was calculated as the sum of escapements during the last three years of a simulation. Scenarios and control rules are described in the text. The horizontal lines represent the means of the distributions.

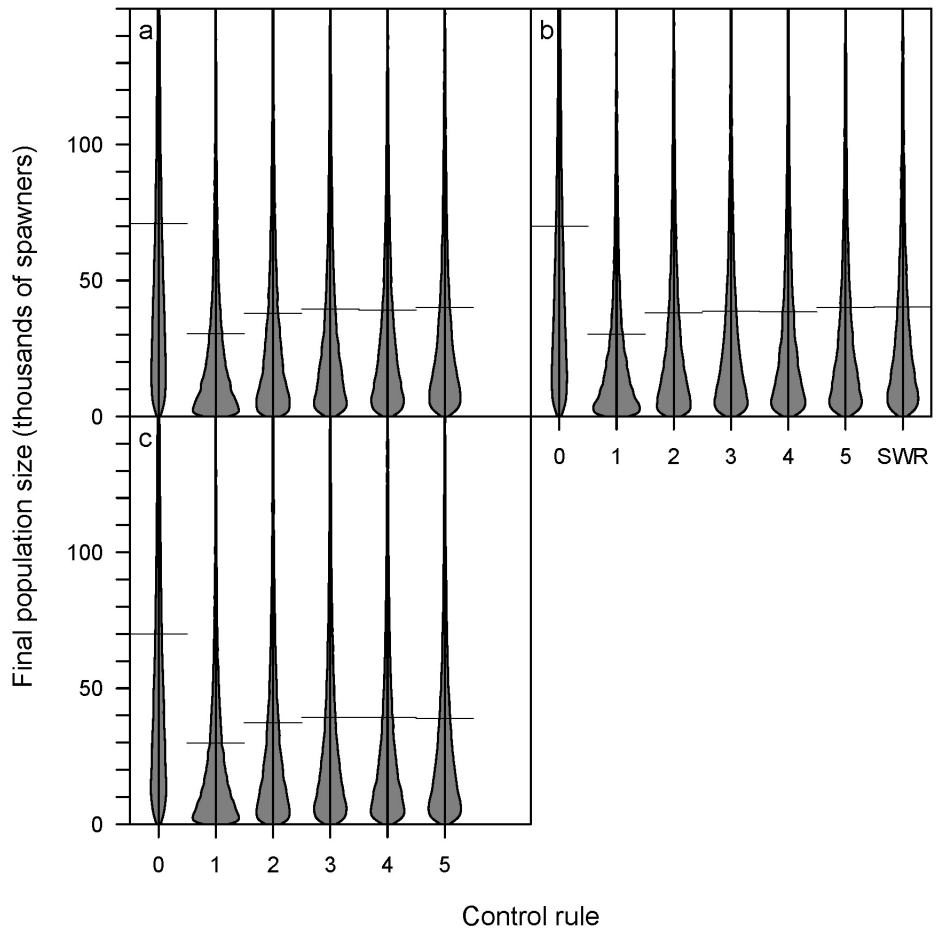

Figure A.7. Distribution of final population size in 20000 100-year simulations for each of three T scenarios (a-c) and 7 control rules (0-5 and 'SWR') assuming a temporal autocorrelation of 0.5 in juvenile survival rates. Final population size was calculated as the sum of escapements during the last three years of a simulation. Scenarios and control rules are described in the text. The horizontal lines represent the means of the distributions.

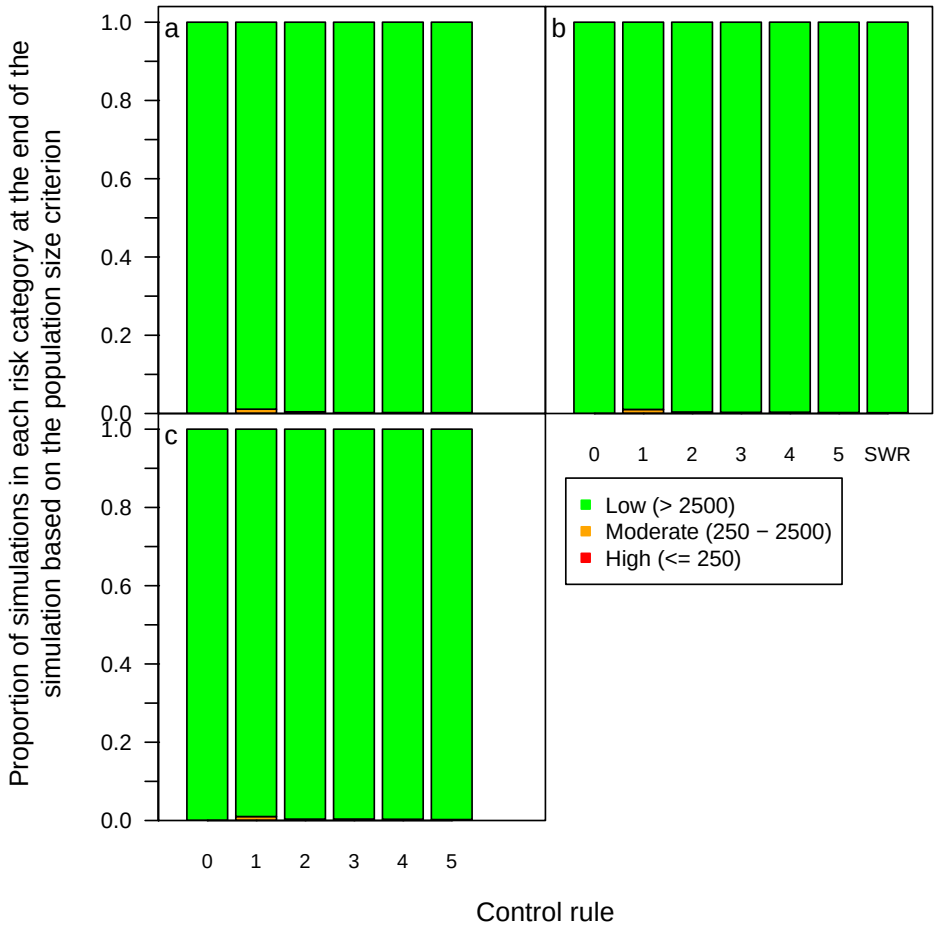

Figure A.8. Proportions of 20000 100-year simulations whose final population sizes met each of three extinction risk categories based on 'population size' defined by Lindley *et al.* (2007). We assumed no temporal autocorrelation in juvenile survival rates. Final population size was calculated as the sum of escapements during the last three years of a simulation. Results are shown for each of three T scenarios (a-c) and 7 control rules (0-5 and 'SWR'), which are described in the text.

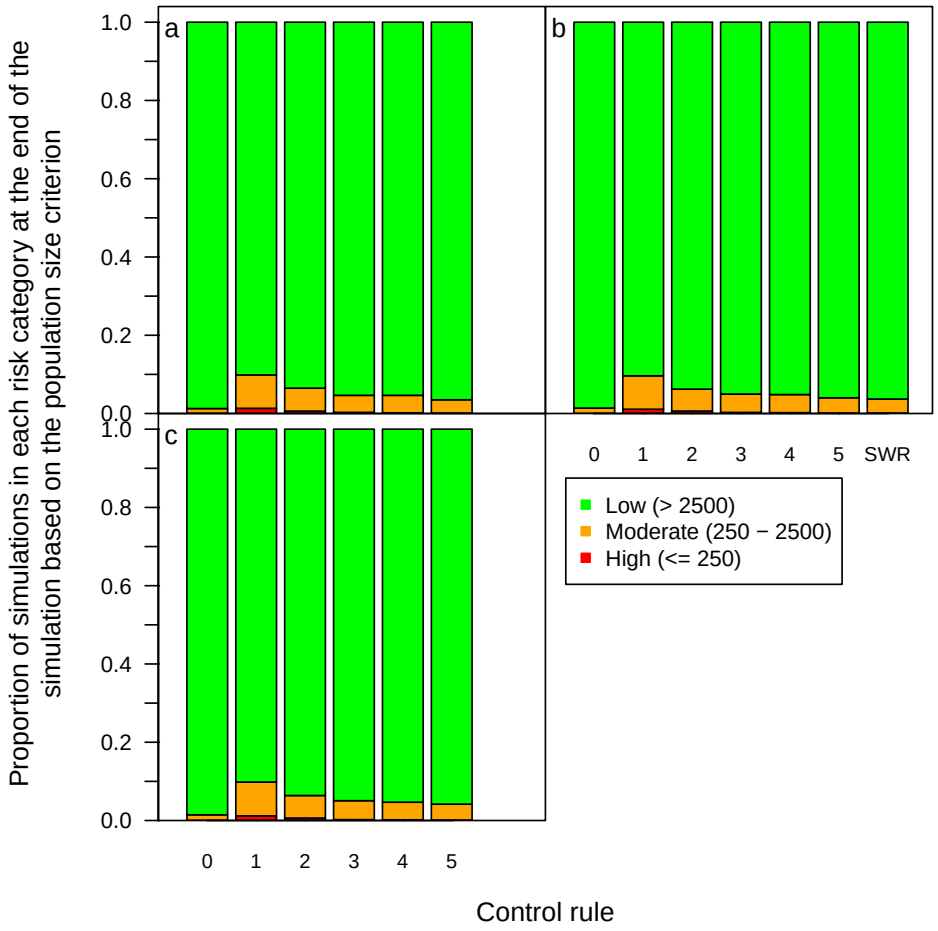

Figure A.9. Proportions of 20000 100-year simulations whose final population sizes met each of three extinction risk categories based on 'population size' defined by Lindley *et al.* (2007). We assumed a temporal autocorrelation of 0.5 in juvenile survival rates. Final population size was calculated as the sum of escapements during the last three years of a simulation. Results are shown for each of three T scenarios (a-c) and 7 control rules (0-5 and 'SWR'), which are described in the text.

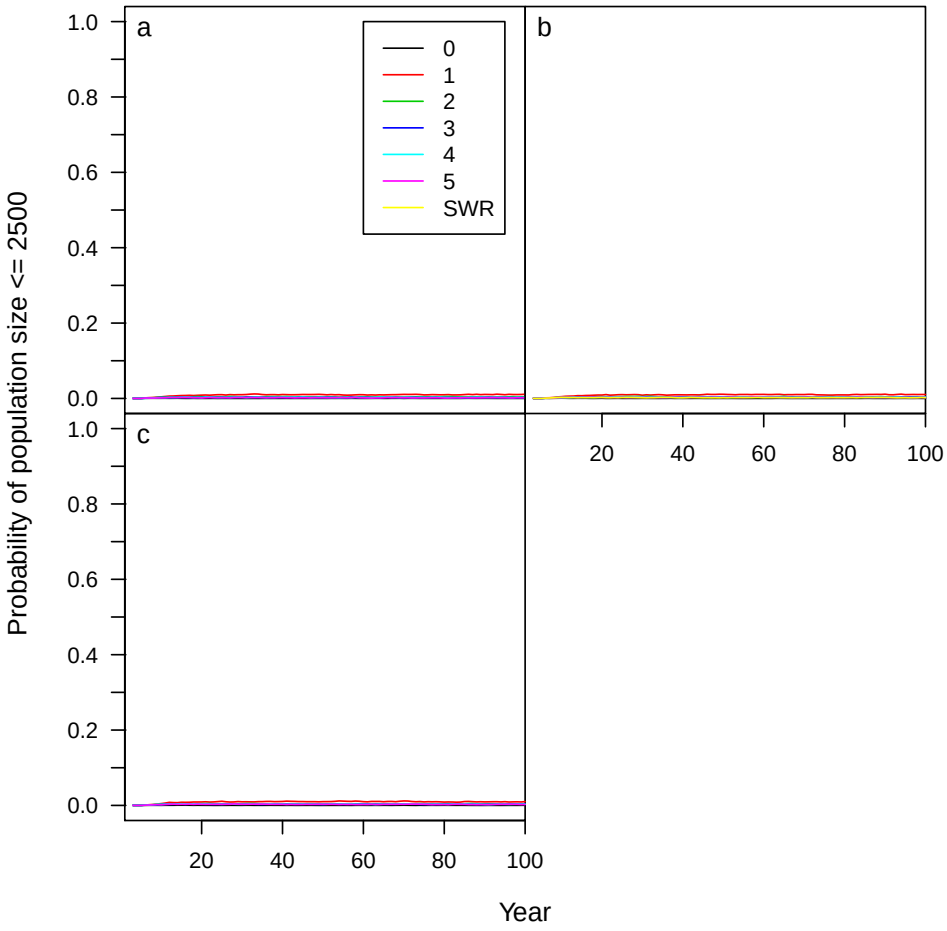

Figure A.10. Proportion of 20000 simulations in which population size was $\leq$ 2500 spawners over the course of a 100-year simulation period. We assumed no temporal autocorrelation in juvenile survival rates. Population size was calculated as the sum of the escapements in the previous 3 years. Results are shown for each of three T scenarios (a-c) and 7 control rules (0-5 and 'SWR'), which are described in the text.

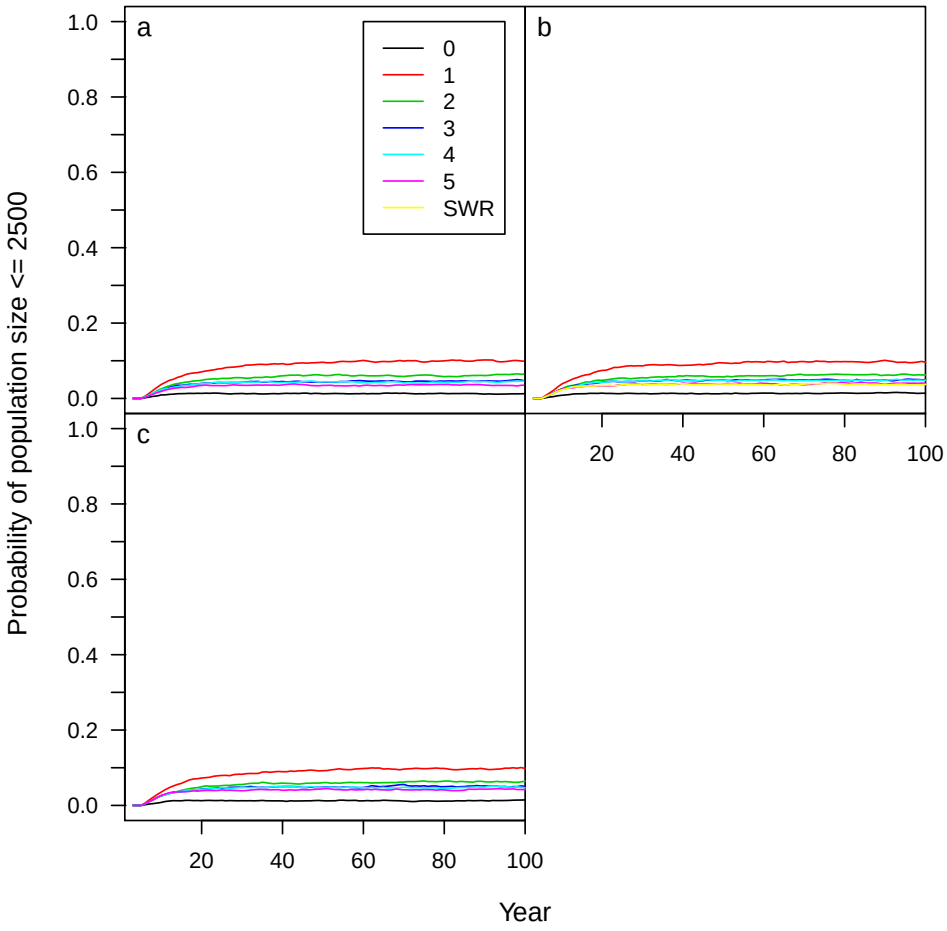

Figure A.11. Proportion of 20000 simulations in which population size was $\leq$ 2500 spawners over the course of a 100-year simulation period. We assumed a temporal autocorrelation of 0.5 in juvenile survival rates. Population size was calculated as the sum of the escapements in the previous 3 years. Results are shown for each of three T scenarios (a-c) and 7 control rules (0-5 and 'SWR'), which are described in the text.

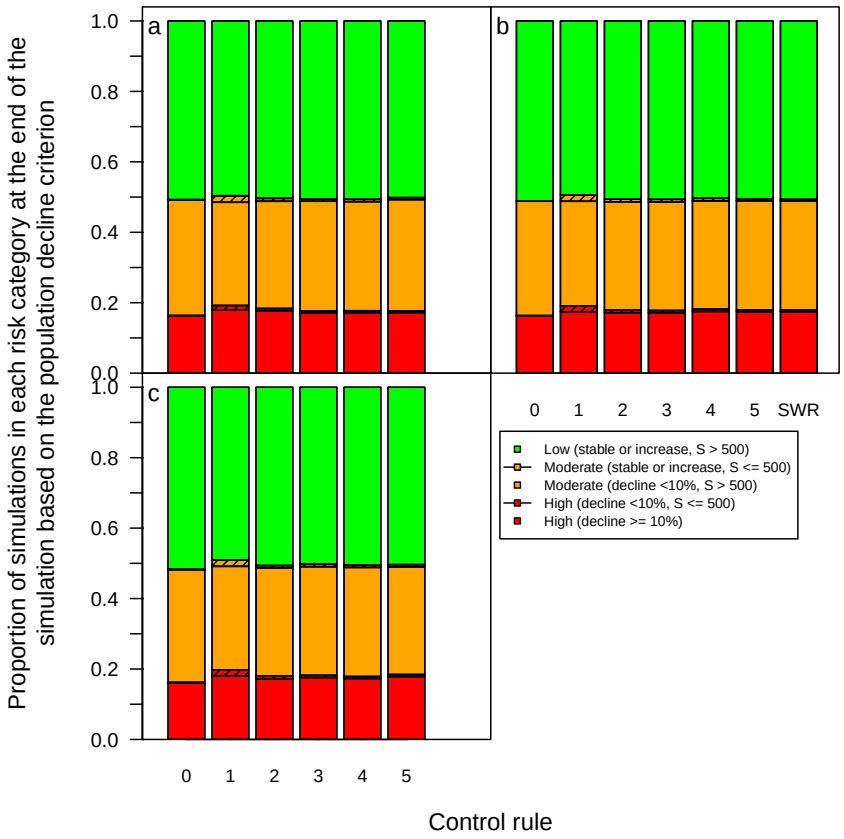

Figure A.12. Proportions of 20000 100-year simulations whose final six escapements (S) and population trends met each of three extinction risk categories based on 'population decline' defined by Lindley *et al.* (2007). We assumed no temporal autocorrelation in juvenile survival rates. S$\leq$ 500 indicates that there was at least one escapement during the final six years (two generations) of the simulation that was $\leq$ 500 spawners, while S$>$ 500 indicates that all of the last six escapements were more than 500 spawners. Population trend was calculated as the slope of the linear regression of the log of the final 10 escapements on year (Lindley *et al.*, 2007). We assumed that a slope $<= \log(0.9)$ indicated a decline $\geq$ 10% and that a slope $> \log(0.999)$ indicated a stable or increasing trend. Trend was not calculated if there was one or more zero escapements during the final 10 years so in some cases the total proportions do not sum to 1. However, zero escapements were rare in the simulations shown here so the sum of the proportions was always very close to one. Results are shown for each of three T scenarios (a-c) and 7 control rules (0-5 and 'SWR'), which are described in the text.

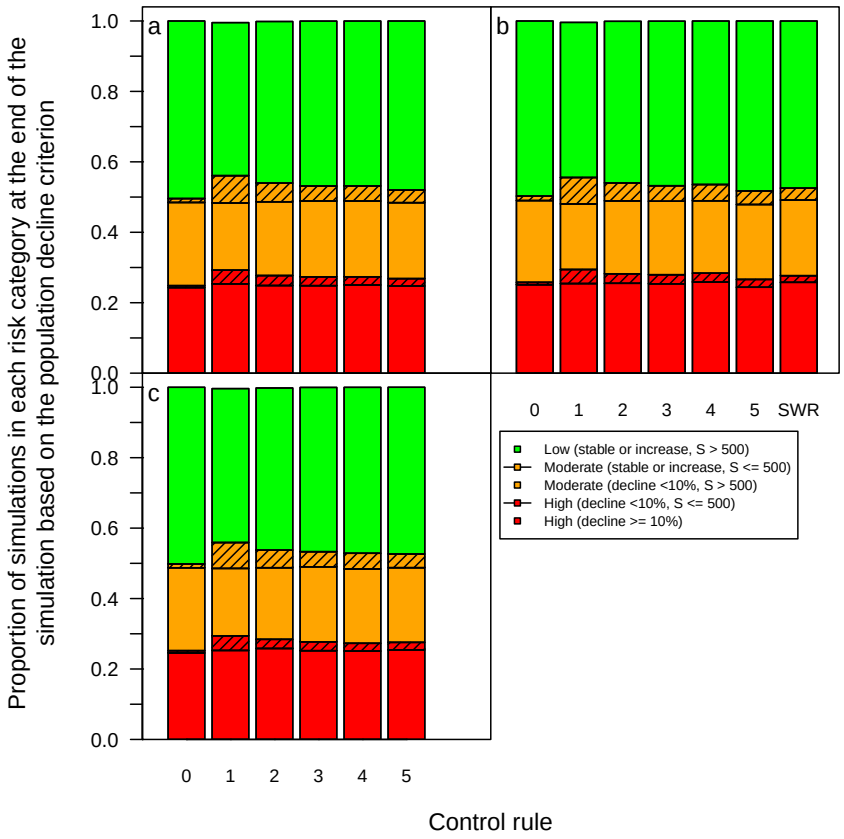

Figure A.13. Proportions of 20000 100-year simulations whose final six escapements (S) and population trends met each of three extinction risk categories based on 'population decline' defined by Lindley *et al.* (2007). We assumed a temporal autocorrelation of 0.5 in juvenile survival rates. S$\leq$ 500 indicates that there was at least one escapement during the final six years (two generations) of the simulation that was $\leq$ 500 spawners, while S$>$ 500 indicates that all of the last six escapements were more than 500 spawners. Population trend was calculated as the slope of the linear regression of the log of the final 10 escapements on year (Lindley *et al.*, 2007). We assumed that a slope $<=$ log (0.9) indicated a decline $\geq$ 10% and that a slope $>$ log (0.999) indicated a stable or increasing trend. Trend was not calculated if there was one or more zero escapements during the final 10 years so in some cases the total proportions do not sum to 1. However, zero escapements were rare in the simulations shown here so the sum of the proportions was always very close to one. Results are shown for each of three T scenarios (a-c) and 7 control rules (0-5 and 'SWR'), which are described in the text.

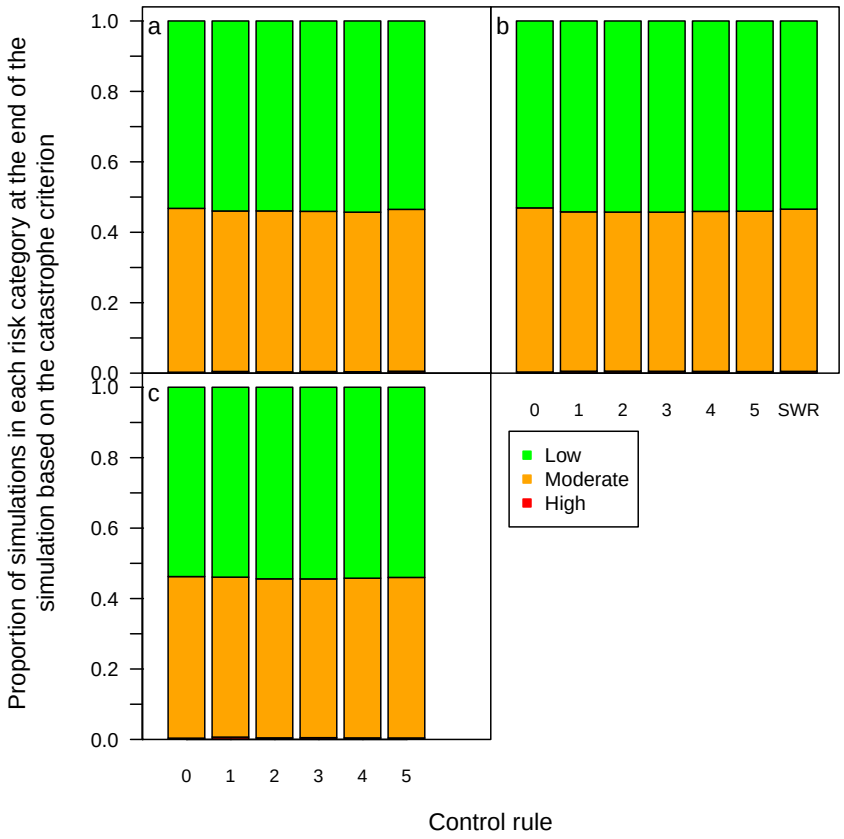

Figure A.14. Proportions of 20000 100-year simulations whose population changes during the last 10 years met each of three extinction risk categories based on 'catastrophe' defined by Lindley *et al.* (2007). We assumed no temporal autocorrelation in juvenile survival rates. Population changes were calculated as proportional differences between pairs of population sizes three years (one generation) apart (Lindley *et al.*, 2007). Thus, during the last 10 years of each simulation there were 7 population changes. High risk was assigned to simulations in which there was at least one population decline $\geq 90\%$. Moderate risk was assigned to simulations in which there was at least one population decline $\geq 50\%$, but none $\geq 90\%$. Simulations that did not meet the conditions for high or moderate risk were assigned low risk. Population changes were ignored if the population went extinct. Results are shown for each of three T scenarios (a-c) and 7 control rules (0-5 and 'SWR'), which are described in the text.

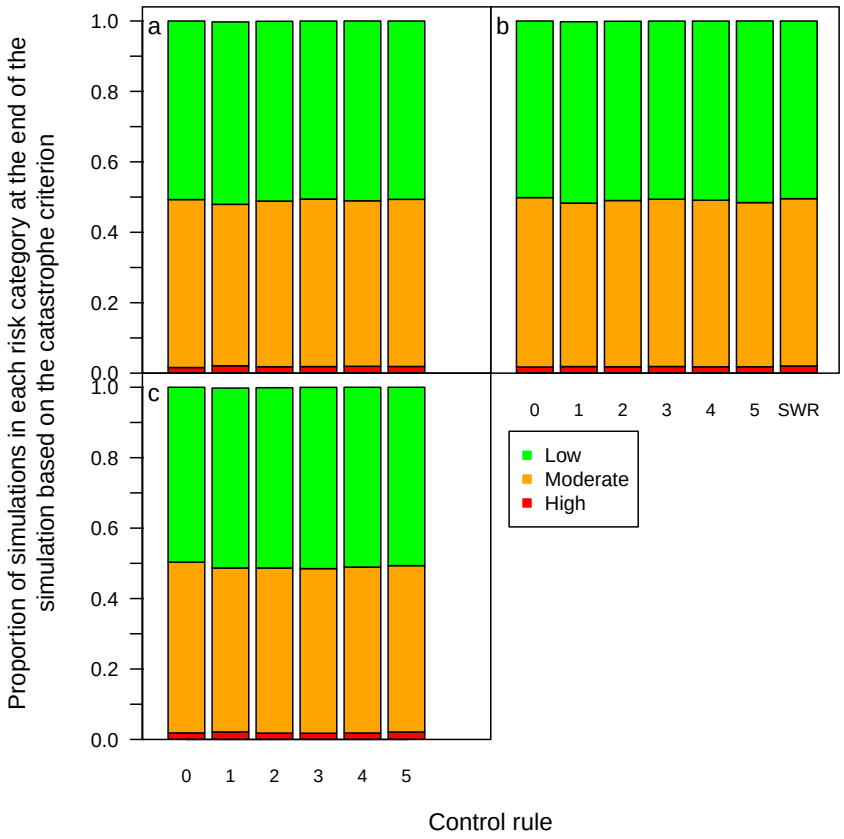

Figure A.15. Proportions of 20000 100-year simulations whose population changes during the last 10 years met each of three extinction risk categories based on 'catastrophe' defined by Lindley *et al.* (2007). We assumed a temporal autocorrelation of 0.5 in juvenile survival rates. Population changes were calculated as proportional differences between pairs of population sizes three years (one generation) apart (Lindley *et al.*, 2007). Thus, during the last 10 years of each simulation there were 7 population changes. High risk was assigned to simulations in which there was at least one population decline $\geq 90\%$. Moderate risk was assigned to simulations in which there was at least one population decline $\geq 50\%$, but none $\geq 90\%$. Simulations that did not meet the conditions for high or moderate risk were assigned low risk. Population changes were ignored if the population went extinct. Results are shown for each of three T scenarios (a-c) and 7 control rules (0-5 and 'SWR'), which are described in the text.

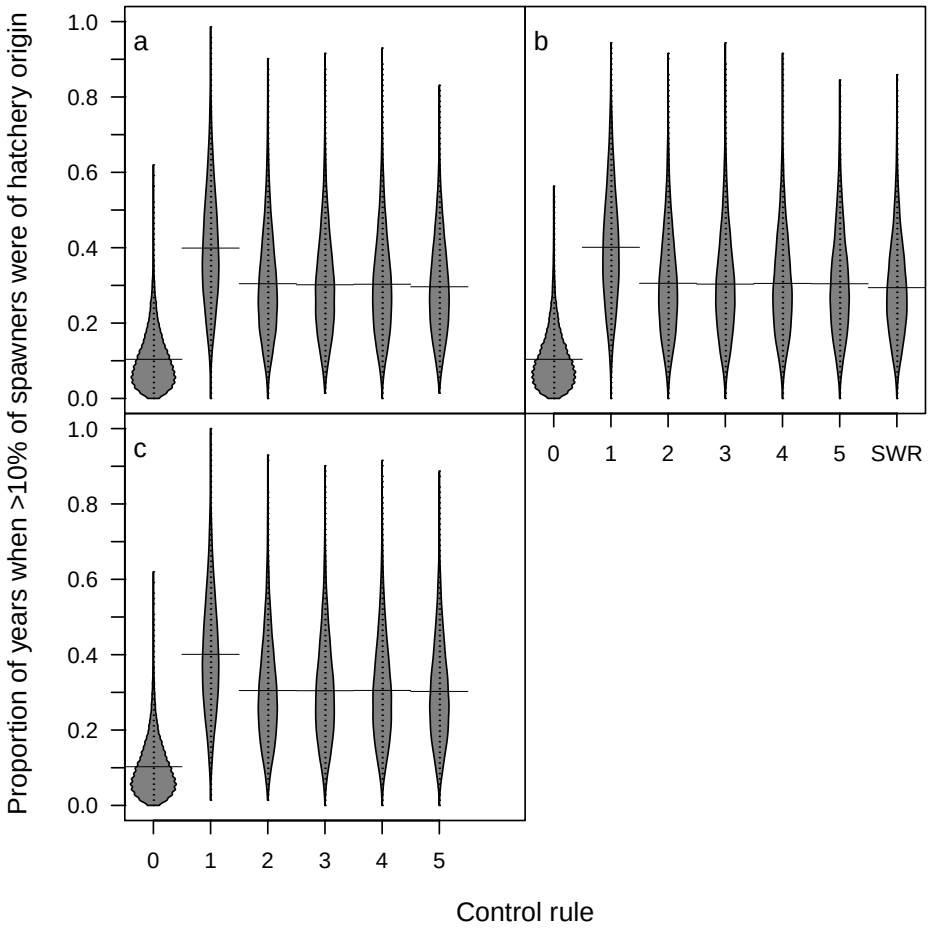

Figure A.16. Distribution of the proportion of years during which $> 10\%$ of spawners were of hatchery origin across 20000 simulations. Proportions were calculated based on years 30-100 of 100-year simulations; the first 29 years were not included to ignore transient changes in spawner composition early in the simulation as a result of initial conditions. We assumed no temporal autocorrelation in juvenile survival rates. Results are shown for each of three T scenarios (a-c) and 7 control rules (0-5 and 'SWR'), which are described in the text. The horizontal lines represent the means of the distributions.

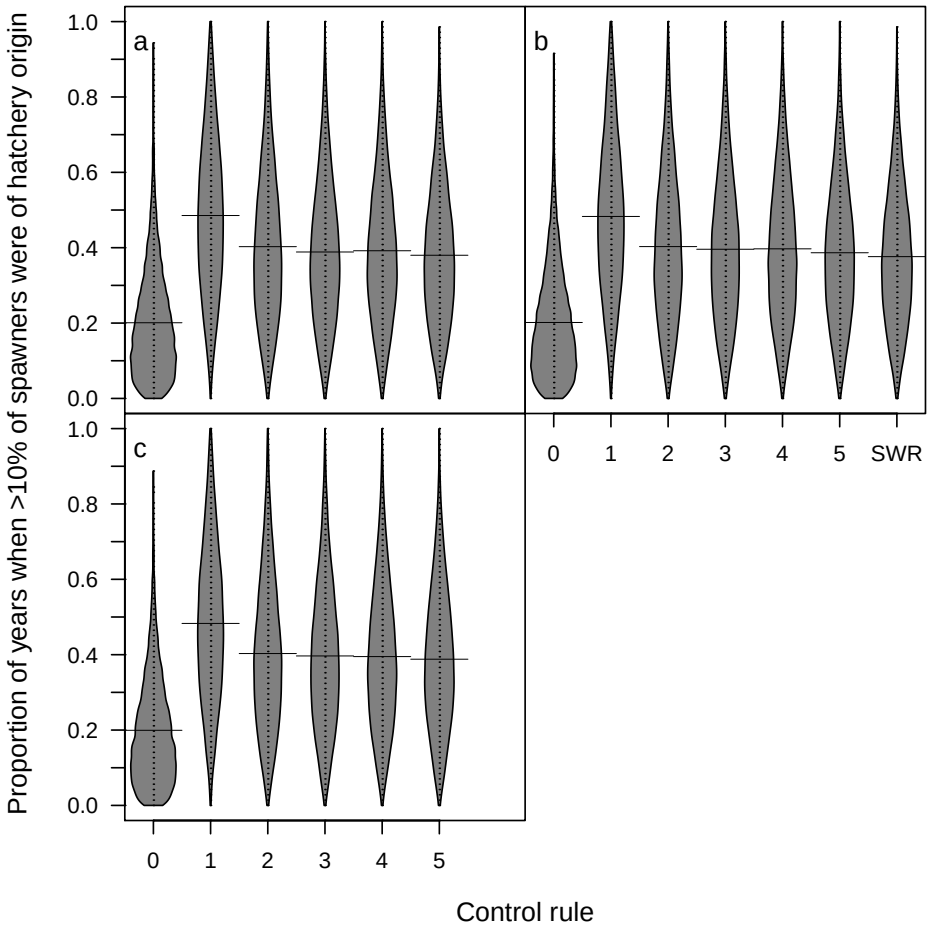

Figure A.17. Distribution of the proportion of years during which $> 10\%$ of spawners were of hatchery origin across 20000 simulations. Proportions were calculated based on years 30-100 of 100-year simulations; the first 29 years were not included to ignore transient changes in spawner composition early in the simulation as a result of initial conditions. We assumed a temporal autocorrelation of 0.5 in juvenile survival rates. Results are shown for each of three T scenarios (a-c) and 7 control rules (0-5 and 'SWR'), which are described in the text. The horizontal lines represent the means of the distributions.

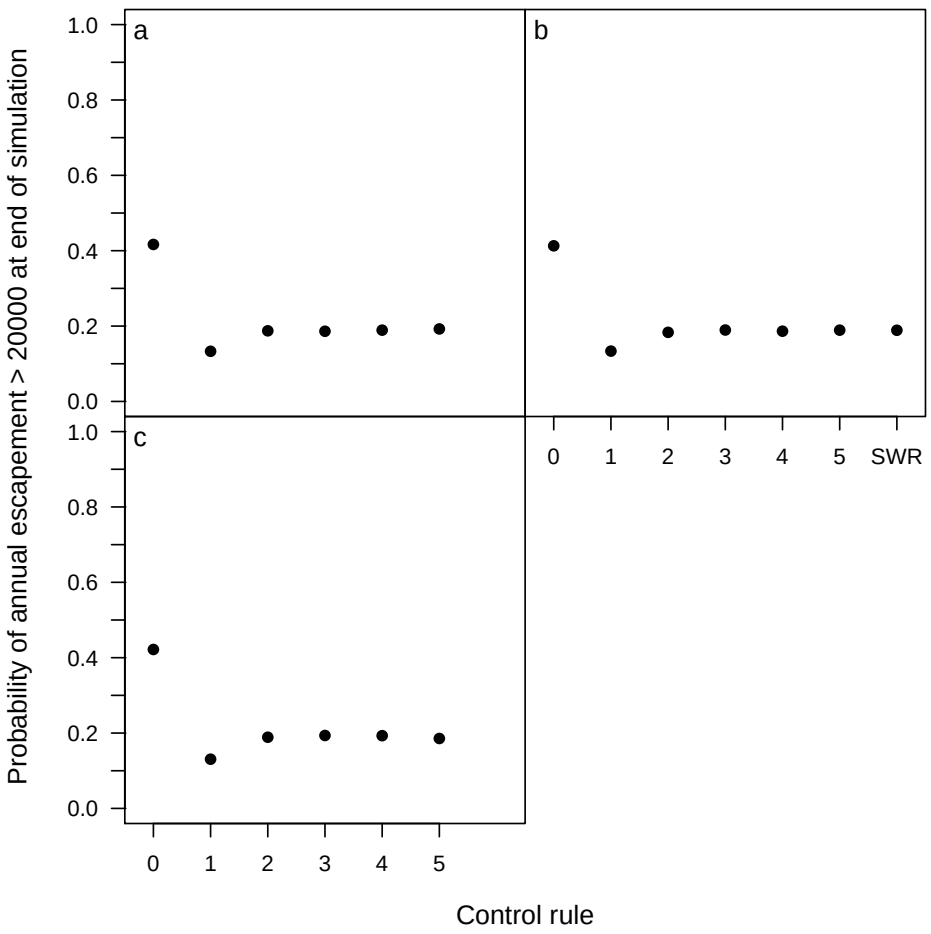

Figure A.18. Proportion of 20000 100-year simulations whose final annual escapement was > 20000 spawners. We assumed no temporal autocorrelation in juvenile survival rates. Results are shown for each of three T scenarios (a-c) and 7 control rules (0-5 and 'SWR'), which are described in the text.

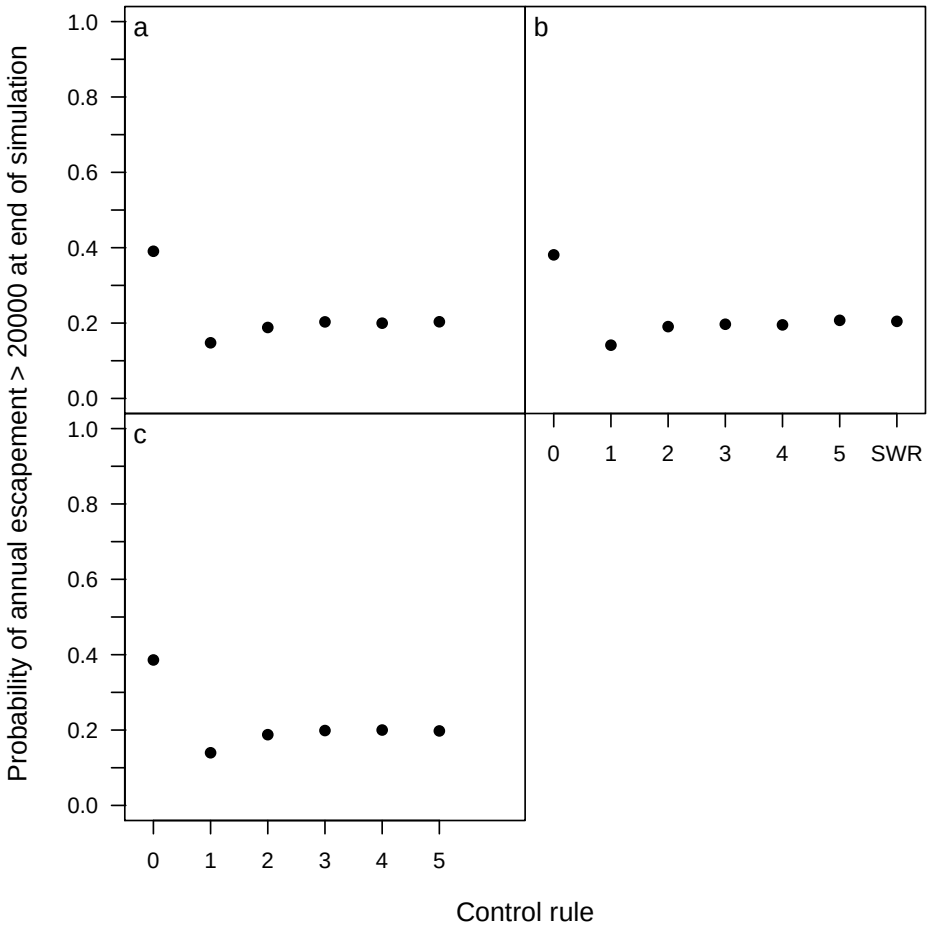

Figure A.19. Proportion of 20000 100-year simulations whose final annual escapement was > 20000 spawners. We assumed a temporal autocorrelation of 0.5 in juvenile survival rates. Results are shown for each of three T scenarios (a-c) and 7 control rules (0-5 and 'SWR'), which are described in the text.

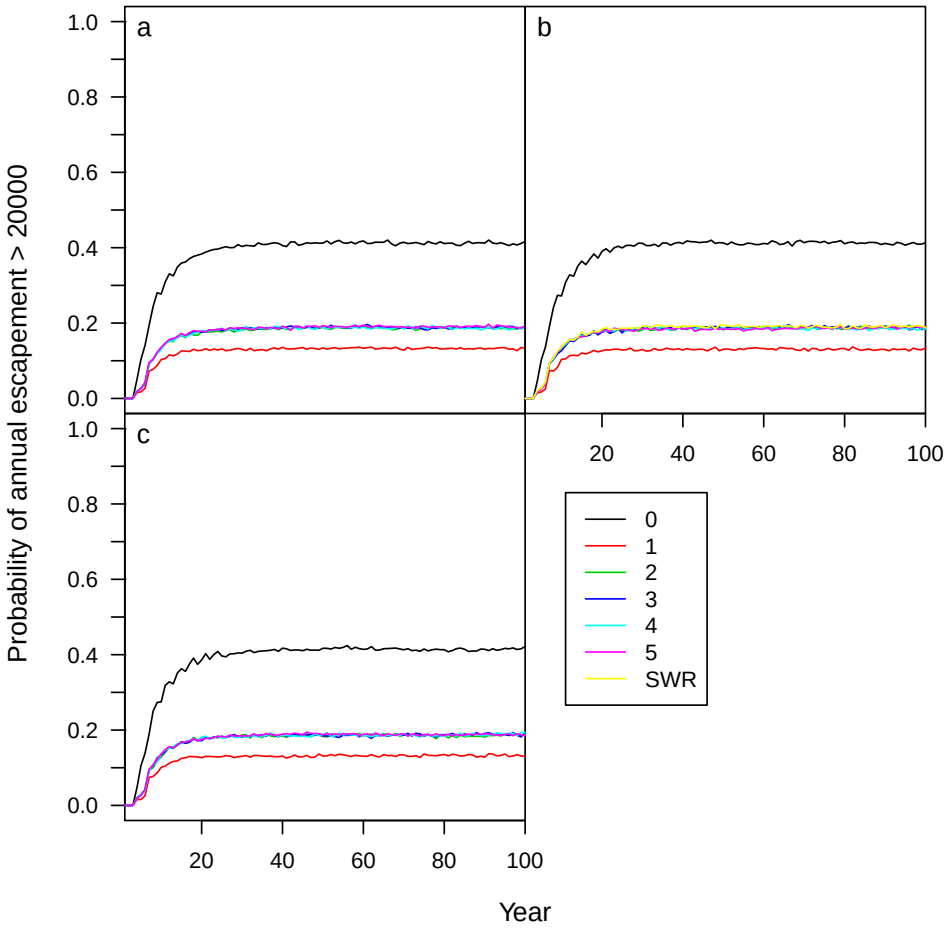

Figure A.20. Proportion of 20000 simulations in which annual escapement was $>$ 20000 spawners over the course of a 100-year simulation period. We assumed no temporal autocorrelation in juvenile survival rates. Results are shown for each of three T scenarios (a-c) and 7 control rules (0-5 and 'SWR'), which are described in the text.

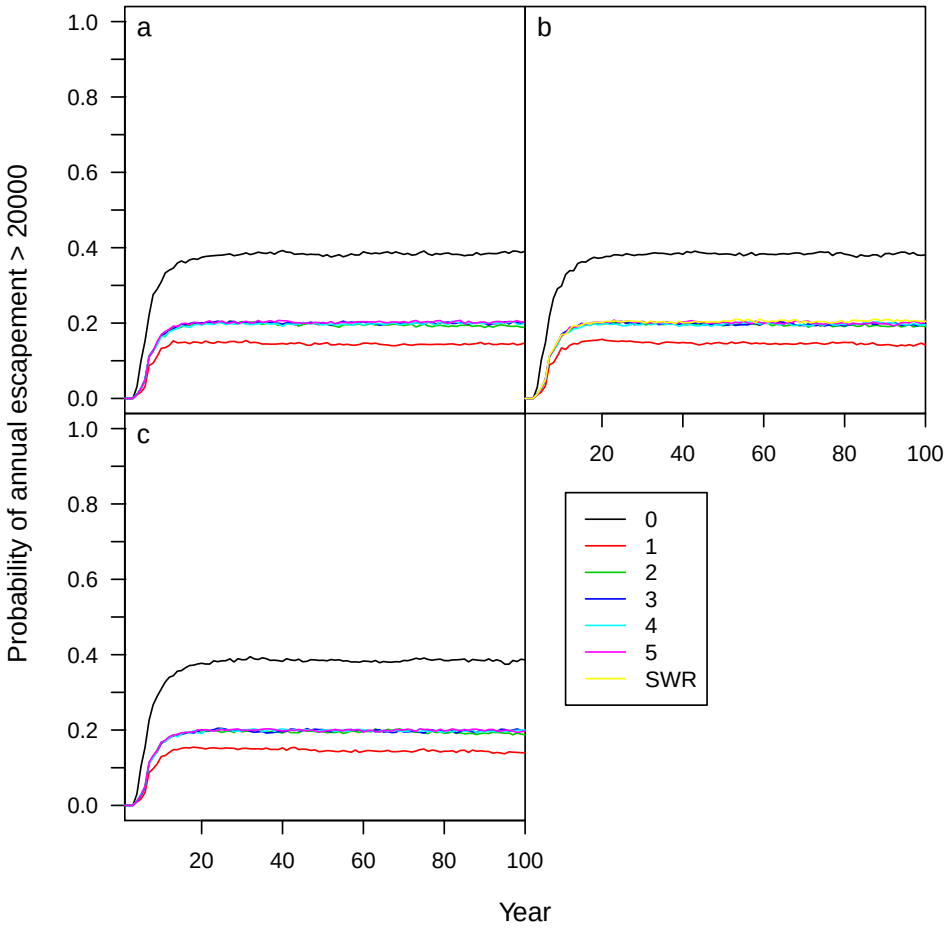

Figure A.21. Proportion of 20000 simulations in which annual escapement was $>$ 20000 spawners over the course of a 100-year simulation period. We assumed a temporal autocorrelation of 0.5 in juvenile survival rates. Results are shown for each of three T scenarios (a-c) and 7 control rules (0-5 and 'SWR'), which are described in the text.

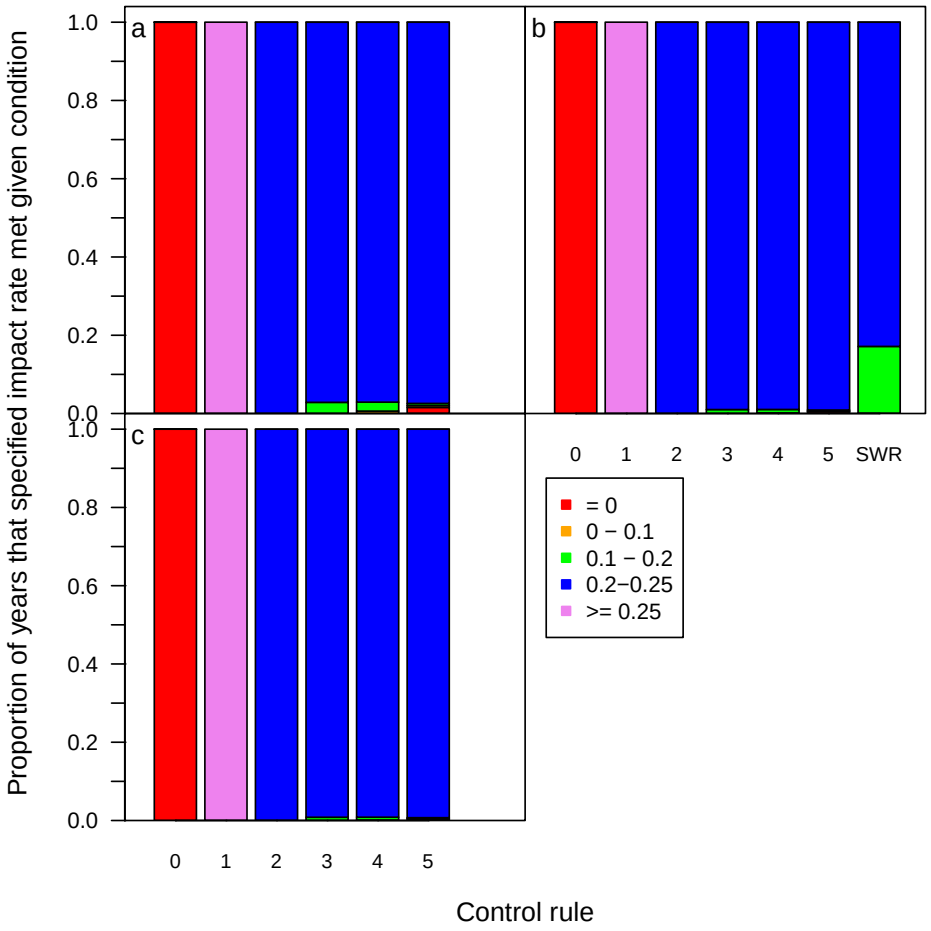

Figure A.22. Proportions of annual impact rates specified by the control rule that met each of four categories across 20000 100-year simulations. Impact rates were only calculated for years 30-99 (i.e., 1400000 impact rates are represented by each vertical bar). The first 29 years were not included to ignore transient changes in population size early in the simulation as a result of initial conditions. We assumed no temporal autocorrelation in juvenile survival rates. Results are shown for each of three T scenarios (a-c) and 7 control rules (0-5 and 'SWR'), which are described in the text.

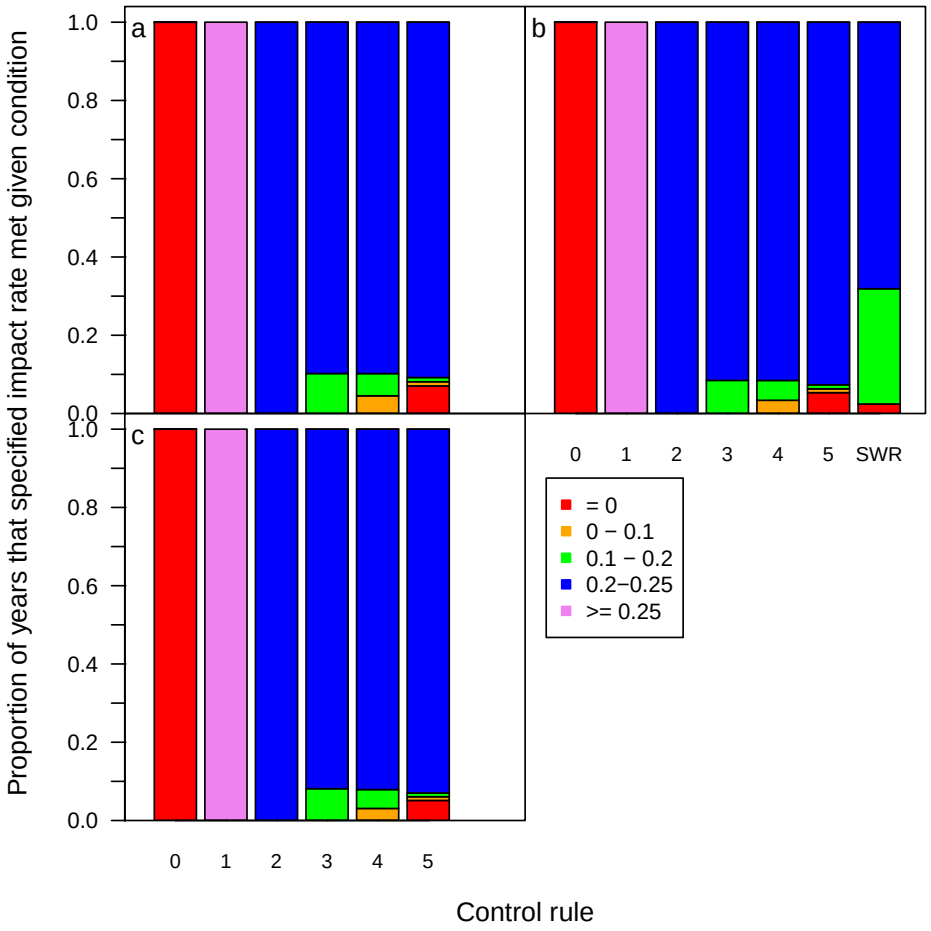

Figure A.23. Proportions of annual impact rates specified by the control rule that met each of four categories across 20000 100-year simulations. Impact rates were only calculated for years 30-99 (i.e., 1400000 impact rates are represented by each vertical bar). The first 29 years were not included to ignore transient changes in population size early in the simulation as a result of initial conditions. We assumed a temporal autocorrelation of 0.5 in juvenile survival rates. Results are shown for each of three T scenarios (a-c) and 7 control rules (0-5 and 'SWR'), which are described in the text.

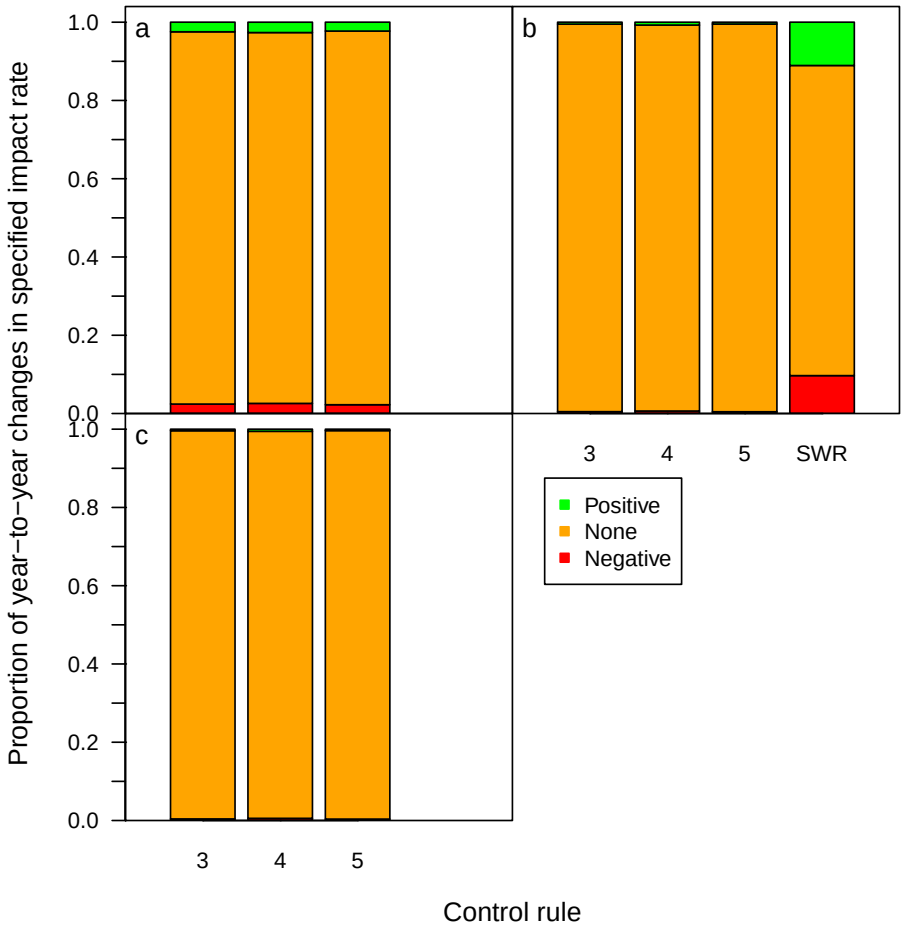

Figure A.24. Proportions of year-to-year changes in the impact rate specified by the control rule that fell into each of three categories: negative, no change, and positive. Results are shown for years 30-99 of 20000 100-year simulations. The first 29 years of each simulation were not included to ignore transient changes in dynamics early in the simulation as a result of initial conditions. We assumed no temporal autocorrelation in juvenile survival rates. Results are shown for each of three T scenarios (a-c) and 4 control rules (3-5 and 'SWR'), which are described in the text.

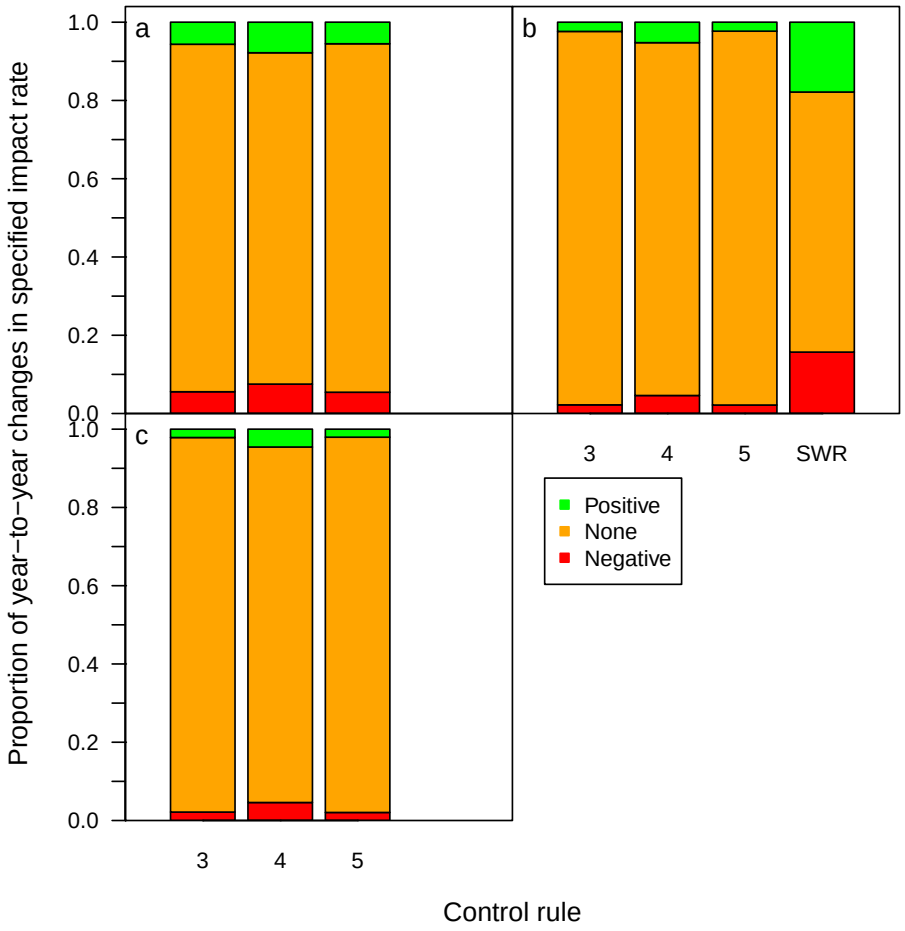

Figure A.25. Proportions of year-to-year changes in the impact rate specified by the control rule that fell into each of three categories: negative, no change, and positive. Results are shown for years 30-99 of 20000 100-year simulations. The first 29 years of each simulation were not included to ignore transient changes in dynamics early in the simulation as a result of initial conditions. We assumed a temporal autocorrelation of 0.5 in juvenile survival rates. Results are shown for each of three T scenarios (a-c) and 4 control rules (3-5 and 'SWR'), which are described in the text.

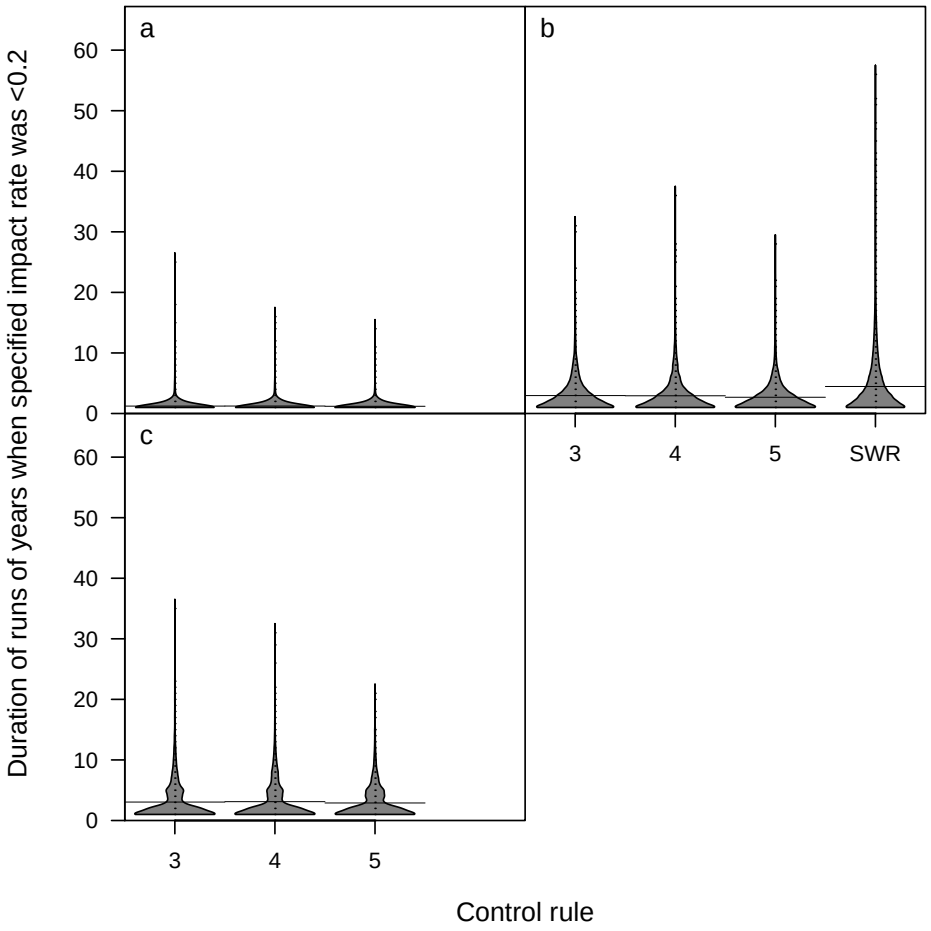

Figure A.26. Distribution of lengths of runs of years when the impact rate specified by the control rule was < 0.2. Results are shown for years 30-99 of 20000 100-year simulations. The first 29 years of each simulation were not included to ignore transient changes in dynamics early in the simulation as a result of initial conditions. We assumed no temporal autocorrelation in juvenile survival rates. Results are shown for each of three T scenarios (a-c) and 4 control rules (3-5 and 'SWR'), which are described in the text. The horizontal lines represent the means of the distributions.

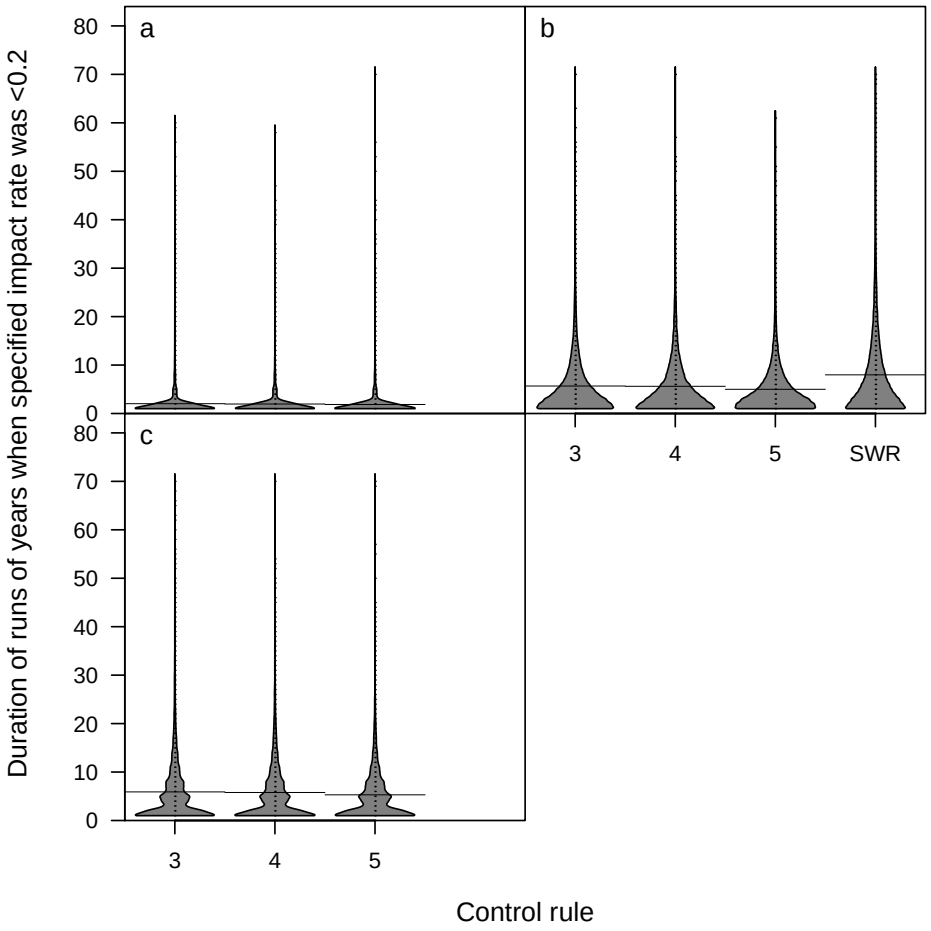

Figure A.27. Distribution of lengths of runs of years when the impact rate specified by the control rule was < 0.2. Results are shown for years 30-99 of 20000 100-year simulations. The first 29 years of each simulation were not included to ignore transient changes in dynamics early in the simulation as a result of initial conditions. We assumed a temporal autocorrelation of 0.5 in juvenile survival rates. Results are shown for each of three T scenarios (a-c) and 4 control rules (3-5 and 'SWR'), which are described in the text. The horizontal lines represent the means of the distributions.

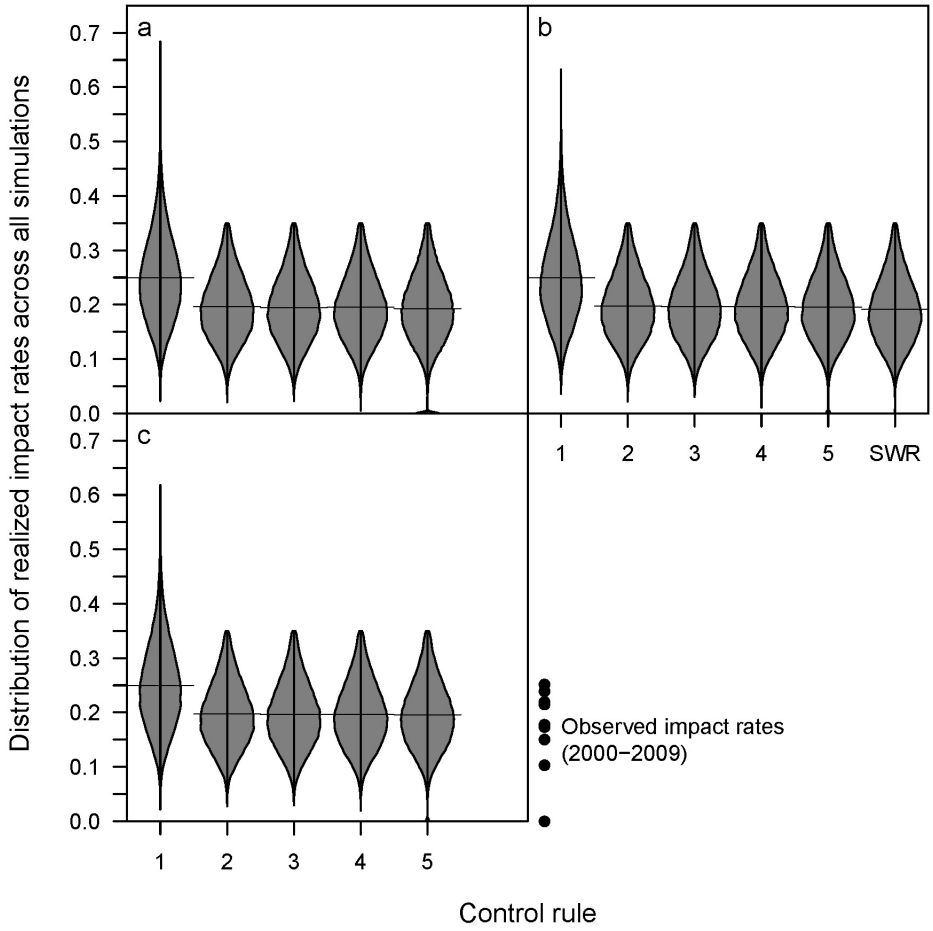

Figure A.28. Distribution of realized annual age-3 impact rates south of Point Arena. Each distribution represents 100000 annual realized impact rates sampled from 20000 100-year simulations. The assumed impact rate north of point Arena ($\delta = 0.006$) was a constant addition to the realized impact rates shown here. Only impact rates from years 30-99 were plotted to exclude transient changes early in the simulation as a result of initial conditions. We assumed no temporal autocorrelation in juvenile survival rates. Results are shown for each of three T scenarios (a-c) and 6 control rules (1-5 and 'SWR'), which are described in the text. The horizontal lines represent the means of the distributions. Actual estimated impact rates for years 2000-2009 are shown as points to the right of the lower panel.

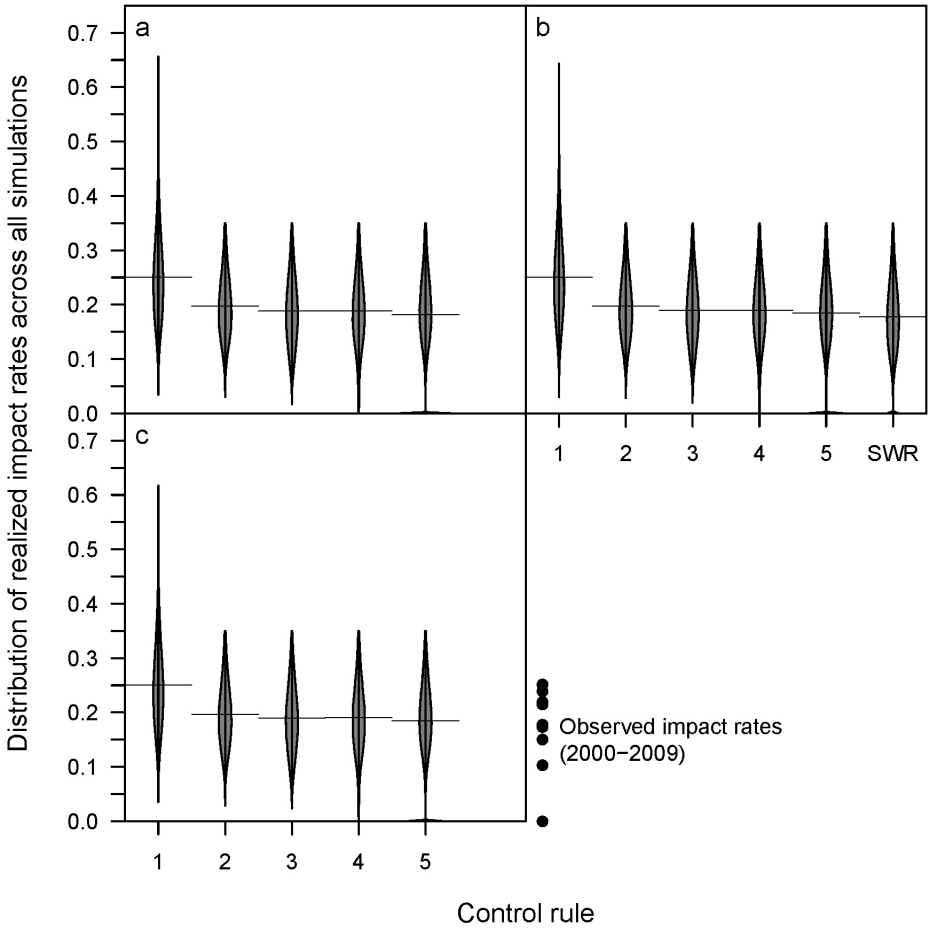

Figure A.29. Distribution of realized annual age-3 impact rates south of Point Arena. Each distribution represents 100000 annual realized impact rates sampled from 20000 100-year simulations. The assumed impact rate north of point Arena ($\delta = 0.006$) was a constant addition to the realized impact rates shown here. Only impact rates from years 30-99 were plotted to exclude transient changes early in the simulation as a result of initial conditions. We assumed a temporal autocorrelation of 0.5 in juvenile survival rates. Results are shown for each of three T scenarios (a-c) and 6 control rules (1-5 and 'SWR'), which are described in the text. The horizontal lines represent the means of the distributions. Actual estimated impact rates for years 2000-2009 are shown as points to the right of the lower panel.